Delivering nanoengineered neural stem cells within neurosurgical grade biomaterials

Louise Finch

Thesis submitted for

Master of Philosophy in Neuroscience

October 2018

Keele University

Bursaries and awards received during MPhil

1. **Royal College of Physicians Wolfson intercalated degree award**

   The Wolfson award is highly competitive, awarding funding to intercalating students nominated by their medical school each year. It is designed to assist medical students who intend to pursue a clinical research career.

2. **Association of Clinical Pathologists Student research fund**

   A competitive, annual award given to intercalating students undertaking laboratory-based research projects.

3. **First prize for poster presentation at the ISTM Annual Symposium**

   I was awarded the prize for best poster presentation at the ISTM Annual Symposium. Here, research from a variety of disciplines is showcased by PhD and masters students.

Abstracts accepted for presentation during MPhil

1. **Royal College of Physicians Innovation in Medicine 2018**

   Abstract accepted for poster and short oral presentation at the RCP Innovation in Medicine conference 2018.

2. **5th International Conference on Nanotechnology in Medicine 2018**

   Abstract accepted for oral presentation at the 5th International Conference on Nanotechnology in Medicine.

3. **British Society of Nanomedicine Early Career Researcher's Meeting 2018**

   Abstract accepted for oral presentation at the British Society of Nanomedicine Early Career Researcher's Meeting.

Abstract

Achieving neural regeneration after spinal cord injury (SCI) represents a significant challenge. Neural stem cell (NSC) therapy offers replacement of damaged cells and delivery of pro-regenerative factors, but >95% of cells die when transplanted to sites of neural injury. Biomaterial scaffolds provide cellular protective encapsulation to improve cell survival. However, current available scaffolds are overwhelmingly not approved for human use, presenting a major barrier to clinical translation. Surgical biomaterials offer the unique benefit of being FDA-approved for human implantation. Specifically, a neurosurgical grade material, DuraGen™, used predominantly for human duraplasty has many attractive features of an ideal biomaterial scaffold. Here, we have investigated the use of DuraGen™ as a three-dimensional (3D) cell encapsulation device for potential use in combinatorial, regenerative therapies. To show the feasibility of enhancing the therapeutic potential of this construct, we genetically engineered the NSCs prior to DuraGen™ encapsulation, which could offer the opportunity to increase expression of therapeutic biomolecules at the site of injury. A combination of magnetofection and minicircle technologies were used for genetic engineering of the NSCs.

I show that DuraGen™ can support the survival (ca 95% viability at 12 days) and 3D growth of NSCs. Key parameters including maintenance of NSC phenotype, proliferative capacity and differentiation into astroglial lineage cells, neurons and oligodendrocytes were unaffected by DuraGen™. Furthermore, proof of concept of the capacity of DuraGen™ to maintain a viable genetically engineered NSC transplant population is demonstrated using reporter protein expression which could be detected for up to eight days (latest time point examined) within the construct. The findings support the concept that a 'combinatorial therapy', consisting of NSCs engineered to produce therapeutic biomolecules and protected within the DuraGen™ construct, is a promising clinically translatable neuro-regenerative therapy.

Contents page

List of figures

List of tables

Acknowledgements

Firstly, and most importantly I owe a significant debt of gratitude to my supervisor Professor Divya Chari. Without her excellent guidance and support I would not have been capable of producing this thesis, which I am incredibly proud of. Thank you for the wealth of ideas and scientific knowledge which guided this project to the success it has become. In addition, I am incredibly grateful that she recognised my potential and empowered me to become the most successful version of myself. I must add, on a more personal note, that I will never forget the care and support Professor Chari provided throughout the year.

I wish to thank Dr Christopher Adams for exceptional supervision and patience throughout the year. His ideas and ability to troubleshoot contributed significantly to this thesis. Thank you to both my clinical supervisors Mr Nikolas Tzerakis and Mr Jon Sen for continually offering knowledge and advice to ensure the consistent clinical relevance of the research. With a special mention to Mr Sen for sourcing the neurosurgical materials, without which this project would have been impossible. In addition, thanks to Nimesh Mithal from Integra LifeSciences who kindly supplied the materials. Thanks to Professor David Furness for providing expertise in scanning electron microscopy.

I am grateful to the Royal College of Physicians and the Association of Clinical Pathologists whose financial support has allowed me to carry out this intercalated degree.

I express my gratitude to Dr Sarah Harris for providing the DNA minicircles for the project. In addition to this, thank you for teaching me molecular biology so patiently and for assisting me with statistics. To Dr Rawa Al-Mayyahi for teaching me NSC culture and Dr Jacqueline Tickle for your expertise throughout this project. To Farhana Chowdhury and Aina Mogas Barcons, thank you for your encouragement, I did not realise I would meet such close friends whilst carrying out this MPhil. Alexander Delaney, thank you for inspiring me to pursue this intercalation.

For all the scientific discussions and support, Dr Arwa Al-Shakli, Dr Stuart Jenkins, Professor Paul Horrocks, Dr Clare Hoskins, Dr David Morgan, Mazin Al-Shallawee, Yolanda Gómez Gálvez, Matthew Kose-Dunn and Sama Al-Shaheeb. To all the staff of the Huxley building I am incredibly grateful for your warm welcome and assistance throughout the year. A special mention should be given to Chris, Nicky, and Jan for looking after me on so many occasions.

Finally, to my parents and the rest of my family and friends for their unwavering support. Thank you Marrigje Nell for your encouragement in all those late nights in the library and to my partner, James Thompson, thank you for continually supporting me, even from Antarctica.

Abbreviations

2D	Two-dimensions
3D	Three-dimensions
aGFP	Anti-green fluorescent protein
AIS	American Spinal Injury Association Impairment Scale
ANOVA	Analysis of variance
Anti-TNFα	Anti- tumour necrosis factor alpha
ASIA	American Spinal Injury Association
BBB	Blood brain barrier
BDNF	Brain derived neurotrophic factor
BSA	Bovine serum albumin
ChABC	Chondroitinase ABC
CNS	Central nervous system
CSF	Cerebrospinal fluid
CSPG	Chondroitin sulphate proteoglycans
CY3	Cyanine 3
DALY	Disability adjusted life year
DAPI	4',6-diamidino-2-phenylindole
DMEM	Dulbecco's Modified Eagle's medium
DNA	Deoxyribonucleic acid
ECM	Extracellular matrix
EGF	Epidermal growth factor
F12	Ham's F12 medium
FDA	Food and Drug Administration
FGF	Fibroblast growth factor
FITC	Fluorescein isothiocyanate
GDNF	Glial cell line derived neurotrophic factor
GFAP	Glial Fibrillary Acidic Protein
GFP	Green fluorescent protein
HIV	Human immunodeficiency virus
ICC	Immunocytochemistry
iPSCs	Induced pluripotent stem cells
ISCS	International Spinal Cord Society
MBP	Myelin Basic Protein
mcGFP	Minicircle plasmids containing GFP
MNP	Magnetic nanoparticles
MRI	Magnetic resonance imaging
MSC	Mesenchymal stem cells
NDS	Normal Donkey Serum
NICE	National Institute for Health and Care Excellence
NPC	Neural progenitor cell
NSC	Neural stem cell
NT3	Neurotrophin-3
OEC	Olfactory ensheathing cell
OPC	Oligodendrocyte precursor cell
OsO_4	Osmium tetroxide

OTOTO	Osmium tetroxide- thiocarbohydrazide- osmium tetroxide- thiocarbohydrazide-osmium tetroxide
PBS	Phosphate buffered saline
PEG	Polyethylene glycol
PFA	Paraformaldehyde
PLGA	Poly lactic-co-glycolic acid
PNS	Peripheral nervous system
PoA	Plane of analysis
RPM	Revolutions per minute
SCI	Spinal cord injury
SEM	Scanning electron microscopy
STACIS	Surgical Timing in Acute Spinal Cord Injury study
SVZ	Subventricular zone
T3	Triiodothyronine
Trk	Tyrosine kinase neurotrophin receptor
TUJ1	Neuron-specific class III beta-tubulin

Chapter 1: General introduction

1.1 Spinal cord injury (SCI)

1.1.1 Epidemiology of SCI

Spinal cord injuries (SCI) have a devastating impact on the individual and their support networks. The global prevalence is estimated at 40-80 cases/ million/ year. The UK prevalence is estimated at 40,000 with an incidence of 12-16 cases per million (1,2). The incidence is increasing particularly in the older population and patients are increasingly likely to survive for longer with a SCI, increasing the number of disability adjusted life years (DALYs) incurred (3,4). SCIs most often occur in those aged 20-29 years. An increasing incidence peak at age 70 years and above is developing due to an ageing population and an increase in falls as the major SCI aetiology (5). Males are disproportionately affected (two: one males: females) (6).

1.1.2 The socioeconomic consequences of SCI

There is a significant social and economic impact of SCI globally. The unemployment rate of those with SCI is greater than 60%. Of children with SCI, fewer will enrol in school than the general population (6). Moreover, in the current NHS climate it is vital to note the cost of SCI. It is very difficult to assess the true cost to the NHS and to the individuals in the UK. In the USA in 1998 a study estimated the cost to an individual in the first year after injury would be $223,261. This cost would be borne by the NHS in the UK and when considered with the estimated incidence of SCI in the UK this suggests the annual cost of new SCI to be in the region of $175,706,407 USD (2,7). In addition, there are the ongoing costs of living with SCI. This comprehensive study suggests that the medical costs and cost due to loss of productivity amounted to $22,573 per person per year beyond the first year. Again extrapolating this to the UK, this would amount to $902,920,000 USD (1,7). This only provides an estimation of the cost; the actual cost is likely to be more as these figures do not

account for home modifications, prescriptions, carers, loss of family member productivity, and the cost of regional SCI centres.

1.1.3 The clinical features of SCI

The mechanism of injury to the spinal cord varies. The most common cause, reported as 90%, is trauma including road traffic collisions, falls, and violence. Other causes include vascular insults such as arteriovenous malformations, degenerative disease including multiple sclerosis, primary and secondary tumour formation and disc prolapse (6). These events can result in a variety of injuries to the spinal cord itself, but most commonly cause a contusive lesion (8).

Symptoms and signs vary depending on the site and extent of the injury. These can include loss of sensory, and/or motor function, loss of autonomic control including bladder and bowel control. In high cervical cord injury there is an appreciable mortality and morbidity rate, largely due to respiratory complications. Furthermore, many patients report chronic pain and depression. Moreover, many experience secondary complications of SCI including pressure ulcers, deep vein thromboses, and infections (6).

Each injury will produce a different set of clinical symptoms depending on the location. The American Spinal Injury Association (ASIA) and the International Spinal Cord Society (ISCS) developed an international system which categorises the extent of SCI; this is called the ASIA Impairment Scale (AIS). Using both anatomical location and extent of injury they developed 5 distinct categories: A-E in descending order of severity. 'A' denotes a complete injury where no sensory or motor function is preserved inferior to the injured cord segment. An injury causing complete motor loss and partial sensory loss would be represented by a category 'B'. 'C and D' represent injuries involving incomplete motor loss with preservation of the most caudal motor segments, including voluntary anal contraction. To be classified as 'D', the patient must display a Medical Research Council grade 3 or above in more than half of the specified 'key' muscles. A category 'E' is given to a patient who

previously had deficits from a SCI but now presents with no deficit. The results of a neurological examination are mapped on to an ASIA chart (9). This criterion is not only useful clinically but also in objectively assessing outcomes in clinical trials.

1.1.4 The pathophysiology of SCI

At the macroscopic level, the primary injury occurs at the time of the event for instance compression or contusion of the cord, then following this a secondary injury occurs where there may be haematoma formation and oedema which can contribute to further compression. Following this the lesion site evolves producing a necrotic epicentre and cyst formation occurs (8).

At the microscopic level, several processes occur in the aftermath of the injury. Firstly, astrocytes at the lesion site are activated and proliferate. These reactive astrocytes hypertrophy and extend their processes. They have been suggested to provide a protective function at this stage. The astrocytes 'seal off' the lesion and in doing so prevent the extension of inflammation and necrosis into the surrounding healthy cord to limit the extent of the injury (10).

Reactive astrocytes release inflammatory cytokines which recruit microglia to the site of injury. Microglia act to clear debris and release pro-inflammatory cytokines which contribute to further tissue damage (11). The damaged neurons retract their axons away from the injury site and this is compounded by the demyelination of the remaining axons due to the loss of oligodendrocytes (8). In the chronic phase of injury, the astrocytes transform into scar-forming astrocytes and inflammatory cells persist and can be found at ten weeks post injury (11,12).

The period post SCI is split into distinct time periods (**figure 1.1**). The initial 48 hours is classified as the acute phase and the subacute phase is after 48 hours up to 14 days. Towards the end of the subacute phase astrocytes become reactive. The period from two weeks to six months is referred to as the intermediate phase of injury. At around four to six months the astrocyte 'scar' has

developed. Beyond six months is categorised as a chronic injury (13). Chronology aids a comparison when using rodent models to investigate human diseases. The response is well categorised in rat models and the astrocytes at the edge of the lesion are reactive by one to two weeks, similar to that in humans. However, the astrocytic 'scar' is established much earlier at two to three weeks (14). In mice, although less well characterised, increased astrocytic staining has been observed at seven days post injury indicating astrocyte reactivity, with intensely reactive astrocytes by day 12 (15). Moreover, the astrocytic scar has been detected in mice at two weeks following injury (16). This suggests that the pathological sequelae in rodents are similar, but shorter than that in humans.

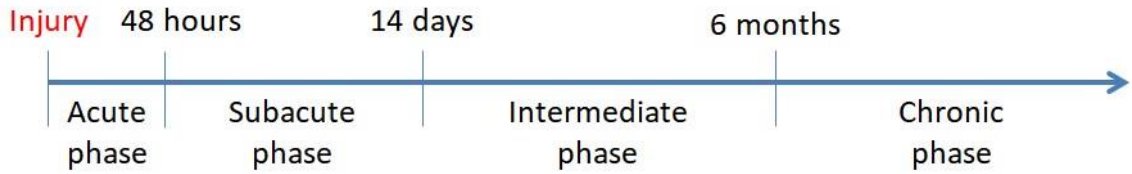

Figure 1.1: *SCI timeline in humans adapted from* (13).

1.1.5 The barriers to regeneration in SCI

It was previously believed that adult spinal cord neurons have no regenerative capacity. In 1928, Santiago Ramón y Cajal published his work describing his observations of nervous system regeneration including theories of neurotropism (17). This was almost forgotten until Richardson et al 1980 proved that spinal cord grey matter axons could cross from the cut edge of a spinal cord lesion to an autologous sciatic nerve graft. Richardson hypothesised that it was the central nervous system (CNS) environment that prevented regeneration (18). Peripheral nerves are capable of regeneration. The peripheral nervous system (PNS) environment is suggested to be promoting of axonal regeneration (19). The process of Wallerian degeneration, which follows PNS axotomy and causes fragmentation of the axon, clears the environment for axonal growth. In addition, Schwann cells are thought to be essential for axonal regeneration, when they are not present the axons do not regenerate (19,20).

The major component of the CNS environment thought to inhibit axonal repair is the astroglial scar. It is not only the physical barrier of the scar that prevents axonal regrowth, but the scar also produces inhibitory factors which prevent axonal regrowth. These inhibitory factors include extracellular matrix (ECM) components such as chondroitin and keratin sulphate proteoglycans which contribute to further tissue damage (21), and factors that specifically prevent neuronal differentiation (22) or cause the collapse of the neuronal growth cone (23) all contributing to the prevention of regeneration. Some vertebrates that can regenerate their spinal cords after injury, produce very little glial scar (24). The astrocytes at the site of SCI in urodele amphibians and teleost fish do not hypertrophy and do not secrete ECM components but instead play a supportive role for neurogenesis by providing guidance for axonal growth (25).

The negative impact of astrocytes in mammalian SCI has been contested. Anderson et al demonstrated detrimental effects when the astrocytic scar does not form after SCI (26). Transgenic mice that did not produce activated astrocytes failed to show spontaneous axonal regrowth after SCI (26). Reactive astrocytes likely play a role in maintaining the blood brain barrier (BBB) immediately following SCI. Bush et al demonstrated that ablation of astrocytes in traumatic brain injury led to a failure of repair of the BBB which resulted in an influx of leukocytes and vasogenic oedema (27). It therefore remains unknown whether the overall impact of the astrocytic scar is disadvantageous or beneficial.

The inflammatory environment immediately following SCI likely has an impact on regeneration, and inflammation is sustained in SCI (12). In general, inflammation is associated with a lack of regeneration and conversely regeneration occurs where there is a reduced inflammatory state (24). Microglia and macrophages play a significant role in the inflammatory state post SCI although their role for regeneration is complex (11). Microglia assume one of two phenotypes after CNS injury,

M1 polarisation or M2 polarisation. M1 microglia are cytotoxic, causing secondary damage and axonal retraction whereas M2 promote axonal growth (11).

The spinal cord has also been identified as a 'non-permissive zone' for neuronal differentiation. Transplantable cells such as spinal cord stem-like cells differentiated into neurons and glia *in vitro* however when implanted into the spinal cord exclusively differentiated into glial cells. This was contrary to their fate in the hypothalamus where the spinal cord stem-like cells did differentiate into neurons (28). This suggests that the environment of the spinal cord is not permissive for neurogenesis (24).

1.1.6 Current and future therapies for SCI

A range of therapies exist for the treatment of SCI which aim to promote functional recovery, but none promote spinal cord regeneration. Currently, a patient experiencing a SCI may expect to receive a combination of anti-inflammatory drugs, immune modulators, and physical rehabilitation. Surgical management may be an option; this would include decompression, stabilisation, or both. In 2012, the Surgical Timing in Acute SCI Study (STACIS) demonstrated two grade improvements on the ASIA criteria after early decompressive surgery (29).

The mainstay of treatments however, tend to focus on specific symptoms of SCI and complications of paralysis, particularly chronic pain management and avoidance of pressure sores (30). Other options include functional electrical stimulation for example peroneal nerve stimulators for associated foot drop, and exoskeletons to improve ambulation (31). Managing SCI patients urologically proves challenging due to the increased risk of urinary tract infections and calculi formation. Many options exist to combat this including catheterisation, urinary diversion and sacral root stimulation (32). In addition, psychological therapies are vital to treat the associated mental health problems (33).

Treatment with high dose methylprednisolone was shown in the National Acute SCI Studies II and III to improve motor and sensory function significantly (34,35) but was later discredited (36) and the National Institute for Health and Care Excellence (NICE) specifically state it should not be administered in their guidance (37). **This leaves an exciting area for development of treatments for SCI that can truly promote regeneration.**

The complex, multifactorial nature of the pathophysiology of SCI means that stand alone treatment options such as pharmaceutical interventions offer some benefit but do not improve regeneration, whilst treating one element of the pathology neglects another. Therefore, **'combinatorial therapies'** combining multiple therapeutic interventions at the site of injury has become the therapeutic target. Figure 1.2 demonstrates the multiplex of treatment goals that exist in SCI and the different potential treatment options that could tackle them. Options include a combination of structural support such as biomaterials, cellular transplants, genetic modification of cells to express specific therapeutic molecules, systemic or local pharmaceutical delivery, epidural stimulation, nanotherapy or scar removal via surgery. Cell transplant, biomaterials and genetic engineering will be discussed in detail in later sections of this introduction. The following are examples of the variety of experimental treatments being investigated.

Inflammation has been identified as a barrier to regeneration in SCI, therefore many new treatments are being investigated which suppress inflammation. Pharmaceuticals directed at specific inflammatory cytokines are being tested. Anti-tumour necrosis factor alpha (anti-TNFa) drugs such as Infliximab, currently used in other inflammatory mediated conditions such as rheumatoid arthritis, are being trialled in SCI. Treatment with infliximab after SCI in rats led to an increased Basso, Beattie, Bresnahan score (38).

Remyelination of axons at an injury site is vital for regeneration. Mature functional oligodendrocytes are essential for myelination within the CNS. Thyroid hormone (specifically

triiodothyronine [T3]) has been shown to encourage NSC differentiation into oligodendrocytes and oligodendrocyte precursor cell (OPC) maturation into oligodendrocytes. Systemic delivery of T3 in rats with SCI caused hyperthyroidism, therefore a local delivery system was developed composed of a T3-impregnated agarose hydrogel. Implantation of this hydrogel led to an increased number of myelinated axons when implanted into rat SCI but did not improve locomotor scoring (39).

To elicit function in the preserved cord distal to the lesion site, epidural stimulation is being trialled. The sacrolumbar regions of the cord contain internal circuits which can control the muscles they innervate even when the central connection is lost. A closed-circuit stimulation device is implanted and along with rigorous training sessions the patient was able to walk and regained some urogenital function. Harkema et al hypothesised that the stimulation either assisted residual descending pathways by summation of the signals allowing the threshold for motor neuron activation to be met, or that it induced axonal regeneration (40).

A combinatorial therapy with multiple targets designed to tackle different elements of the pathophysiology is currently considered to be the most promising strategy to improve SCI regeneration.

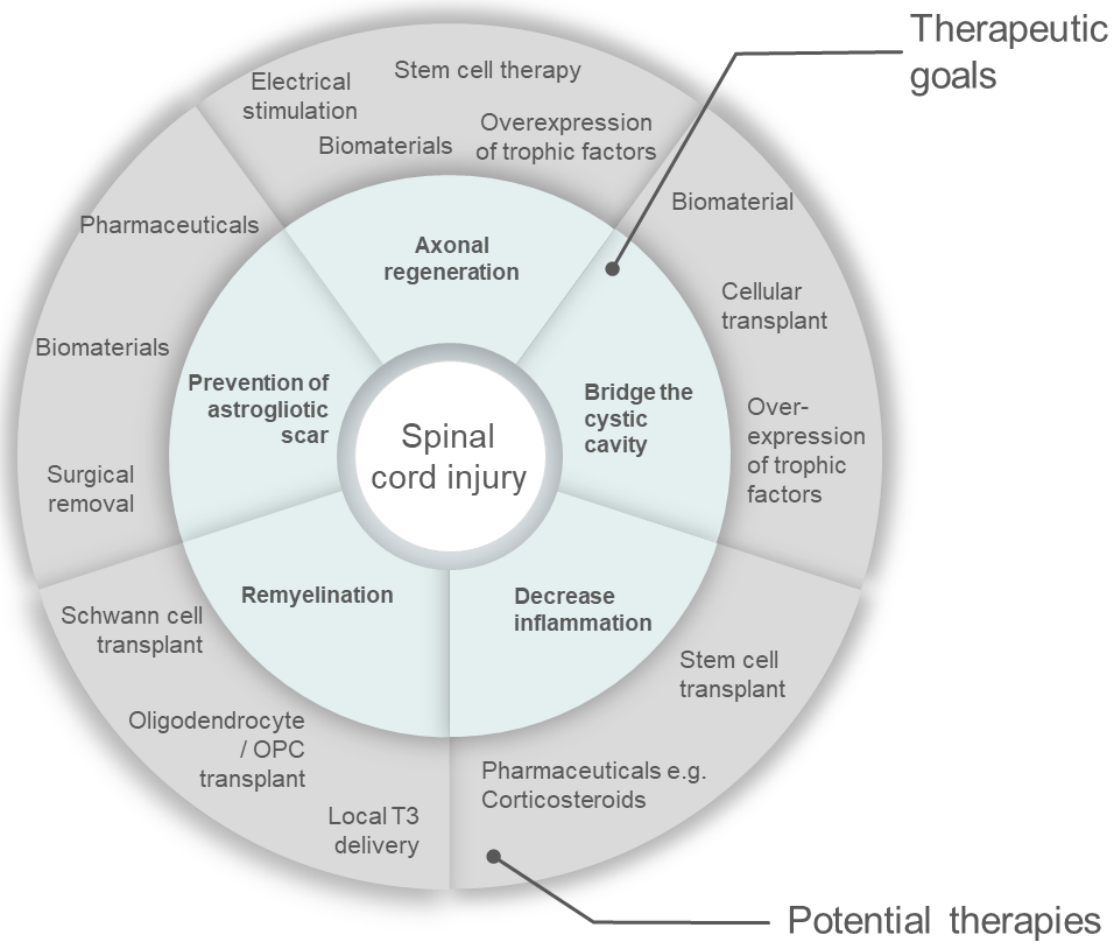

Figure 1.2: *The multiple therapeutic goals of SCI and some potential associated therapies. Diagram design adapted from* (41).

1.2 Cell transplantation can promote regeneration in SCI

1.2.1 Cell transplantation enhances regeneration

The CNS is not a conducive environment to growth and repair (18,42). Following an injury, the endogenous NSCs and progenitor cells become activated and migrate to the site of injury or inflammation (43–45). This is the innate CNS regeneration process, the aim being for NSCs that have migrated to replace lost cells and encourage regeneration. However, due to the inhibitory nature of the environment and often the extent of the injuries, the endogenous response is not sufficient

to promote repair. Therefore, significant attention in the field of regenerative medicine has been given to therapies that involve the delivery of neural cell transplant populations.

When considering a cell transplant therapy, there are many features that are desirable. In general, for any cell transplant regardless of which system is the target the graft must achieve the desired benefit whilst causing minimal harmful effects. The cells should be accessible and commercial scale up must be possible for the population to become a realistic clinical therapy. When considering CNS therapy, the target is often to re-establish or improve neuronal function. This requires more complex cell therapy designs. Dunnett and Björklund describe the key mechanisms by which a neural graft can improve function in the CNS. These include full reconstruction of all the tissues at the site of injury or more specifically focussing on graft-host reinnervation where the therapeutic target is to produce functional integration of transplanted cells with host neurons. Researchers may also aim to provide trophic stimulation by delivering exogenous trophic factors. 'Bystander effects' are also important benefits of stem cell treatments. This occurs when the presence of the grafted cell exhibits beneficial effects on the host tissue by paracrine effects. It is referred to as 'bystander' because there is no long-term survival of the transplanted cells. The 'bystander effects' are commonly immunomodulatory (46,47).

Barker outlines four essential features of a stem cell transplant population with a CNS target for translation to clinical trial. The first is that the stem cells must differentiate into neurons. Secondly, the properties of the stem cells must be reproducibly demonstrated within the laboratory. Thirdly, the neurons must survive long-term *in vivo* and produce functional benefits in animal models. Finally, all three of the above must occur without evidence of malignant transformation (48).

1.2.2 Types of neural cells for transplantation

There are multiple neural cell populations available for transplantation, each with different beneficial properties. Table 1.1 outlines the pros and cons related to each of the major neural cell transplant populations in relation to the treatment of SCI.

Cell transplant population	Pros	Cons
Astrocytes	Maintain homeostasis after CNS insult (49). Repair the BBB/ Blood-spinal barrier (27,50). Release neurotrophic factors (51–53). Reduce astrocytic scar volume (54,55). Reduce secondary injury (27,56).	Historically considered preventative of axonal regeneration (49). Release factors detrimental to axon growth such as chondroitin sulphate proteoglycans (CSPGs), reactive oxygen species and cytokines (57). Modest benefits in experimental trials so far (54,58,59).
NSCs	Differentiate into the three major cell types of the CNS (60). Capable of self-renewal (60). Produce immunomodulatory bystander effects (61). Produce neurotrophic factors (61). Exhibit pathotropism (43–45). Option for protected delivery as neurospheres (62). Can be autologously generated from iPSCs (63).	Risk of teratoma formation (64,65). *In vivo* differentiation yields low number of neurons (66). Sourcing autologous cells is problematic for instance the process to derive iPSCs requires four months (63).
Olfactory ensheathing cells (OECs)	Unique neuro-regenerative properties throughout life (67). Remyelinate axons (68). Release neurotrophic factors (69). Can be obtained from olfactory mucosa biopsies for autologous transplant (70).	Wide variation in results of regeneration studies (71). No robust benefit after transplantation into moderate and severe thoracic contusion injuries (72). Requires adjuvant therapy to improve efficacy (72).

	Can be purified and grown in large quantities (67).	
OPCs	Mature into oligodendrocytes which can remyelinate axons (73). Under specific conditions can give rise to astrocytes and neurons (74,75).	Evidence suggests they may contribute to the glial scar (76). Increase CSPGs at the injury site (77).
Schwann cells	Remyelinate axons (78). Can be readily harvested from peripheral nerves and cultured in large numbers (67).	Schwann cells will not myelinate axons in the presence of CNS astrocytes (79). Requires adjuvant therapy to improve efficacy (72).

Table 1.1*: The pros and cons of the major neural transplant populations with respect to SCI therapy.*

1.2.3 NSC transplantation for SCI

NSCs are an ideal clinical transplant population for the treatment of SCI. They offer a multitude of beneficial effects for the treatment of SCI. NSCs differentiate into three cell types: astrocytes, neurons and oligodendrocytes. These three cell types form the basis of neural circuitry and the ability to transplant all three provides a unique opportunity to replace lost cells like for like (60). Moreover, NSCs naturally produce a variety of neurotrophic factors to encourage growth at the site of injury including brain-derived neurotrophic factor (BDNF) and neurotrophin-3 (NT3), both essential factors in development of the CNS (61). NSCs have been shown to decrease astrogliosis and they exert immunomodulatory effects on the microenvironment of SCI (61).

There are three main ways to generate a culture of neural precursor cells or NSCs. Firstly, they can be derived from primary sources and cultured with growth factors to remain undifferentiated and continue to proliferate. In adult rodents, they can be obtained from the striatum, subependymal region, the dentate gyrus of the hippocampus, the thoracic spinal cord, periventricular regions and the olfactory bulb (80–82).

Secondly, neural precursor cells can be differentiated from pluripotent stem cells. Two main sources of neural cells in trials are embryonic stem cells and induced pluripotent stem cells (iPSCs). Embryonic stem cells are acquired from *in vitro* fertilisation clinics where the cells are donated with consent. This has ethical implications and the law differs internationally (80,83,84). Due to the controversial nature of embryonic stem cells they do not represent a popular source of NSCs. iPSCs on the other hand, are a favourable source of NSCs. They are induced from host tissues such as bone marrow and adipose tissue, so hence would be exempt from immune reaction issues. However, they do require a significant amount of time to be cultured and this may not always be possible due to ideal treatment time scales (80).

Thirdly, neural cells can be obtained via transdifferentiation of one type of mature cell. The process involves inducing 'transdifferentiation' in a mature cell such as a fibroblast to become another type of mature cell such as a neural cell avoiding the pluripotent phase. For transdifferentiation to occur the cell population requires induction most commonly by addition of transcription factors such as Sox-2 (85). Transdifferentiation can also be induced via cocktails of chemical compounds (86) or via growth in 3D culture (87). There are multiple cell types from which this could be carried out for instance fibroblasts, Sertoli cells, hepatocytes and B lymphocytes. These cells could be obtained from the individual, transdifferentiated, and returned to the individual hence avoiding an immune reaction (80).

There are two ways in which laboratories propagate NSCs. They can either be cultured as a single layer of cells normally on glass termed a 'monolayer' culture or they can be maintained as balls of NSCs, termed 'neurospheres'. This is a free floating, 3D culture system where the cells are not adherent to a substrate.

The concept of transplanting neural tissue was first demonstrated in Santiago Ramón y Cajal's laboratory in the early 20th century, Jorge Francisco Tello, Cajal's student, transplanted pre-

degenerated segments of peripheral nerves onto the proximal stumps of the optic nerve. He observed retinal axons growing into the nerve providing the first documented proof that grafted neural tissue could provide the solution to neuronal injury (17). In 1975, Richard Bunge developed an *in vitro* culture of Schwann cells and hypothesised that this cell type could be transplanted to treat SCI (88).Then in 1980, Richardson et al demonstrated long distance axonal growth after the transplantation of peripheral nervous tissue (18). Continuity across the rostral and caudal stumps of partial SCIs in rats was demonstrated post transplantation of rat fetal spinal cord tissue by Reier in 1986 (89). The concept that fetal neural tissue can encourage CNS repair was further proven by Björklund et al in models of Parkinson's and Huntington's disease (90).

The field of neural tissue engineering has evolved significantly over the last decade having now reached clinical trials. The following section describes some of the major pre-clinical and then clinical trials utilising NSCs for the treatment of SCI.

There has been significant success with the use of NSCs from a variety of sources in animal models of SCI. Rodents are the most commonly used model, although primates have also been utilised. SCIs are induced in different ways including dropping a weight on the spine, the use of devices such as impactors to produce a compression injury or surgically producing a partial or complete transecting injury (80,91–96). Many studies have demonstrated functional and histological improvement post implantation of NSCs.

One of the major outcome measures of these studies is locomotor recovery. Salazar et al injected human fetal derived NSCs at the SCI site 30 days after creating T9 compression injuries in mice (97). Mice demonstrated a significant improvement in locomotor function compared to the baseline pre-transplant assessment. There was evidence of successful cell engraftment in both grey and white matter. Interestingly, NSCs differentiated predominantly into oligodendrocytes (~40%) and neurons (~38%) at the injury site. This differs from previous work, which suggests astrocytic differentiation

within the spinal cord predominated (66). In 2014, Nemati demonstrated improved locomotor performance and sensation in primates after transplantation of adult monkey subventricular zone (SVZ)-derived NSCs. Animals were subjected to a weight drop over the spinal cord at T9-10. Significant and faster improvements were observed in the NSC-transplant group compared to the control in tail movement tests and sensation assessments (98). This demonstrates that NSC-transplant can improve locomotor function.

Another major outcome measure is axonal regrowth. Recently, Brock et al utilised a rat contusion model of SCI to investigate neural progenitor cell (NPC) transplantation. In this study, rats underwent a unilateral cervical (C6) contusion injury created by an impactor device. 14 days post-injury, embryonic (E14) derived spinal cord NPCs were injected into the site. Graft axons extended to form synapses with host axons (bouton-like structures were observed that co-localised with a pre-synaptic protein, synaptophysin). The glial scar was not removed at the time of NPC transplantation, and these findings demonstrate that graft axons can extend into host tissue despite the presence of the glial scar. Additionally, rats in the NPC-graft group out-performed the control and fibroblast-graft groups in forelimb performance assessments (99). Kumagai et al demonstrated axon growth when NSCs cultured as neurospheres were implanted into contusive SCI models. They also described an increase in angiogenesis and remyelination in the NSC transplant group (100).

In 2006, NSCs were used to treat two patients with SCI. Moviglia et al utilised a co-culture of transdifferentiated NSCs and autoimmune T-cells to promote regeneration at the site of injury. The delivery of the cell suspension was via selective catheterisation of feeder arteries to the lesion sites. This provided a more targeted delivery of cells compared to systemic intravenous delivery. Many safety measures were put in place. Both patients underwent an intensive neurorehabilitation programme post treatment. Ultimately, both patients made significant improvements in motor function including regaining the ability to perform some activities of daily living. Patient one

regained the ability to walk assisted. No adverse events were recorded. This study is very promising for the development of NSC therapy for SCI, however it is important to note that it is a study of two patients only and there was no comparison group (101).

In another small clinical trial of just one ASIA A patient, olfactory bulb derived OECs were transplanted into the site of a SCI. Tabakow et al used multiple microinjections to transplant autologous OECs into the site of a transection injury caused by a knife. The gap between the two spinal cord stumps was bridged with a sural nerve graft. 11 months after the operation and neurorehabilitation the patient had achieved ASIA C classification. The patient had regained lower limb sensation and had motor improvement (102). Although the results of this trial appear highly promising, it must be considered that this patient had a rare transecting lesion. This may not be transferable to the general SCI population.

Recently, a clinical trial involving four thoracic SCI patients was conducted to assess the safety of NSC transplantation. NSCs from an established cell line were injected into the site of SCI. Three out of the four patients showed neurological improvement at follow-up and there were no adverse events (103). Again, this represents a small scale clinical trial. Nonetheless, the potential success of utilising neural cell transplants for the treatment of SCI is evident in these studies but further research is required.

1.2.4 Barriers to clinical translation of stem cell therapies

While such data appears promising, many problems have been encountered and no single therapy appears to be successful. There are some general risks associated with cell transplantation. Firstly, the transplanted cells must provide benefit to the patient. There is a risk that the transplant population could fail and not provide any function. Secondly when implanting stem cells there is a risk of uncontrolled cellular proliferation leading to malignant transformation (104). With stem cells derived from an embryonic origin there is a risk of teratoma. 20% of rats injected with blastocyst

derived embryonic stem cells developed a teratoma in a study investigating stem cell therapy for Parkinson's disease (64). Furthermore, there is evidence to suggest that NSC implantation leads to glioma formation; this was reported in a single case report where the patient returned four years after repeated intrathecal human fetal NSC treatment with evidence of a non-host glioneuronal neoplasm (65).

Thirdly, whenever a therapeutic intervention includes transplantation of allogenic cells or tissue there is the issue of immune rejection (105,106). In organ transplantation, this is counteracted with the use of immunosuppressant therapy. This does not come without risk. In stem cell transplantation trials immunosuppression has been utilised and authors suggest that it should be used for a few months to a year following implantation (93,104). However, in the case of SCI the patient is likely to have complex health needs including an increased susceptibility to infection, meaning that immunosuppression may not be a favourable option.

There are more specific challenges facing stem cell transplantation. These are poor cell survival and cell migration. Cell survival is a major barrier to the success of neural cell transplantation. If cell survival is poor, then less cells persist at the target location to provide the desired beneficial function. Further, if cells die during transplantation, implanting dead cells into the injury site may encourage an immune response. As the prolonged inflammatory response at the site of SCI is a barrier to regeneration, implanting dead cells could cause further damage. It is also important to consider that if a high proportion of cells do not survive then it would be necessary to increase the number of cells transplanted to maintain levels of viable cells. This poses its own issues. Cells are a precious commodity, particularly when derived from embryonic sources or autologously derived. When considering clinical translation, pharmaceutical companies will need to scale up production of cells to make them commercially viable. High cell death on implantation will increase expense and may lead to a lack of support from the pharmaceutical industry. In general <3% of cells will be

engrafted during transplantation (107,108) - in fact Lepore found that no transplanted fetal neuroepithelial stem cells survived at three days (96).

There are many reasons for high stem cell death during transplantation. Most cells are injected into SCI sites via a needle. This process exerts mechanical forces on the transplant cells. The narrow gauge of the needle and ejection force is suggested to cause cell death and was demonstrated by Mahetab et al. In this study, cell viability was improved by protecting the fibroblasts in alginate hydrogels (109).

Pearse et al demonstrated low viability after transplantation of OECs and Schwann cells into SCI sites and suggested some theories as to why the cell survival was so low (110). Firstly, allograft rejection could explain the high cell death. If an immune response is mounted to the implantation of exogenous cells it would explain why Brock et al transplanted NPCs into inbred rats to intentionally avoid an immune rejection (99). Secondly, Pearse suggests that inadequate vascularisation of the injury site could create an inhospitable environment for cell survival. Lack of oxygen delivery and carbon dioxide removal which increases the pH could be responsible for cell death. To combat this, many studies pre-expose transplant cells to hypoxia and this improves outcomes (111). Furthermore, the presence of cytotoxic and oxidative free radicals at the lesion site due to the breakdown of cellular debris could impact cell survival. Finally, when cells previously cultured at optimal conditions are transplanted into the lesion site they are abruptly deprived of serum, growth factors and structural support. This change termed ‘environmental shock’ may lead to the lack of cell viability seen post transplantation (110).

For the success of the transplantation procedure, it is important that the majority of cells remain at the lesion site where they can differentiate and replace lost cells. In some cases, a proportion of the implanted NSCs will have migrated away from the site of injury (93,95). For instance, in one study which investigated the use of human NSCs in a mouse model of SCI, it was shown that the

NSCs had migrated throughout the full length of the spinal cord (97). This not only poses the issue that there are less cells at the site to provide the intended benefits, but there is the risk of off-target effects. If cells migrate to distant anatomical locations, they may act differently in the environment and potentially lead to malignant transformation. In addition, if cells are genetically engineered to produce specific biomolecules, then the secretion of those in unintended anatomical locations may lead to further detrimental effects.

1.3 Encapsulation in biomaterial scaffolds offers improved cellular outcomes

1.3.1 What are biomaterial scaffolds and why are they important?

To address the challenges that present when utilising cellular transplants, a lot of attention has been focused on biomaterial scaffolds that encapsulate cells and provide a construct for their growth and differentiation. Figure 1.3 indicates the major benefits of biomaterial scaffolds. At the site of a SCI there is often a degree of cavitation; a physical structure must be used to bridge that gap. This also allows guidance for the immature axons to follow, encouraging the rostral and caudal ends of the injury site to unite (112). It is also vital that the implanted cells remain at the site of the injury; an encapsulating structure may maintain them in situ.

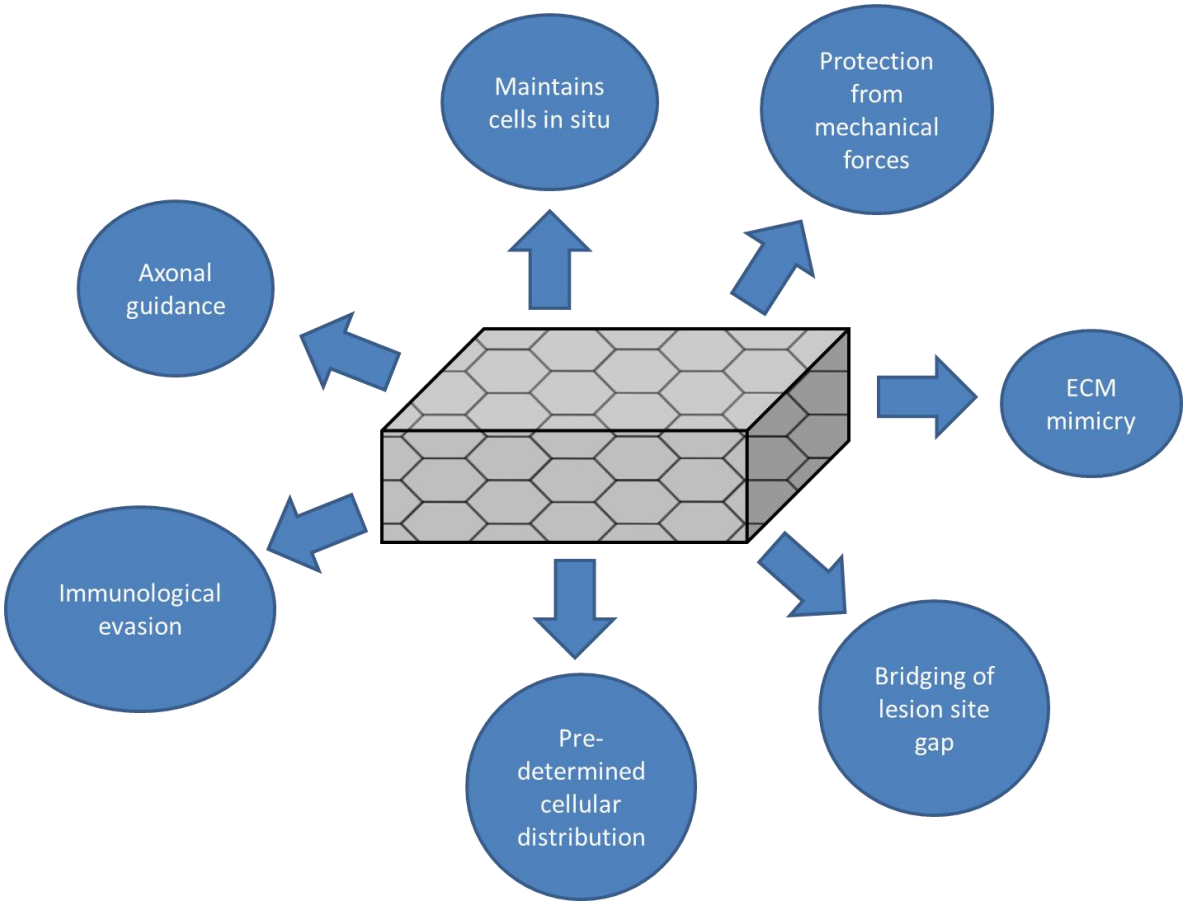

Figure 1.3*: Benefits of a biomaterial scaffold for cellular transplant into sites of neurological injury.*

1.3.2 The ideal properties of a biomaterial for cell transplant

There are multiple properties of biomaterials that are deemed desirable to create a cellular scaffold for delivery of transplant cell populations. Importantly, the material should be minimally immunogenic so as not to increase the inflammation at the site of SCI. It should also have mechanical strength but balanced against ability to conform to the site. The material would have to support the cells but also fit into the SCI site. The scaffold must be of such a design that nutrients can move freely within it to allow proliferation and maturation of the cells. Preferably, the scaffold would allow angiogenesis to occur within it, mimicking a natural restoration process and allowing delivery of nutrients, inflammatory cells, and cytokines. Moreover, the material must be degradable. After completing its task of transplanting the cells and supporting their initial growth it

must degrade to not hinder further growth. The cells must be able to either adhere to the material or be encapsulated within it. This would allow for safe and efficient transplantation. Additionally, transplantation of the material would ideally be simple, for instance an injection, to prevent inter operator discrepancies (113).

Origin	**Biomaterial**
Natural	Agarose
	Alginate
	Chitosan
	Collagen
	Fibrin
	Fibronectin
	Gellan gum
	Hyaluronic acid
	Protein mixture
Synthetic	Calcium sulfate cement
	Oligo[poly(ethylene glycol) fumarate]
	Poly(ethylene glycol)
	Poly-b-hydroxybutyrate
	Poly(2-hydroxyethylmethacrylate)
	Poly(D, L-lactic acid)
	Poly(lactide-co-glycolide)
	Poly(lactic-co-glycolic acid)

Table 1.2*: The variety of biomaterials used for stem cell transplantation studies in SCI. Adapted from* (105).

1.3.3 Current uses of biomaterials for cell transplantation

A plethora of materials have been explored in pre-clinical research including naturally existing substances and synthetic ones, network structures and gels. Table 1.2 demonstrates the variety of biomaterials utilised in animal studies. Many materials have been patented, demonstrating the growing interest.

There has been success *in vitro* with NSCs demonstrating cell survival, normal phenotypic expression and importantly differentiation into neurons in fibrin hydrogels (114), 3D gelatin-electrospun poly (lactide-co-glycolide)/polyethylene glycol (PEG) scaffolds (115) and poly(L-lactic acid) nanofibers (116). Functional improvement was reported with NSCs *in vivo* when cultured in a fibrin matrix (117,118), poly lactic-co-glycolic acid (PLGA) scaffold (119,120), gelfoam scaffold (121), porous collagen scaffold (122) and 3D gelatin-electrospun poly (lactide-co-glycolide)/PEG scaffolds (115). With other cell types functional improvement is also possible, for instance a Schwann cell transplant in Matrigel (123) or an OEC transplant in a PLGA scaffold (124). Even acellular biomaterials can provide functional improvement (125). Each material has favourable qualities, but none has emerged optimal thus far.

1.3.4 Problems encountered whilst utilising biomaterials for stem cell transplant

In the process of investigating various materials for the use in CNS pathologies some major factors have come to light regarding the design of such materials. Firstly, the clinical safety of the material is paramount. The majority of the biomaterials in table 1.2 are not Food and Drug Administration (FDA) approved for CNS applications. When researchers wish to pursue a material to the next phase of clinical trial many safety aspects must be addressed.

Many materials thus far have inhibited cell growth, and importantly neuronal growth, rather than promoting it. King et al investigated the use of fibronectin and fibrin as scaffolds for SCI therapy.

Fibronectin had few neurons growing within it at four weeks post transplantation and large cavities had developed between the material and the host spinal cord making it an inefficient graft material (126). Collagen scaffolds and gels have been found to promote glial scar formation or provide uneven axonal growth due to dense inclusions in the gel formulations (126). Alginate has many desirable properties in theory, however when used to support a variety of cells including OECs, Schwann cells and bone marrow derived stromal cells, it inhibited their growth and led to atypical, rounded phenotypes. In addition, when alginate was added to an embryonic dorsal root ganglion culture, neurite outgrowth was greatly reduced suggesting that this biomaterial would not support axon regeneration (127). Hyaluronan and methyl cellulose did not achieve a high level of cell survival at eight weeks post implantation (<0.05%) (108).

The material must be degradable as mentioned above. However, it must also be able to remain intact until the transplanted cells are fully integrated at the host site and no longer need the material for support. It is suggested that in the field of orthopaedic implantations a scaffold should last at least two weeks (128). A CNS implant, on the other hand is likely to require a slower degradation rate, likely to be required up to two to four months (128). Unfortunately, hyaluronic acid based hydrogels for example degrade rapidly and demonstrate up to 90% degradation after 14 days (129).

Many materials require a complex assembly procedure with multiple components and steps that are often time dependent (130). Cell survival is likely to be increased with fewer steps for assembly and hence less disturbance to the culture. For clinical translation, products will be more appealing if they are simpler. This will reduce the amount of inter-operator variance and will be more appealing to surgeons once the product becomes commercially available.

Finally, many studies describe significant *in vitro* success with the use of encapsulating biomaterials including improved cell survival and axonal growth. However, when tested *in vivo* they do not

provide any improvement in functional ability (108,131–133). It is vital for a successful transplant material that it is able to prove *in vivo* benefits in rodent models before moving to clinical trials.

1.3.5 Approved surgical grade materials to act as cell encapsulation devices

The FDA is widely considered the gold standard for the regulation of the development of medical drugs and devices (134). The average time for a device such as a biomaterial scaffold to go through FDA-approval is seven years (134). This process adds additional costs to the already mounting cost of developing a new medical device (135). The need for a biomaterial scaffold has been outlined above, however most biomaterials used in pre-clinical trials are not FDA-approved. Another group of biomaterials exist that are already FDA-approved and are used regularly in clinical practice (**table 1.3**). These are surgical materials used for various indications including haemostasis and duraplasty. **These pre-approved matrices could offer an existing regenerative solution for stem cell transplantation in SCI.** The following are examples of these materials, with more specific details on their properties and previous experimental experience with their use.

Biomaterial	**Manufacturer**	**Clinical indication**	**Components**	**Evidence of use for cell encapsulation**
DuraGen™	IntegraLife Sciences	Duraplasty	Type 1 bovine collagen	Yes
DuraSeal™	IntegraLife Sciences	Dural sealant	Amine solution and PEG - based solution	No
Tisseel™	Baxter	Haemostasis	Fibrin	Yes
Floseal™	Baxter	Haemostasis	Gelatin based	Yes
Surgicel™	Ethicon	Haemostasis	Oxidised regenerated cellulose	Yes

Table 1.3: *Details of surgical materials that have the potential to be utilised for NSC encapsulation.*

1.3.6 DuraGen™ (Integra LifeSciences) for duraplasty

DuraGen™ Plus matrix is a medically approved biomaterial made from type one bovine collagen. It is predominantly used for duraplasty, where it allows infiltration of fibroblasts and then after six to eight weeks is resorbed to leave endogenous dura mater (136). Other indications include acting as a separation layer between the dura and overlying tissues and to prevent peridural fibrosis in procedures where nerve roots are exposed (137). The collagen is obtained from bovine deep flexor tendon; this is known to be one of the purest sources of type one collagen available. It has no detectable infectivity for Bovine Spongiform Encephalopathy. This specific type of collagen is also used for artificial skin, absorbable haemostatic sponges, and absorbable wound dressings (138). Integra LifeSciences boast engineered porosity to provide the optimal environment for cell infiltration and conformability. Moreover, research demonstrates a 0% foreign body response and a 1.9% infection rate (no difference compared to controls). The FDA have approved DuraGen™ for use as a dural substitute and have confirmed its lack of immunogenicity, cytotoxicity and pyrogenicity. They also verify its conformability, sterility and biocompatibility (139).

1.3.6.1 Rationale for the use of DuraGen™

DuraGen™ is a popular biomaterial for use in a variety of different regenerative medicine research areas (**table 1.4**). It has been shown to provide a restorative environment in traumatic brain injury. Traumatic cortical brain injuries were induced in rats and following implantation of DuraGen™ the lesion volume, neuronal loss, and cortical dysfunction were decreased compared to the control (140). This suggests that DuraGen™ is the ideal material for producing a restorative environment for axonal regrowth.

The properties of DuraGen™ make it an ideal material for cellular engraftment. Firstly, DuraGen™ is composed of collagen which has been shown to facilitate growth of CNS cells (141). It has been shown to support cells when acting as a dural substitute, by allowing infiltration of fibroblasts and

allows angiogenesis to occur within the material (142). It is highly porous which would allow adequate distribution of cells and removal of debris, plus circulation of medium during *in vitro* trials. Degradation time has been highlighted as a problem for scaffolds, the ideal being two to four months (128). DuraGen™ when utilised as a dural substitute degrades over a period of two months (142). Most importantly DuraGen™ has been proven safe for a CNS indication- dural graft- and is therefore an appealing cellular scaffold option.

1.3.6.2 DuraGen™ for the delivery of cell transplant populations

DuraGen™ has become a popular choice for researchers testing different cell types at different anatomical locations and for differing pathologies (**table 1.4**). Although never the direct focus of the studies it has played the part of guide, mould, and cell delivery mechanism. In these studies, they do not compare to a group where the cells are delivered without the DuraGen™ implant so therefore it is difficult to delineate DuraGen™'s effect on cell survival in these studies. However, from their success, it would suggest that DuraGen™ is a suitable host for cellular growth.

Orthopaedic researchers have found DuraGen™ to be especially useful for delivery of mesenchymal stem cells (MSC) at the site of bone defects. In a study conducted by Gafni et al, DuraGen™ was loaded with human bone marrow derived MSCs and implanted at the site of a rodent calvarial defect, which was compared to an acellular DuraGen™ control (143). MSCs were detected within the lesion site at eight days. After four weeks and with the addition of bone morphogenetic protein-two delivered by the human parvovirus adeno-associated virus, they detected bone formation in the defect site radiographically and histologically. Similar results were found when Steinhardt et al implanted human MSCs loaded at $5x10^6$ cells/ mL in DuraGen™ into mandibular defects in mice after eight weeks (144). Again, the MSCs required bone morphogenetic protein- two for differentiation. Non-union radial fractures were tested in the same way with $2x10^6$ genetically engineered MSCs/mL loaded onto the DuraGen™. This yielded similarly promising results (145).

Other orthopaedic based research has found DuraGen™ to be a suitable scaffold for cellular growth. Kimelman-Bleich et al utilised acellular DuraGen™ at the site of a non-union radial fracture in rodents as a guide for host progenitor cells to infiltrate. After ten days, they described the HPCs as being 'abundant' on the DuraGen™ and subsequently with the aid of targeted gene therapy, at five weeks immature bone formation had occurred (146). DuraGen™ has also been used as a scaffold for culturing human meniscal fibrochondrocytes (147).

Murphy et al investigated a series of orthopaedic implants for their properties when seeded with human MSCs, one of these was DuraGen™. They concluded that this collagen sponge was unable to adequately retain cells and that hydration caused a significant decrease in pore size unable to sustain cell cultures (148). However, the experimental evidence shown here contradicts those findings and demonstrates high numbers of cells maintained within the material and able to regenerate tissues.

In renal research, DuraGen™ soaked in MSCs was utilised to encapsulate the kidneys of mice. The mice had rhabdomyolysis-induced acute kidney injury. Biochemical markers such as creatinine and blood urea nitrogen were significantly reduced by the addition of MSCs in DuraGen™. The intervention in question in this study was the addition of MSCs so there was no comparison of MSCs without the DuraGen™. Geng et al explains why they used DuraGen™ by saying it was used to prevent leakage of cells and increase cellular survival for longer periods (149).

DuraGen™ has also been used to deliver cells in human trials. A study of two cases was carried out by Gersey et al in which DuraGen™ implanted with autologous Schwann cells was placed at the site of two traumatic sciatic nerve injuries. In both cases, the patients regained motor function in the tibial distribution and the latter regained some sensation. In this study, DuraGen™ was used to transport the cells and to guide the regrowth of the sciatic nerve. Notably no tumour formation was recorded at 36 months follow up (150).

The previous studies involving DuraGen™ provided specific insights into how to utilise the DuraGen™ for *in vitro* cellular experiments. For instance, most studies that use DuraGen™ for a variety of cell types directly seed their cells at the desired concentration (144,145,151). However, Adesida et al utilised a step wise protocol to achieve cell attachment to the material. They initially seeded $1x10^6$cells suspended in 10µl onto the DuraGen™ matrix, allowed a total of 45 minutes and at two stages added more medium to produce a total volume of 1110µl (147).

The safety of DuraGen™ as a dural substitute has been investigated widely. However, one study specifically looked at DuraGen™'s effects on neurons with the intention of establishing its safety as a dural substitute. To evaluate DuraGen™'s effect on the CNS when used for duraplasty, Rabinowitz et al grew rat cortical neurons in DuraGen™. When compared to the poly-L-lysine control, there was no difference in the viability of the neurons at three and ten days. Moreover, there was no difference in the length of axons or dendrites either grown on glass or DuraGen™. DuraGen™'s effect on injured neurons was also investigated, after an excitotoxic injury was induced in the neurons. In this experiment DuraGen™ samples were added to the monolayer culture of neurons to establish if its presence exacerbated the injury. The presence of DuraGen™ did not exacerbate the glutamate-induced injury (152). This makes DuraGen™ a highly favourable biomaterial for use as a cell encapsulating device as its lack of neurotoxicity has been demonstrated.

Research area	Study design	Cell type	Indication	Outcome	Ref
Orthopaedic	*In vitro*	Human MSCs	Biocompatibility assessment	DuraGen™ unable to sustain cells	(148)
	In vivo	MSCs	Non-union fracture	Bone formation	(145)
	In vivo (rodent)	Human MSCs	Calvarial defect	Bone formation	(143)
	In vitro	Human meniscal fibrochondrocytes (MFC)	Meniscal cartilage repair	DuraGen™ supported MFCs in culture	(147)
	In vivo (rodent)	MSCs	Mandibular defect	Bone formation	(144)
	In vivo (rodent)	Acellular	Non-union fracture	Bone formation	(146)
	In vivo (rodent)	MSCs	Calvarial defect	Bone formation	(153)
	In vivo (human)	Acellular (loaded with bone morphogenetic protein)	Maxillary sinus floor augmentation	Bone formation	(154)
	In vitro	Human meniscal fibrochondrocytes (MFCs)	Meniscal cartilage repair	DuraGen™ supported MFCs in culture	(155)
	In vivo (rodent)	MSCs	Non-union radial bone defect	Bone formation	(156)
	In vivo (rodent)	MSCs	Tendon repair	Tendon regeneration	(151)
Renal	*In vivo* (rodent)	MSCs	Acute Kidney injury (AKI)	Reduced biochemical markers of AKI	(149)
Neurology	*In vivo* (Human)	Autologous Schwann cells	Sciatic nerve damage	Improved motor/sensory function	(150)
	In vivo (rodent)	Acellular	Traumatic brain injury	Reduced contusion volume, neuronal loss and cognitive deficit	(140)
	In vitro	Rat cortical neurons	Biocompatibility assessment	Compatible with neuron growth	(152)

***Table 1.4**: DuraGen™ has been used in a multitude of in vitro and in vivo trials to support a variety of transplantable cell types in a range of different medical specialities.*

To the best of our knowledge DuraGen™ has never been seeded with NSCs or been shown to allow their survival or differentiation. Although evidence exists demonstrating DuraGen™'s use in orthopaedic, renal, and PNS implants (**table 1.4**), it has never been considered as a CNS therapeutic option beyond its current indications.

1.3.7 DuraSeal™ (Integra LifeSciences) acts as a dural sealant

Other surgical materials also offer potential as cell encapsulation devices. DuraSeal™ is a hydrogel sealant used to prevent cerebrospinal fluid (CSF) leaks post operatively (157). It resembles hydrogel formulations used for stem cell delivery in pre-clinical trials. It is composed of a PEG ester solution and a trilysine amine solution which cross-link when mixed together at the point of administration (158). Many PEG-based hydrogels exist and have been utilised to encapsulate NSCs (159). PEG has been used as a therapy for SCI in pre-clinical trials; it has neuroprotective effects including repair of damaged cell membranes and reduction of the secondary injury (160–163). In addition, DuraSeal™ is compatible with the CNS with a low rate of adverse events (157).

DuraSeal™ is absorbed after nine to 12 weeks (158), in line with the ideal time of two to four months for degradation (128). DuraSeal™ is injected as a fluid so therefore can fill irregular cavities formed at the lesion site allowing it to be mouldable. It should be noted that in several case studies DuraSeal™ expanded within the spinal column and caused spinal cord compression or cauda equina syndrome (164,165). To utilise an expandable material in the confined space of the spinal column with its hydrophilic properties may prove more damaging than beneficial. This swelling would need to be taken in to account when designing a therapy.

1.3.7.1 DuraSeal™ demonstrates benefits in the PNS

Unlike DuraGen™, no reports exist describing the use of DuraSeal™ to encapsulate transplant cell populations. It has however, been used in a pro-regenerative capacity for peripheral nerve injury.

In these cases, DuraSeal™ permitted the regeneration of a peripheral nerve across two cut sections. Lin et al repaired five-millimetre gaps in rat sciatic nerves with DuraSeal™. Within the DuraSeal™ group restoration of motor and electrophysiological function was demonstrated and there was an increase in the regeneration compared to tissue glue. Regeneration was defined as achievement of continuity in the nerve and remyelination. Moreover, DuraSeal™ did not demonstrate any neurotoxic effects evidenced by a decreased amount of Schwann cell apoptosis at the injury site compared to other groups (166). Isaacs et al also utilised DuraSeal™ to repair transected sciatic nerves in rats. The findings demonstrated nerve regeneration equivalent to that of the suture-only control, but more promisingly a decrease in scar formation (167). These findings suggest that DuraSeal™ can facilitate regeneration and in some circumstances enhance it. From the literature, there is no evidence of transplant populations being grown within the gel. This may be an ideal injectable material for cellular transplantation.

1.3.8 Fibrin glue for haemostasis

There are multiple types of fibrin glue available, they are designed for assisting haemostasis in surgical procedures. Examples include Tisseel™ (Baxter), Evicel™ (Ethicon), Vitagel™ (Stryker), Cryoseal™ (Thermogenesis) and Vivostat™ (Vivostat). Tisseel™ for instance, much like DuraSeal™, begins as two separate components: fibrinogen and thrombin, which when combined mimic the clotting cascade to form a fibrin mesh. This fibrin mesh has been suggested to be an ideal cellular scaffold (168). There are multiple reports of survival of cell populations within fibrin glue. For instance, in cardiology research, adipose derived stem cells were combined with fibrin glue and injected into the left ventricular wall of rats after myocardial infarction, this produced an improvement in cardiac function across all parameters measured indicating muscle regeneration (169). MSCs were loaded in fibrin glue for the treatment of rotator cuff injuries (170). Fibrin glue has also supported stem cells in a rat model of cerebral ischaemia providing functional

improvement (171). Vivostat™, a fibrin glue made from the patient's own blood is licenced for neurosurgical use and sprayed into the site (172), this could prove a non-immunogenic option. It has demonstrated the ability to support keratinocytes for dermal regeneration and this combination was sprayed onto the site (173). Spray application would be highly beneficial in the complex space of a SCI. Fibrin glues demonstrate the ability to encapsulate cells and transport them to the target so hence may be a favourable option in SCI.

1.3.9 Floseal™ (Baxter) for haemostasis

Floseal™ created by Baxter, is a gelatin based haemostatic agent utilised in surgical procedures. It has many desirable properties of a cellular scaffold. It has successfully been used to transport MSCs into rat sciatic nerve injuries (174). Moreover, when tested as a haemostatic agent in peripheral nerve repair they reported it led to a faster motor function recovery (175). This suggests that Floseal™ may be a supportive environment for cellular transplant and endogenous neuron growth.

1.3.10 Surgicel™ (Ethicon) for haemostasis

Ethicon's Surgicel™ is also a haemostatic agent. The matrix is made from oxidised regenerated cellulose. This biomaterial offers the specific advantage compared to the other materials of being used within the brain in close association with the brain parenchyma. It is used to line cerebral cavities after intracerebral tumour removal. This demonstrates its robust safety when used in the CNS. In addition, it has previously been used for controlled drug release. In this study, Surgicel™ was coated with PLGA containing the drug and an evaporating solvent used to release the drug (176). This demonstrates its potential as a carrier substrate. Furthermore, when Surgicel™ was used at the site of canine iliac crest defects, as an acellular implant, radiographic and histological evidence of bone formation was found (177). Most importantly, Surgicel™ has been previously used to support MSC transplant into the site of sciatic nerve injuries. Pan et al implanted MSCs

within Surgicel™ into 5mm sciatic nerve defects in rats. Axon length increased in this group compared to the control (178). This evidence of PNS cellular implantation suggests the potential of Surgicel™ as a cell encapsulation device for CNS pathology.

1.4 Genetic engineering of cell transplant populations

1.4.1 The need for augmented cell therapies for SCI

When considering the complex nature of the events that occur after SCI it is helpful to consider the process of CNS development. At this time, many processes occur simultaneously, orchestrated by cell signalling pathways particularly associated with the timely expression of proteins such as BDNF. It is suggested that recreating appropriate protein expression at the site of SCI, may encourage axonal growth, myelination and cellular organisation (179–187). One way to do this is to genetically engineer transplanted cells to express specific beneficial proteins. Genetic engineering offers the potential to control the complex micro-environment of SCI. This site-specific release of proteins avoids any undesirable systemic effects. Overexpression of proteins at the site of injury can improve endogenous regeneration and improve the survival of transplanted populations (188).

1.4.2 Potential biomolecules that are beneficial for SCI regeneration

There are multiple different proteins to choose from, each providing a distinct set of therapeutic targets (**table 1.5**). Most commonly research has focused on the increased expression of trophic factors, but the techniques can also be used to express enzymes that can degrade inhibitory factors such as CSPGs. Carwardine et al effectively engineered OECs to express chondroitinase ABC (ChABC), using a lentiviral vector (189).

BDNF and NT3 are popular choices for therapeutic molecule expression for SCI. These neurotrophic factors promote neuronal survival and axonal regeneration. When used in combination by Zhao et

al, they produced synergistic effects. In this study, MSCs were transfected using lipofectamine to express BDNF and NT3. After transplantation into a SCI transection model, axonal sprouting was observed and hindlimb function improved (190). Glial cell line derived neurotrophic factor (GDNF) has also demonstrated benefits in animal models of SCI. This factor improves neuronal survival and promotes axonal regeneration similar to BDNF and NT3. It has added benefits of encouraging remyelination and synapse formation too. Deng et al used lentiviral vector transfection to engineer Schwann cells to express GDNF. When GDNF expressing Schwann cells were transplanted into a rat hemisection model regeneration was achieved. Parameters of regeneration included axon lengthening, synapse formation, new myelin production and improved hindlimb function (191).

Stromal-derived factor 1 is a chemokine which has been used for its regeneration promoting properties. It provides guidance for axonal growth and due to the presence of a stromal-derived factor receptor on most CNS cell types, it is thought to promote cell survival. Stewart et al engineered MSCs to express stromal-derived factor-1, these cells were implanted into a contusion model of SCI. The results were promising, demonstrating decreased cavitation and an increase in axonal numbers (179).

Study design	**Transplant population**	**Protein being over-expressed**	**Therapeutic goal**	**Gene vector**	**Outcome**	**Ref**
In vitro	OECs	BDNF	Axonal growth, neuronal plasticity	Magnetic nanoparticles (MNP) and minicircle deoxyribonucleic acid (DNA)	Safe and efficient transfection	(192)
In vitro	OECs	ChABC	Digestion of inhibitory CPSGs	Lentivirus	Safe and efficient genetically engineered population	(189)

In vitro	MSCs	BDNF and GDNF	Synaptic plasticity and repair(BDNF), neuronal survival promotion (GDNF)	Lentivirus	Safe and efficient genetically engineered population	(193)
In vitro	Dorsal root ganglion neurons	Silencing of non-muscle myosin II	Axon growth by targeting growth cone	Electroporation	Axon growth	(194)
In vitro	NSCs	BDNF	Increase in neuronal numbers and maturation, plus neuro-protection	MNP and minicircle DNA	Safe and efficient genetically engineered population	(195)
In vitro	Schwann cells	FGF-2	Nerve regeneration across long gaps	Electroporation	Safe and efficient genetically engineered population	(196)
In vivo rat contu-sion SCI model	MSC and NSC	Stromal derived factor-1	Axonal growth	Retrovirus	Improved Basso, Beattie, Bresnahan score, tumour formation	(180)
In vivo rat contu-sion SCI model	MSC	Stromal derived factor-1	Axonal growth	Retrovirus	Decreased cavitation, increased axon numbers	(179)
In vivo rat comp-lete transect ion SCI model	MSC	NT3 or BDNF	Neuronal survival and axon regeneration	Lipofectamine	Axonal sprouting and improved hind limb function	(190)
In vivo rat tran-section of	Schwann cells	NT3	Neuronal development,	Lipofectamine or PAMAM dendrimer	Axonal regeneration	(182)

sciatic nerve			survival and regeneration			
In vivo mouse comp-ression SCI model	Schwann cells	Cell adhesion molecule L1	Remyelination	Retrovirus	Faster locomotor recovery, axonal sprouting	(183)
In vivo rat hemi-section SCI model	Schwann cells	GDNF	Neuronal survival and axon regeneration	Lentivirus	Axon regeneration, synapse formation, myelin production, improved hindlimb function	(191)
In vivo rat hemi-section SCI model	NSCs	NT3	Neuronal development, survival and regeneration	Lentivirus	Improved Basso, Beattie, Bresnahan score	(184)
In vivo rat ventral horn comp-ression SCI model	Fetal NPCs	HB9, Nkx6.1, Neurogenin 2	HB9 – Motor neuron specification, axon extension Nkx6.1 – Ventral spinal cord patterning	Lentivirus	Motor neuron differentiation, axonal growth initiation	(185)
In vivo rat uni-lateral tran-section SCI model	OECs	NT3	Neuroprotecti on and neurite outgrowth	Adenovirus	Tissue sparing, corticospinal tract sprouting, no functional change	(186)
In vivo rat hemi-section	OECs	NT3 and BDNF	Neuroprotecti on and neurite outgrowth	Adenovirus	Decreased lesion volume, axonal sprouting,	(187)

SCI model					functional improvement	

Table 1.5: *Successful outcomes of genetic engineering of cell transplant populations for therapeutic use in SCI.*

1.4.3 Barriers to clinical translation of genetically engineered cell transplant populations

Genetic engineering offers major benefits for the treatment of SCI; however, many issues present themselves when considering translation to clinical practice. The issue of safety surrounding genetic engineering is of paramount importance. Genetic engineering poses the risk of insertional mutagenesis, particularly when using retroviral vectors, which can lead to oncogene expression and tumour formation (188,197).

Many ethical issues surround the use of genetic engineering techniques. The long-term consequences of genetic engineering on individual's health and the environment remain unknown. The use of viral vectors to deliver the DNA presents the risk of viral DNA changes leading to new strains of potentially deadly infections. In addition, the use of bacteria to produce the DNA poses the risk of bacterial resistance (198).

From a practical perspective, many factors in the research and production of genetically engineered therapies pose barriers to clinical translation. There are an increased number of regulatory challenges involved when utilising genetic engineering technologies. These can slow development of therapies. Abou-El-Enein et al describe the challenges to the clinical translation of their human immunodeficiency virus (HIV)-therapy which involves the use of genetically engineered haematopoietic stem cells. They discuss the prominent level of regulatory challenges and the expense associated. In addition, they also highlight the lack of validated safety and quality assessments. These factors have inhibited the advancement of this therapy to the clinic (199). Clinical scale-up of genetic engineering presents issues. The use of some vectors can only engineer

a small number of cells at a time. Advancement in the field of genetic engineering is required for clinical translation of such therapies.

1.4.4 Combining genetic engineered cell transplant populations with biomaterial scaffolds

Constructs combining genetically engineered cells and biomaterial scaffolds have been designed and utilised for regenerative indications before (**table 1.6**). Hwang et al utilised retroviral vectors to engineer a line of NT3-overexpressing NSCs. This cell population was loaded into poly-ε-caprolactone scaffolds and implanted into rat SCIs. The use of this advanced construct increased behavioural scores and induced increased motor evoked potentials after transcranial stimulation when compared to the control, the scaffold alone and the scaffold with NSCs. Interestingly, the addition of ChABC increased behavioural and electrophysiological outcomes further implying that combinatorial therapies are the most effective for SCI (200).

The function of NT3 can be enhanced by the additional expression of its receptor, tyrosine kinase neurotrophin receptor (Trk). Du et al transfected two populations of NSCs to express either NT3 or TrkC. When both populations were co-cultured in parallel channels of poly(lactic-co-glycolic acid) and transplanted into rat SCIs maximal regeneration was detected compared to one cell type in the scaffold or the scaffold alone. Regenerative parameters included decrease in cystic cavity size, increased neuronal survival, evidence of myelination and improved locomotor scores (120). Similar regenerative outcomes were established with NT3/Trk-expressing NSCs transplanted within a gelatine sponge scaffold (201).

Deng at al used a combination of Schwann cells engineered to express GDNF encased in a poly-acrylonitrile/ poly-vinylchloride scaffold to promote regeneration in a hemisection model of SCI. GDNF encouraged astrocyte migration into the graft allowing Schwann cells and astrocytes to co-exist. The expression of GDNF improved the lesion environment for regeneration by reducing astrocyte reactivity and decreasing CSPG expression. This led to axonal regeneration and

remyelination (202). Gao et al constructed an agarose scaffold supporting BDNF-expressing MSCs. When transplanted into a SCI there was an increase in linear axonal growth into the lesion site. The study did not report functional analysis (203). The aforementioned studies corroborate that multi-faceted combinatorial therapies for SCI are the most effective. Furthermore, it provides an evidence base for the concept of a biomaterial scaffold protectively encapsulating genetically engineered cells for therapeutic transplantation in SCI.

Scaffold	**Cell population**	**Therapeutic molecule**	**SCI model**	**Outcome**	**Ref**
poly-ε-caprolactone	NSC	NT3 ChABC	Hemisection	Improved behavioural and electrophysiological measures	(200)
poly(lactic-co-glycolic acid) (parallel channels)	NSC	NT3 TrkC	Transection	Improved behavioural scores, electro-physiological measures and neuronal survival with myelination	(120)
Gelatine sponge	NSC	NT3 TrkC	Transection	Improved behavioural scores, electro-physiological measures and neuronal survival with myelination	(201)
Poly-acrylonitrile/ poly-vinylchloride (parallel channels)	SC	GDNF	Hemisection	Astrocyte migration, decreased reactivity and decreased CSPG expression	(202)
Agarose	MSC	BDNF	Transection	Axonal growth	(203)

Table 1.6*: Examples of constructs combining genetically engineered cells with a biomaterial scaffold for SCI. Adapted from* (204)*.*

1.4.5 Commonly used viral vectors present disadvantages

There are several different methods of achieving a genetically engineered population of cells (**table 1.7**). The most common method is the utilisation of viral vectors. The virus integrates its DNA into the host's genome which is then expressed by the host. The daughter cells of transfected cells also contain the integrated DNA, facilitating continued transgene expression (205). Examples of viral vectors include adenovirus, lentivirus and many retroviruses. Although highly efficient at transfecting high proportions of cells and relatively easy to use, they are immunogenic and can cause host cell death (206). Viral vectors have been used for their ability to produce stable gene expression over the life span of the cell. However this is not always beneficial, and prolonged release of some factors may lead to tumourgenicity so a timed decrease in expression of product can be highly useful particularly in the complex SCI pathology (180). Stewart et al utilised a retroviral vector to engineer MSCs and NSCs to express the beneficial protein stromal derived factor-1. The benefits included improved locomotor scores but at the cost of tumour formation. The tumours were thought to be NSC in origin (180).

1.4.6 Non-viral vector alternatives

The newer generation of transfection vectors appear much more favourable (**table 1.7**). Options include chemical and physical methods. Chemical methods such as lipid-based transfection relies on the negatively charged phosphate group of DNA forming a complex with the positively charged lipid. The overall positive charge of the complex is attracted to the negatively charged cell membrane where it passes through the cell membrane. The methods by which the complex does this and reaches the nucleus are unknown (205). It has high success rates and is relatively inexpensive but can be cell-type dependent (205). Other chemical options include calcium phosphate, this method works on the same principles as lipid-based transfection but its efficiency can be affected by the medium's components (207).

Physical vectors include direct injection which is a simple principle but labour-intensive, plus electroporation and laser-transfection techniques which are easy but can be very costly to set up initially (208). The mechanism of electroporation is not known but it is thought that short electrical pulses disrupt the cell membranes, allowing DNA to pass through (209). Laser-transfection uses a laser to form a pore in the cell membrane temporarily, to allow DNA in (210).

Transfection techniques	Pros	Cons
Viral		
Adenovirus/ lentivirus/ retrovirus etc	High efficiency Easy to use (206)	Difficult scale-up Sustained release (tumourgenicity) Immunogenic Cytotoxicity DNA cargo size limit Potential hazard to laboratory personnel (206)
Non-viral		
Calcium phosphate	High efficiency Low cytotoxicity (207)	Affected by medium components Cell-type dependent (207)
Direct injection	Straightforward	Need special instruments Cell death Labour-intensive
Electroporation	Easy to use No need for a vector (208)	Expensive (208)
Laser-irradiation	Easy to use (210)	Expensive (210)
Lipid-based/ lipofection	Easy to use No DNA cargo size limit High success rate Inexpensive Low cytotoxicity (205)	Cell-type dependent (205)
Magnetofection	Easy to use Low cytotoxicity High dose-response profile (211)	

Table 1.7*: The pros and cons of the major methods of transfection, split into viral and non-viral methods. Adapted from* (205)*.*

1.4.7 Magnetofection offers clinically translatable benefits as a non-viral alternative for genetic engineering

Magnetofection, utilising MNPs in a magnetic field, has proven successful. Initially a complex is formed between the DNA and nanoparticle. This is then placed in a magnetic field with the cells where the complexes can be taken up by endocytosis (**figure 1.4**). Pickard et al demonstrated an efficient method of magnetofection utilising iron oxide nanoparticles that formed complexes with DNA plasmids which effectively transfected NSCs- known to be difficult to engineer (212). Magnetofection is easy to use and offers rapid transfection compared to other vectors. Moreover, it has an increased dose-response profile meaning that less DNA is required for high transfection levels (213) and large quantities of cells can be transfected at once. These factors are particularly important when considering clinical scale-up. For targeting specific host tissues *in vivo*, magnetic fields can be externally applied to the host tissue target to attract nanoparticle-DNA complexes (214).

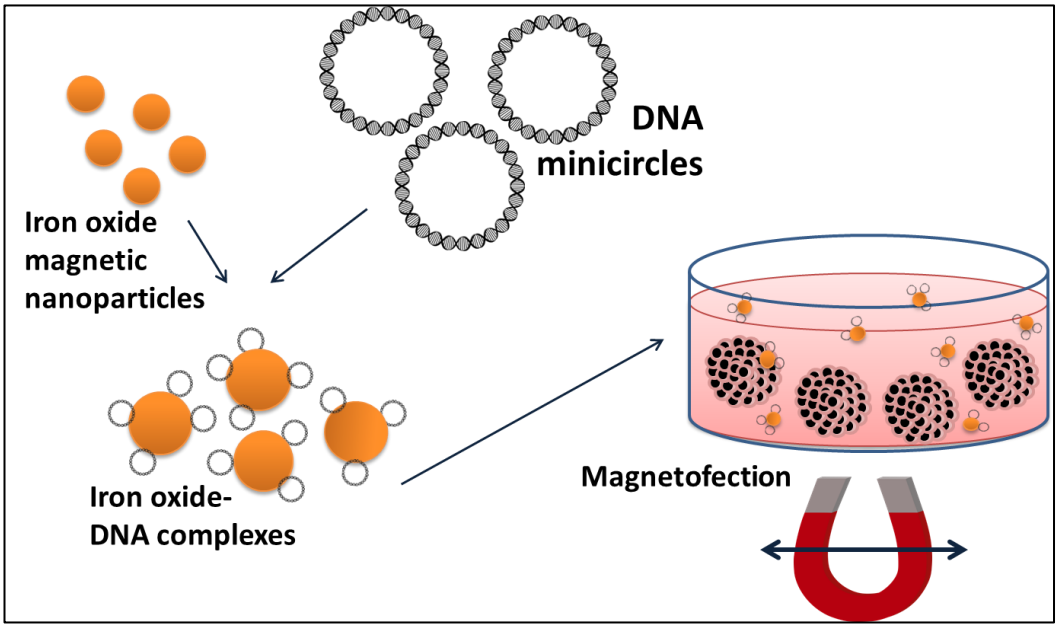

***Figure 1.4**: Process of magnetofection – Iron oxide nanoparticle- DNA complexes taken up into NSCs on an oscillating magnetic field.*

1.4.8 DNA minicircles provide significant benefits over DNA plasmids for genetic engineering

DNA minicircles are small circular DNA sequences that, unlike DNA plasmids, do not have a bacterial backbone. Minicircles contain primarily the promoter, transgene and polyadenylation signal. This has major advantages due to the decrease in size of the DNA. It is known that a larger DNA cargo is associated with a decrease in nanoparticle mediated transfection efficiency (215). Without the excess DNA, the immune response to the process is decreased and the gene expression is sustained due to decreased silencing (216). Moreover, the bacterial backbone contains the antibiotic resistance gene, required for isolation of the plasmid in culture; the absence of this is very reassuring when considering clinical application. Minicircles are easy to produce and store, and require relatively small amounts of DNA for high transfection yield (217). This makes clinical scale up highly possible which is a problem for many transfection techniques particularly viral vectors (206). Fernandes and Chari utilised DNA minicircles to transfect populations of NSCs with BDNF successfully (195,217).

1.4.10 A genetic engineered NSC population encapsulated in DuraGen™

DuraGen™ has demonstrated properties of a suitable biomaterial scaffold for the encapsulation of NSCs for transplantation in SCI. In line with the studies in table 1.4, DuraGen™ holds the potential to provide a pre-approved scaffold to support genetically engineered NSCs creating a combinatorial therapy offering a multitude of benefits. However, unlike the materials utilised in table 1.6, DuraGen™ is approved for human use and is used regularly in the CNS (137). The NSCs would provide cell replacement and attenuation of the growth inhibitory environment (61,128). Additional benefit would be provided by the therapeutic molecule or combination of molecules expressed by the engineered NSCs. The majority of transfection for the cell populations in table 1.5 utilised viral vectors, this construct would use a non-viral transfection method, magnetofection, and minicircle technology in its production adding further clinical translation benefits. To the best

of our knowledge DuraGen™ has never been utilised as an encapsulation matrix for NSCs which have been genetically engineered utilising a non-viral transfection method.

1.5 Conclusion

It is clear that the next step for SCI treatment will be a regenerative therapy. There has been a wide variety of cell types and biomaterials used with none standing out as the ideal transplant therapy. Many problems have presented throughout leading to no revolutionary clinical trial outcomes. Surgical materials offer an exciting opportunity for the field of regenerative neuroscience. **To the best of our knowledge, DuraGen™ has never been tested as a scaffold for NSC growth.** Genetically engineered cell populations provide useful functions to control a complex pathological environment. **The combination of both the structural support of the DuraGen™ matrix and a genetically engineered clinical transplant population of NSCs appears never to have been tested before.** If this construct is successful, it could produce a microenvironment conducive to neural growth and the consequences would be far reaching for the regenerative medicine field.

Chapter 2: Methods

2.1 Materials

Primary rodent NSC culture: All culture grade plastics were from Thermo Fisher Scientific (UK). Media components included Dulbecco's Modified Eagle Medium (DMEM), Ham's F12 Medium (F12), B27 Supplement, Penicillin-streptomycin solution, N2 supplement all from Thermo Fisher Scientific plus, heparin from Sigma Aldrich (Dorset, UK). Human recombinant Epidermal Growth Factor (EGF) was from R&D Systems (Minnesota, USA), Human recombinant basic Fibroblast Growth Factor (FGF) was from Peprotech (London, UK). Fetal bovine serum was from Biosera (Nuiallé, France). Other culture reagents included DNAse, accutase, trypan blue, poly-ornithine and laminin from Sigma Aldrich, and TrypLE™ Express enzyme which was from Thermo Fisher Scientific.

Surgical materials: DuraGen™ and DuraSeal™ were from Integra LifeSciences (New Jersey, USA).

Characterisation of NSCs in DuraGen™: The McIlwain tissue chopper was from The Mickle laboratory engineering co. Ltd (Guilford, UK). Calcein was from VWR (Pennsylvania, USA), Ethidium homodimer-1 was from Invitrogen, Hoechst was from Thermo Fisher Scientific, UK, and Click-iT EDU Imaging Kit was from Invitrogen (California, USA). Bovine serum albumin (BSA) and paraformaldehyde (PFA) were from Thermo Fisher Scientific, normal donkey serum (NDS) was from Stratech Scientific (Suffolk, UK), and Triton X-100 was from Sigma Aldrich.

Antibodies for immunocytochemistry (ICC): Primary antibodies were nestin from BD Biosciences (Oxford, UK), anti-sox-2 from Millipore (Massachusetts, USA), purified anti-neuron-specific class III beta-tubulin (TUJ1) from Biolegend (California, USA); anti-Glial Fibrillary Acidic Protein (GFAP) from Thermo Fisher Scientific; anti-Myelin Basic Protein (MBP) from BioRad (California, USA).

Secondary antibodies were Fluorescein isothiocyanate (FITC)-conjugated donkey anti-mouse, -rabbit and -rat, cyanine 3 (CY3) donkey anti-mouse, -rabbit and -rat, and AMCA donkey anti-rabbit which were all from Stratech Scientific. Vectashield mounting medium with 4', 6-diamidino-2-

phenylindole (DAPI) and Vectashield mounting medium for fluorescence were from Vector Laboratories Inc. (Peterborough, UK).

Minicircle plasmids containing GFP (mcGFP) production: pMC.EF1-MCS-IRES-GFP-SV40PolyA, GelRed, MC-Easy™ Growth Medium and MC-Easy™ Induction Medium were from Cambridge Biosciences (Cambridge, UK). MC-Easy™ Minicircle DNA Production kit was from System Biosciences (California, USA). QIAprep miniprep kit and QIA maxiprep kit were from Qiagen (Manchester, UK). LB Agar and LB broth were from Thermo Fisher Scientific. Kanamycin was from Sigma Aldrich. EcoRI was from Promega (Wisconsin, USA). Agarose was from Appleton Woods (Birmingham, UK). TAE buffer was made in house by Dr Sarah Harris.

Transfection of NSCs and development of NSC-DuraGen™ construct: NeuroMag transfection reagent was from Oz Biosciences (Marseilles, France). Magnefect-nano 24-magnet array system was from NanoTherics (Stoke-on-Trent, UK). Fisherbrand pH indicator paper sticks and TurboGFP Polyclonal Antibody were from Thermo Fisher Scientific.

2.2 Primary rodent NSC culture

All experiments were conducted in accordance with the Animals (Scientific Procedures) Act of 1986 and approved by the local ethics committee.

2.2.1 NSC culture

NSCs were derived and maintained as previously described (212). For this, eight to ten CD1 mouse pups per litter at postnatal day one to three were anaesthetised with 0.04 mL pentabarbitone via intraperitoneal injection. Each brain was dissected by sagittal cuts in the skin and skull, and then placed in PBS on ice. The SVZ of each brain was then dissected under microscopic guidance to identify the structures (**figure 2.1**). The SVZs were then dissociated using DNAse, centrifuged and resuspended in neurosphere medium composed of DMEM: Ham's F12 (3:1), 4 ng/mL Heparin, 2%

B27, 20 ng/mL Epidermal Growth Factor (EGF), 20 ng/mL basic Fibroblast Growth Factor (FGF), 50 U/mL penicillin and 50 U/mL streptomycin at 37°C. After being passed through a 40 µm cell sieve the cell density was calculated using a haemocytometer, and then plated at a density of $1x10^5$ cells/mL into T25 flasks containing 5 mL of neurosphere medium. Cultures were maintained at 37°C in 5% CO_2/ 95% humidified air. The culture was then passaged after the cells reached confluence (six to ten days) and used up to passage three. Every two to three days 50% of the medium was replaced with fresh neurosphere medium. To prevent the cells adhering to the surface of the flask, a sharp tapping force was applied each day.

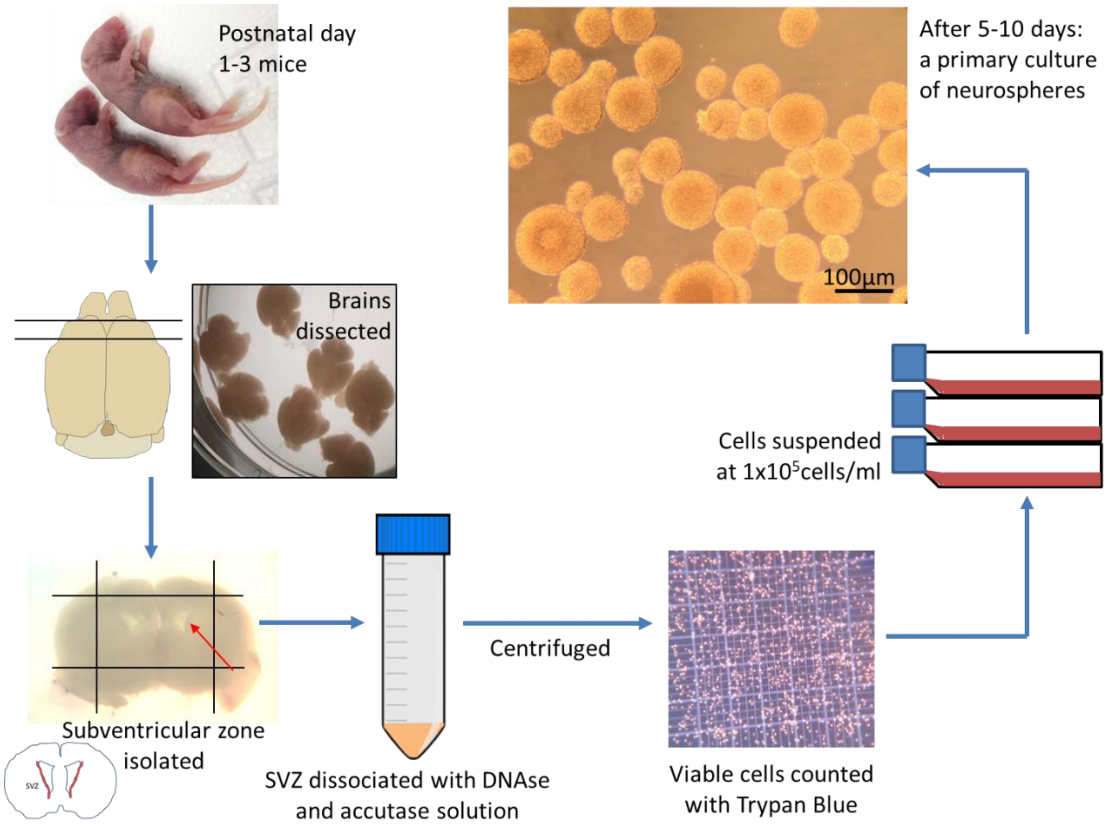

Figure 2.1: *Schematic representation of the process of producing a primary culture of NSCs.*

2.2.2 Subculture of NSCs

The culture was passaged when it reached confluence between six and ten days. Neurospheres were pooled into a 50 mL Falcon tube and centrifuged (all centrifugation steps were performed at 1000 revolutions per minute (rpm) for five minutes). The cell pellet was then washed using phosphate buffered saline (PBS) and centrifuged again before addition of accutase and DNAse at a ratio of 9:1 and incubation at 37^{o}C for five to ten minutes. Dissociation was confirmed under the microscope and media added to inactivate the accutase and DNAse. The suspension was centrifuged once more, resuspended in media and passed through a 40µm cell strainer producing the final cell suspension. Cells were plated into T25 flasks at a density of 0.2x10^{5} cells/mL.

Occasionally, the cells adhered to the surface of the flask. Therefore prior to passage, the cells required trypsinisation to detach them from the surface. Firstly, the medium was collected into a fresh tube. 5 mL Tryple was added to each flask and observed under the microscope after 20 seconds, more time was allowed if not visibly detaching. Detached cells were then added to the tube of medium and passage completed as described above.

2.2.3 Monolayer NSC culture set up

NSCs can be cultured as neurospheres as described above or as single cell layers known as monolayers. To achieve a monolayer culture, coverslips first had to be prepared for NSC growth. For this, coverslips were shaken overnight with 1% nitric acid on an orbital shaker. Following this, the coverslips were shaken in deionised water for 60 minutes with water changes every ten minutes. Coverslips were then shaken three times in 70% ethanol for ten minutes each and then sonicated in 70% then 95% ethanol for 15 minutes each. Washed coverslips could then be stored in 70% ethanol until use. For coating, each coverslip was placed in a well of a 24-well plate and washed with 70% ethanol for ten minutes. A 20% poly-Ornithine in deionised water solution was incubated on the coverslips for one hour. After aspiration of the solution, a 0.5% laminin in deionised water

solution was incubated on the coverslips for a further hour. Coverslips were then washed three times with deionised water before use.

Dissociated NSCs were then seeded onto coverslips at a density of $1.5x10^5$ cells/ mL in 600µl per well. Cells were grown in monolayer media composed of 1:1 DMEM: F12, N2 supplement, 40 µg/mL EGF, 40 Mg/mL basic FGF, 5 µg/mL heparin, 50 U/mL penicillin and 50 U/mL streptomycin at 37^{o}C. 50% of monolayer media was replaced every two to three days and to differentiate NSCs all monolayer media was removed and replaced with differentiation media. Differentiation medium was composed of DMEM: F12 (3:1), 2% B27 Supplement, 40 ng/mL Heparin, 50 U/mL Penicillin, 50 U/mL Streptomycin and 1% fetal bovine serum.

2.3 Initial trial studies of surgical materials

2.3.1 Investigation of the porosity of surgical materials

(1) **DuraSeal™**: To test the ability of DuraSeal™ to allow permeation of medium, a pilot test was carried out utilising food colouring dye. The product DuraSeal™ came as two components which required mixing together within the device before use. For the pilot experiment, the two components were injected into a bijou tube utilising the syringe like device. Food colouring dye was then added to the tube and observed over the next 24 hours.

(2) **DuraGen™**: To test the ability of DuraGen™ to allow permeation of medium, DMEM was added to a cut sample and observed. The DuraGen™ product was supplied as a dry square piece of material. Using a sterile scalpel, a 5mm by 5mm piece was cut. Within a petri dish, DMEM was added in a dropwise fashion. The material was then observed immediately under light microscopy.

2.3.2 Trial seeding of NSCs into DuraGen™

NSCs were seeded into samples of DuraGen™ under sterile conditions. Observations were made under a Zeiss light microscope immediately. Later, the pilot samples of DuraGen™ were investigated using the following initial assays: live-dead at 24 hours, nestin staining at 48 hours, differentiation profile at eight days (details given for each in section 1.4).

2.3.3 Scanning electron microscopy (SEM) of DuraGen™ and DuraSeal™ to assess pore size

SEM samples were prepared in the Keele EM Unit. Samples of each material were prepared using the osmium tetroxide (OsO_4) and thiocarbohydrazide multiple step protocol known as OTOTO. OTOTO is carried out as follows. Samples of each material were provided in their original state and in PBS. The dry DuraGen™ sample did not survive SEM processing. Samples were first fixed in 2.5% glutaraldehyde diluted in 0.1M Sodium Cacodylate buffer with 2mM calcium chloride for two hours. All washes were carried out in Sodium Cacodylate buffer. After the first wash, samples were incubated with 1% OsO_4 for one hour then washed again. A series of four incubations followed this: (1) thiocarbohydrazide for 20 minutes then (2) OsO_4 for two hours, (3) thiocarbohydrazide for 20 minutes, and (4) OsO_4 for two hours. Samples were then dehydrated in a series of ethanol solutions of increasing concentration. Critical point drying was carried out using liquid carbon dioxide. Samples were then mounted on aluminium stubs in preparation for SEM. SEM was carried out at the standard setting of 5Kv. Images were taken at x100, x1000 and x10,000 magnification.

For quantification of the pore size in DuraGen™, five fields were selected: four corners and one central field from the x100 image. Using ImageJ (free software found at www.imagej.net), the largest diameter from each pore was measured. The mean and standard deviations were calculated to provide an estimate of the average pore size and variance in pore size.

2.4 Optimisation to establish methods for characterising NSC growth in DuraGen™

Prior to these investigations the methods for utilising DuraGen™ had not been systematically established. Studies investigating MSCs transplanted in DuraGen™ had utilised differing conditions including a variety of cell seeding densities (see section 1.3.6). This necessitated a structured approach to establishing the optimal parameters for NSC growth in DuraGen™ including developing appropriate ICC and microscopy protocols. The flowchart below demonstrates the steps taken to determine the methods used for the main body of chapter three (**figure 2.2**).

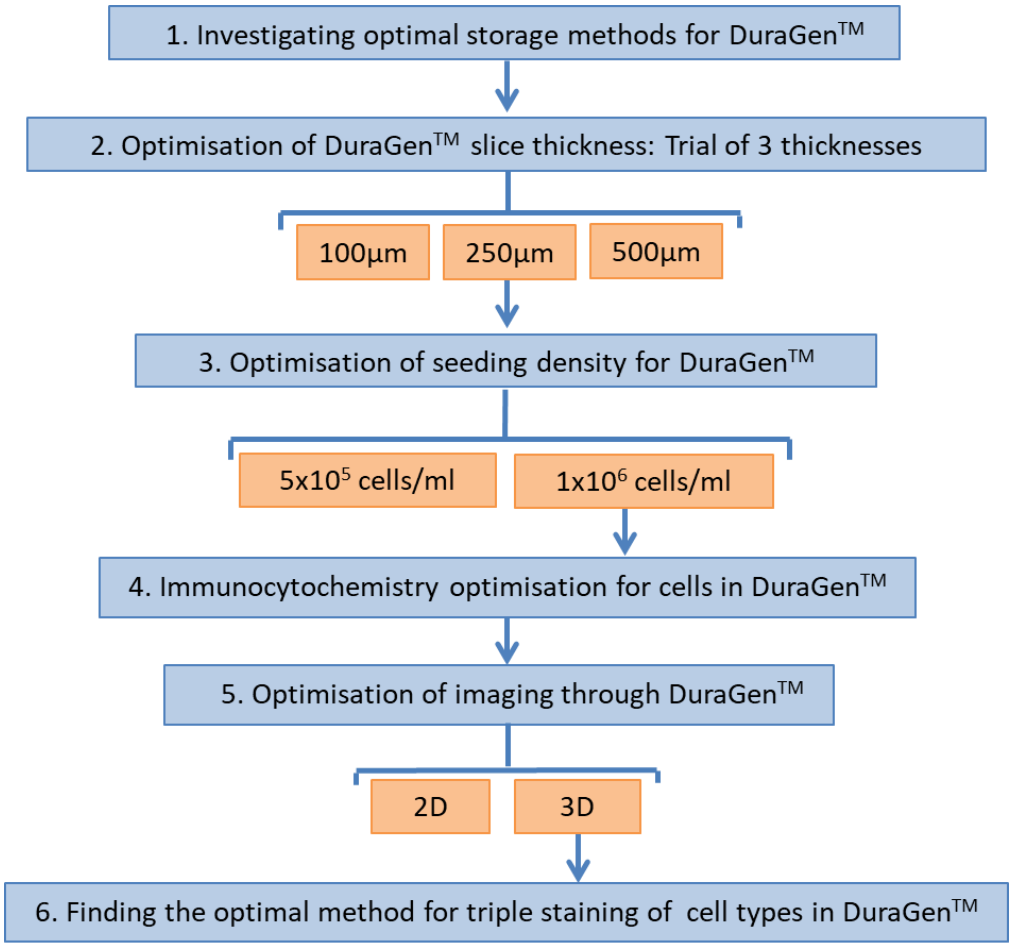

Figure 2.2*: Flowchart demonstrates the various stages of optimisation to produce a NSC-DuraGen™ construct.*

2.4.1 Finding the optimal storage conditions for DuraGen™

A standard DuraGen™ prototype with intact packaging was received by the laboratory. To ensure sterility once opened it was treated with ultraviolet light. Furthermore, once a small section had been removed for processing the remainder was stored in its original packaging. This packaging came as two plastic layers. After each use, both layers would be sealed to ensure sterility of the sample. After processing of the DuraGen™ matrix it would most often be used immediately. In the event that it needed to be stored beyond this point, it was kept in medium at 4°C. Both dry storage and storage in medium was trialled.

2.4.2 Optimisation of DuraGen™ thickness

A McIlwain Tissue Chopper was used to slice equal thickness pieces of DuraGen™ under sterile conditions. DuraGen™ was first sliced using a scalpel and stainless-steel ruler to produce a uniform piece at 5mm width (**figure 2.3a**). A pilot study utilising these 5mm by 5mm by the pre-determined depth of the material was carried out. Parallel experiments were being carried out within the laboratory investigating other cell types. A pure astrocyte culture courtesy of Farhana Chowdhury was seeded into full thickness DuraGen™ sample.

The McIlwain tissue chopper is used regularly by members of the Chari tissue engineering group for producing organotypic slice culture (15). An adapted protocol for DuraGen™ was trialled. Firstly, dry 5mm by 5mm pieces were placed on the chopping table and the chopper was set to 500µm. The piece could not be secured on the chopping table and was not immobilised for slicing accurately. Next, the piece was secured using tape or a sterile plaster to allow slicing. The tape/plaster was sliced with the DuraGen™ sample, potentially leading to contamination and making it unsuitable for culture. Finally, a drop of sterile medium was added to the DuraGen™ sample once on the chopping table (**figure 2.3b**) stabilising it for the slicing process. This method produced a sequence of uniformly thick slices on the chopping table by visual inspection (**figure**

2.3c). For ease of access to the slices and for storage, they were then washed using medium into a small petri dish where they separated. The medium used was always that which the cells would be later seeded in to maintain consistency. To decide the optimum thickness of DuraGen™ for culture three sizes were investigated: 500, 250 and 100µm. The tissue chopper was set to each thickness in turn producing three sets of uniformly sized slices for cell seeding. Later, 250 microns was agreed upon to be the most appropriate thickness (see section 3.3.3.1) and all quantitative assays were carried out on slices of 250µm thickness.

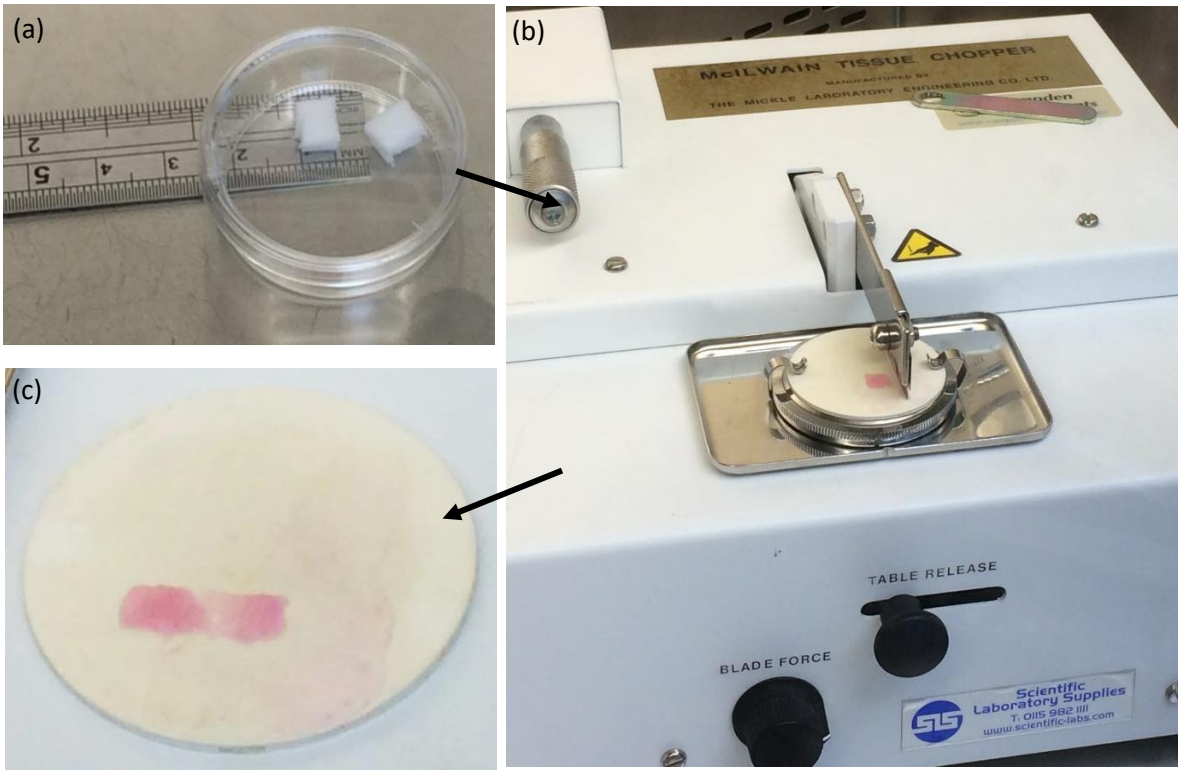

Figure 2.3: Thickness optimisation of DuraGen™ *(a) 5mm uniform DuraGen™ pieces cut with a scalpel with ruler for guidance (b) McIlwain tissue chopper set to 250µm ready to slice 5mm sample of DuraGen™ lined up on chopping table and dampened with neurosphere medium. (c) Chopping disc after slicing demonstrating 250µm slices of DuraGen™ ready to be washed into a petri dish.*

2.4.3 Optimisation of seeding density of DuraGen™

Two densities were tested: $5x10^5$ cells/mL and $1x10^6$ cells/mL. Densities for investigation were selected based on the most common cell densities used in studies investigating DuraGen™ as a cell encapsulation device (see section 1.3.6). Cells were counted using a haemocytometer after passage and then suspensions were made up to the given densities. These were then seeded on to separate sets of DuraGen™. A cell viability assay, proliferation assay and ICC for NSC, astrocyte, neuron and oligodendrocyte markers were carried out to assess for any differences between cell densities (for details of these assays see section 2.5.4-7).

2.4.4 ICC optimisation for cells in DuraGen™

Initially ICC was carried out following the standard protocols for monolayer cultures on coated coverslips. Incubation times were increased to optimise penetration of the collagen scaffold and numbers of washes were increased to prevent scaffold staining. For details of final optimised incubation times and washes see section 2.5.4-7.

Initially, each DuraGen™ construct was mounted in Vectashield mounting medium with DAPI. It was discovered that Vectashield with DAPI caused staining of the DuraGen™ fibres; therefore, all subsequent constructs for quantification purposes were incubated with Hoechst (see section 2.5.7 for details). Initially, the incubation time was for 15 minutes but this was not sufficient for complete penetration of the collagen matrix, therefore the incubation time was increased to one hour.

2.4.5 Optimisation of imaging through DuraGen™

Both two-dimensional and three-dimensional imaging techniques were deployed on DuraGen™ samples treated with ICC. A Zeiss Axioscope A1 microscope in combination with an AxioCam ICc1 digital camera with Axiovision software (Carl Zeiss MicroImaging GmbH, Göttingen, Germany) was utilised to image DuraGen™ samples in two dimensions (2D), taking different channel images and

then later merging relevant channels. A Zeiss Axio Observer.Z1 in combination with an AxioCam MRm with Zen 2.0 (blue edition) software (Carl Zeiss MicroImaging GmbH, Göttingen, Germany) was used to take stacks of images at varying distance intervals for 3D images. These could be converted to a video or a set of individual images at a later stage utilising Zen 2.0 software.

Constructs were observed and imaged using epifluorescence microscopy whilst immersed in PBS in a 24-well plate. This was problematic as it moved during 3D imaging. Withdrawing a small volume of liquid helped but the construct was large and required a high number of slices to image the full thickness. In addition, the construct displayed hazy staining, possibly due to high diffraction of light through the large constructs, which was difficult to quantify. Subsequently, each construct was mounted on a microscope slide in Vectashield mounting medium (without DAPI) and covered with a coverslip. This allowed for stability when 3D imaging and improved image quality throughout the DuraGen™ samples.

2.4.6 Finding the optimal method for triple staining of three daughter cell types in DuraGen™

To visualise all three cell types growing in DuraGen™ after differentiation, triple staining protocols were applied. Due to the risk of non-specific staining when multiple antibody protocols are used, two different methods were trialled. These methods were named for the purpose of this thesis the 'combined approach' and the 'sequential approach'. Primary antibodies utilised were as follows anti-GFAP donkey anti-rabbit, anti-TUJ1 donkey anti-mouse and anti-MBP donkey anti-rat for astroglial lineage cells, neurons and oligodendrocytes respectively. Secondary antibodies used were AMCA donkey anti-rabbit (astroglial lineage cells), FITC donkey anti-mouse (neurons) and CY3 donkey anti-rat (oligodendrocytes).

All DuraGen™ samples were fixed in 4% PFA in PBS following the method described in section 2.5.6. A 5% NDS-0.3% Triton-X100-PBS blocker was added to each sample for 30 minutes.

(1) *Combined approach*: Here, all three primary antibodies detailed above were diluted in 200µl of blocker per well and added to the sample. This was then incubated overnight at 4°C. The following day the samples were washed three times for five minutes each in PBS. A further 30 minutes of blocker was applied at room temperature. Next all three secondary antibodies as detailed above were diluted in 200µl of blocker per well and incubated for up to three hours at room temperature. Samples were washed three times for five minutes each in PBS.

(2) *Sequential approach*: This involved the same primary and secondary antibodies as detailed above. The first primary antibody anti-TUJ1 was incubated overnight. The following day this was removed and washed as before. These samples were then blocked for 30 minutes and then the secondary antibody associated with anti-TUJ1, FITC donkey anti-mouse was incubated with the sample for up to three hours. This was then removed, washed and blocked for 30 minutes again. The process was repeated twice for each of the remaining antibodies. After four days the sample was then ready for mounting and imaging. Both approaches produced sufficiently specific staining, so the combined approach was utilised for all other triple cell type staining.

These optimisation studies allowed us to determine the optimum methods for growth and characterisation of NSCs in DuraGen™. Once the pilot studies were completed, a full characterisation of NSC growth, proliferation and differentiation was carried out.

2.5 Characterisation of NSC growth and differentiation in DuraGen™

2.5.1 Seeding NSCs on to DuraGen™

Each slice of DuraGen™ was placed into the bottom of a well in a 24-well plate, with one sample per well. Each DuraGen™ sample often adhered to forceps used for transferring it into the well plate. To aid in releasing the sample into the well plate, a small drop of medium was required in the base of the plate, when the DuraGen™ touched the medium it separated from the forceps. A 200µl

cell suspension was applied to the surface of the DuraGen™ dropwise to allow time for absorption of the cell suspension. Once the DuraGen™ sample was fully saturated by the cell suspension, the remainder was introduced into the surrounding area within the well. Each well was fed every other day by replacing 100µl of medium with 100µl of fresh neurosphere medium.

2.5.2 Differentiation of NSCs in DuraGen™

To allow the stem cells to differentiate into their three main cell types – astrocytes, neurons and oligodendrocytes, the medium was changed 48 hours post passage. All medium from each well was removed then 200µl of differentiation medium was added. Each 250µm DuraGen™ slice was free-floating within the well. Whenever medium was replaced or the scaffold was washed with PBS caution was taken to avoid drawing up the 3D construct with the pipette. To prevent drawing up the sample, the pipette tip was placed at the side of each well, away from the scaffold, and medium was removed gently whilst visually monitoring the slice.

2.5.3 Assay time points

To ensure the material had no adverse effects on the properties of NSCs the following parameters were measured: cell viability, cell proliferation, NSC marker expression and NSC differentiation on the DuraGen™ at various time points (**table 2.1**). Details of each assay are given below.

INVESTIGATION	ASSAY	MECHANISM	TIME POINT
CELL VIABILITY	Calcein/ ethidium homodimer-1	Calcein crosses intact cell membranes (live cells) and ethidium homodimer-1 crosses disrupted cell membranes (dead cells)	24 hours 8 days 12 days
CELL PROLIFERATION	EdU	EdU is modified thymidine which is incorporated into new DNA (proliferating cells)	24 hours 8 days
NSC MARKER	Nestin Sox-2	NSC cytoskeleton protein NSC transcription factor	48 hours
CELL DIFFERENTIATION	GFAP TUJ1 MBP	Astrocyte cytoskeleton protein Neuronal microtubule protein Major constituent of myelin – produced by oligodendrocytes	8 days 12 days 16 days

Table 2.1*: Demonstrating each experimental goal, the assay used to address it and time points used.*

2.5.4 Cell viability assessment of cells in DuraGen™

Cell culture medium was removed from wells, and the DuraGen™ washed with PBS once. A 2 mL solution of PBS containing 4 µM calcein, 6 µM ethidium homodimer-1, and 2 µg/mL Hoechst was added to each well and incubated at 37°C in 5% CO_2/ 95% humidified air for one hour to allow the solution to penetrate the matrix. The samples were fixed, mounted and then imaged. Three washes with PBS were added prior to fixing to ensure full removal of residual reagents.

2.5.5 EdU Proliferation assay of cells in DuraGen™

For assessment of proliferation of NSCs in DuraGen™ a Click-iT EdU imaging kit was used according to the manufacturer's instructions except where incubation times and washes were increased as follows. Component A was incubated for 16 hours with NSCs or differentiated cells in DuraGen™. Constructs were then fixed with 4% PFA for 30 minutes. Samples were washed four times with 3% bovine serum albumin (BSA) in PBS. 0.5% triton X-100 was added to each well for 40 minutes to

allow permeabilization of the cell membranes. Once again, the construct was washed four times with BSA. The EdU detection cocktail was prepared in accordance with the Invitrogen guidelines and incubated with the sample for one hour, protected from light. Constructs were washed in BSA twice and then PBS twice before the ICC protocol was carried out to identify nuclei and either nestin positive cells at 24 hours or GFAP positive cells at eight days (the two proliferating cell types, see section 2.5.7 for the full ICC protocol).

2.5.6 Fixation of cells in DuraGen™

Unless otherwise stated, all fixation was carried out using these conditions. Firstly, medium was removed from the wells, and then washed with PBS. 4% PFA was added for 20 minutes. Then the well was rinsed with PBS three times for five minutes each.

2.5.7 ICC of cells in DuraGen™

Each well was blocked for 30 minutes with a solution of 5% NDS in PBS-0.3% Triton X-100. Details of antibodies used are in table 2.2. Primary antibody diluted in blocker solution at the concentration given in the table, was added and incubated overnight. Following this, the primary antibody was removed and the construct was washed with PBS three times for five minutes each. Again, the sample was blocked for a further 30 minutes with the same blocker. Then secondary antibody diluted in blocker was added for up to three hours, to allow penetration of the DuraGen™. Secondary antibody was matched to the origin of the primary antibody for instance when utilising MBP antibody which is donkey anti-rat, the secondary antibody would be either FITC Donkey anti-rat or CY3 Donkey anti-rat. Finally, each well was washed with PBS three times for five minutes each.

Primary antibodies	Nestin (mouse) Sox-2 (rabbit) TUJ-1 (rabbit/ mouse) GFAP (rabbit/ mouse) MBP (rat)
Secondary antibodies	FITC Donkey anti-mouse FITC Donkey anti-rabbit FITC Donkey anti-rat CY3 Donkey anti-mouse CY3 Donkey anti-rabbit CY3 Donkey anti-rat AMCA Donkey anti-rabbit

Table 2.2*: Antibodies used in ICC.*

Each construct was incubated for a further hour with a solution of 2 µg/mL Hoechst in PBS to allow nuclear staining. This was washed three times with PBS before being mounted on to a microscope slide with Vectashield and covered with a coverslip.

2.5.8 2D and 3D imaging of cells in DuraGen™

All quantitative imaging was carried out using an Axio Observer.Z1 in combination with an AxioCam MRm (black and white camera) with Zen two (blue edition) software. For all assays five fields were selected at x200 magnification as demonstrated in figure 2.4. A stack of images was taken as the focus moved upwards to produce a Z-stack; this was carried out at each field with the interval fixed

at 5µm between each image (**figure 2.4**). The top and bottom of the stack was allocated when the last visible cell went out of focus.

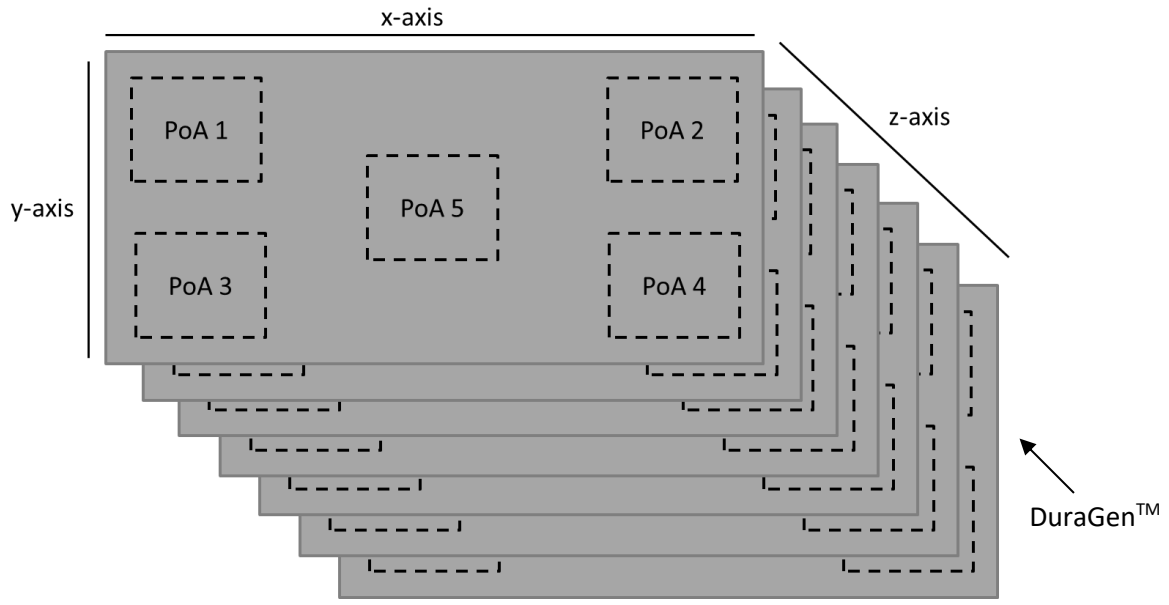

Figure 2.4*: Demonstration of acquisition of 3D Z-stack images for quantification including allocation of fields for analysis termed plane of analysis (PoA).*

2.5.9 Quantitative analysis of images

Quantification was carried out utilising ImageJ free software. Each field contained around 10-15 images which were loaded onto the ImageJ software as a stack allowing quantification throughout the layers of the 3D image. Cell nuclei were counted using the cell counter plugin for each field. For each assay cells positive for the antibody in question were counted. For live-dead assays, cells positive for calcein (green) were counted and nuclei positive for ethidium homodimer-1 (red) were counted. There was some bleed through from ethidium homodimer-1 which produced fluorescence into the green channel at high exposures. The exposure was set so the bleed-through was minimal across all channels. Then this exposure was used for all live-dead imaging.

For quantification of axon length, each TUJ1 field was surveyed for axons extending within the same plane. Often due to the 3D nature of the construct axons would transverse the layers of the stack making measurements difficult. Axons were only selected for measurement if the cell body and full length of the axon could be visualised in one plane. In future experiments confocal microscopy may be employed to generate 3D images of the construct within which axonal length measurements can be made in all directions. Of the axons that met the stated criteria, the freehand line tool in ImageJ was utilised to mark from the cell body to the furthest point of the axon, following its curvature. This distance was measured. From each DuraGen^{TM} slice made up of images from five fields, axons from 30-63 neurons were measured. This was carried out for samples stained with TUJ1 at day eight, day 12 and day 16.

The cellular distribution was quantified in two planes, horizontal and vertical. The horizontal analysis was carried out by counting the number of nuclei per field. There were five fields per DuraGen^{TM} sample as described above. The average number of cells per corner field or central field were calculated to decipher if there was a preferential distribution in one of the sections (**figure 2.5**). This was carried out at 48 hours and eight days. Analysis of the vertical distribution was also carried out by imaging cell nuclei. Z-stacks were imaged at 5µm intervals. The top and bottom of the matrix was defined as the point where the first/ last fibre was in focus using phase. Nuclei per image were counted and converted to a percentage of the total number of images in that z-stack. The average number of cells at each one percent interval was calculated (**figure 2.5**).

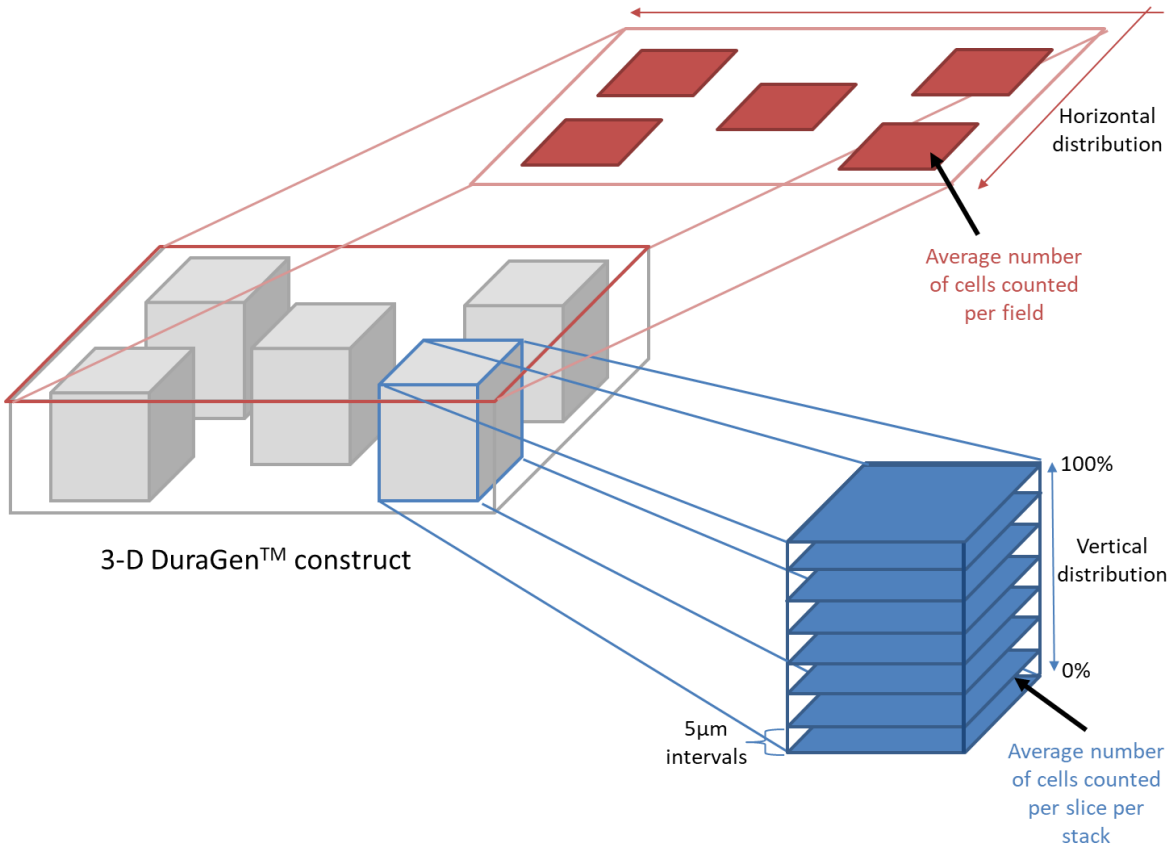

Figure 2.5*: Schematic representing how the distribution analysis was carried out. The red schematic represents the method for analysing the distribution of cells in the horizontal plane. The blue schematic represents the method for analysing the distribution of cells in the vertical plane.*

2.5.10 Statistical analysis

At each time point for each experiment where DuraGen™ was investigated the mean; standard deviation and standard error were calculated of the quantified percentages. All results are given as the mean ± the standard error of the mean. Furthermore, to establish if there was a difference between the lower and higher cell seeding density in cell viability at 24 hours a two sample T test was used to compare the means. A two sample T test was also used to compare the proliferation rates of cells at 24 hours and eight days. When analysing the cell viability or cell type proportions at the three different time points a one-way analysis of variance (ANOVA). For comparison of axon

length at the three different time points again a one-way ANOVA with Tukey and Fisher post hoc multiple comparison tests were utilised. To compare the spatial distribution of cells in both the horizontal and vertical planes, one-way ANOVAs were used. All statistical tests were performed using MiniTab software.

2.6 Genetic engineering of NSCs using MNPs with magnetofection and minicircle DNA vectors

2.6.1 Producing mcGFP

mcGFP were used to allow assessment of levels of transfection in NSCs. mcGFP were produced by Dr Sarah Harris in the Neural Tissue Engineering group. mcGFP were produced using the parental plasmid pMC.EF1-MCS-IRES-GFP-SV40PolyA and the MC-Easy^{TM} Minicircle DNA Production kit.

100ng of parental plasmid was transformed into *Escherichia coli* (strain ZYCY10P3S2T) by heat-shock. *E. coli* cultures were grown on LB agar plates containing 50 µg/mL kanamycin for 16h at 37°C. Three to five colonies were selected and cultured in LB broth containing 50 µg/mL kanamycin for 16 h at 37°C and 250 rpm. To ensure the parental plasmid was present in the bacteria a QIAprep miniprep kit was used followed by a restriction digest using EcoRI. Gel electrophoresis was performed to confirm the size of the plasmid DNA. All electrophoresis was performed using 1% agarose in 1xTAE buffer containing 0.5µl GelRed for 120 minutes at 100V.

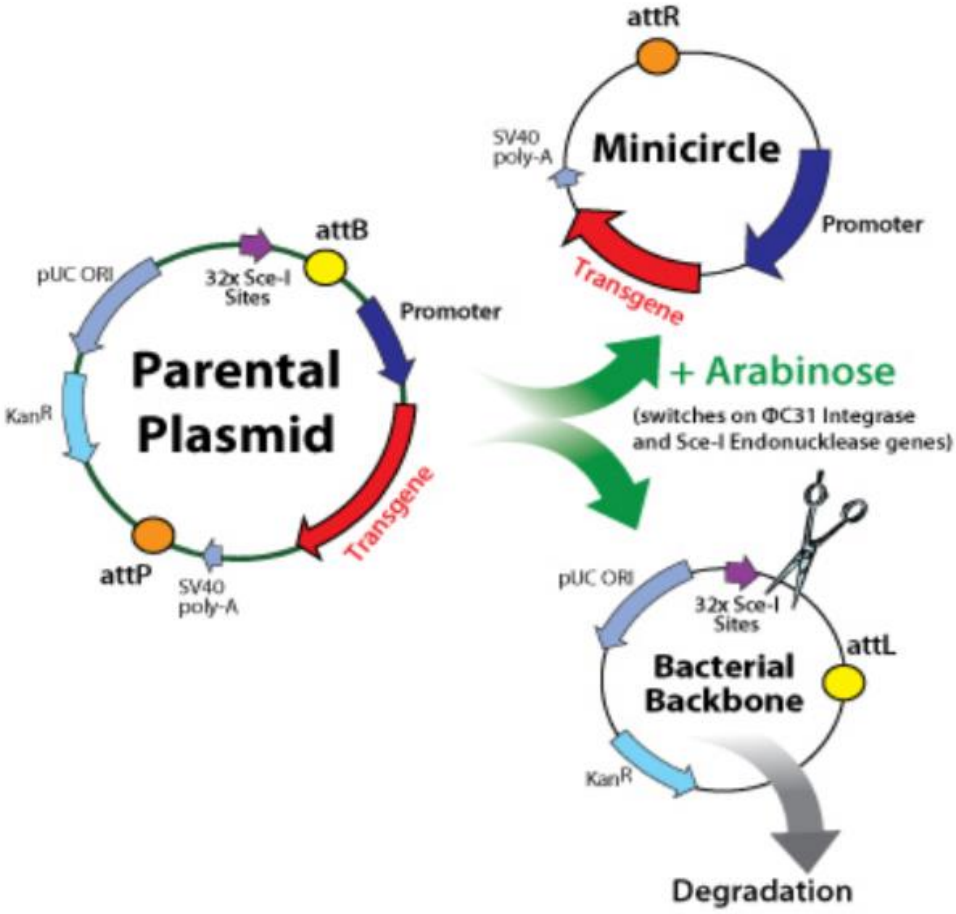

Figure 2.6*: DNA minicircle production from the parental plasmid* (218) .

After confirmation of successful transformation, 200 mL of MC-Easy™ Growth Medium was inoculated with *E. coli* and cultured for 16 hours at 30°C and 250rpm. pH and optical density (600nm) were measured and for pH 7 and OD_{600} = 0.6-0.8, 400 mL of arabinose containing MC-Easy™ Induction Medium was added. The broth was incubated at 30°C and 250 rpm for a further five hours and 30 minutes to liberate the minicircle from the parental backbone (**figure 2.6**). Confirmation of the presence of a plasmid the correct expected size for mcGFP was performed using a miniprep kit and restriction digest (EcoRI as previously described). Bacterial cells from the remaining broth were pelleted for harvest by centrifugation at 3220 x *g* and 4°C for 20min per 50 mL broth (300 mL broth into one single pellet). A QIAprep maxiprep kit was used to isolate mcGFP

from bacteria pellets as per the manufacturer's instructions with the following amendments: 20 mL of Buffers P1, P2 and P3 were used. Successful isolation of mcGFP using the maxiprep kit was confirmed via restriction digest using EcoRI as previously described (**figure 2.7**). The concentration of the mcGFP solution was confirmed using spectrophotometry prior to each transfection.

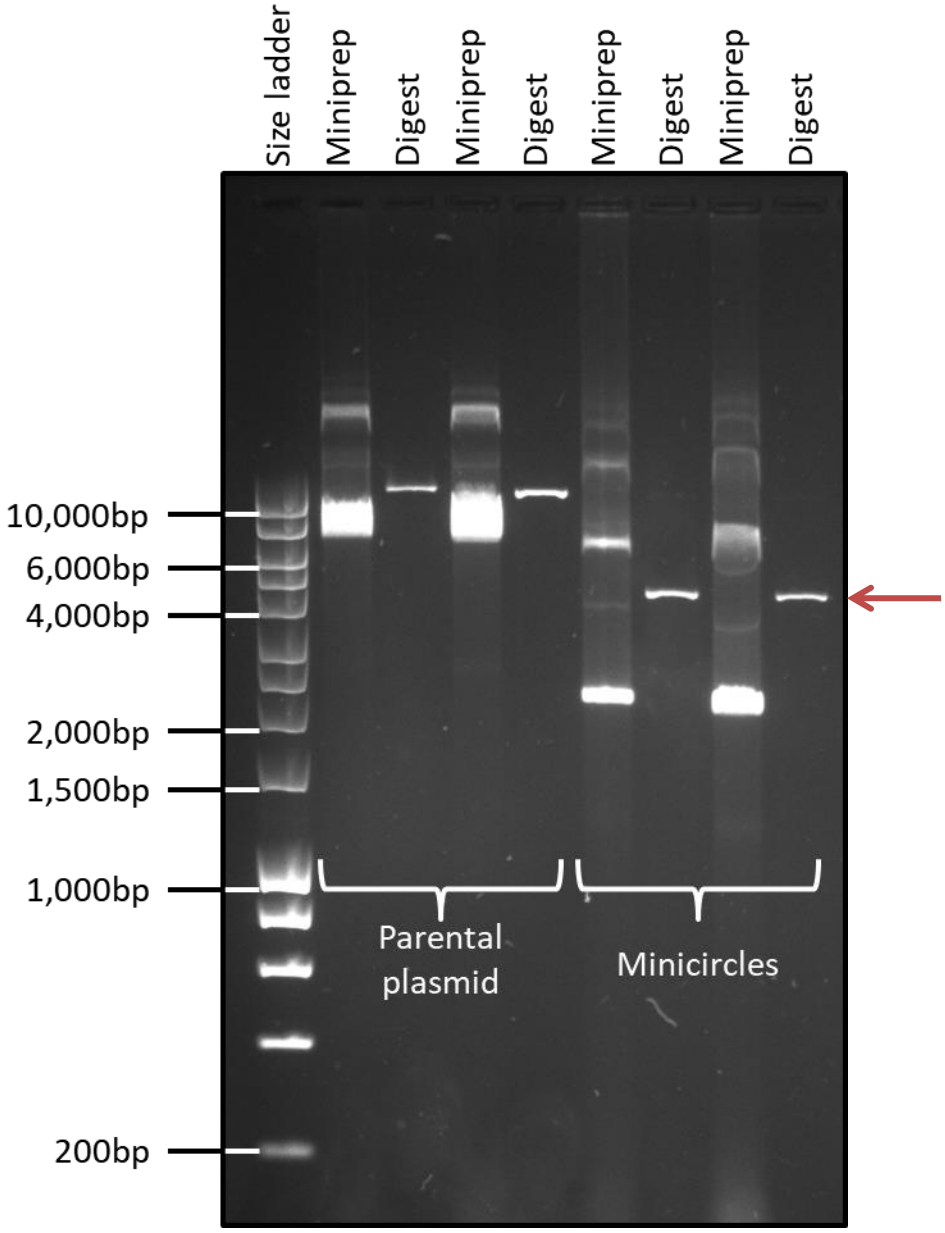

Figure 2.7*: Gel electrophoresis demonstrating mcGFP at the correct size after restriction digest (arrow). Image was taken by Dr Sarah Harris.*

2.6.2 Magnetofection of NSCs

The method of transfection of neurospheres used here has previously provided efficient transfection (195,217). NSCs were passaged after reaching confluence and 500 µL of a single cell suspension at 1 x10^5 cells/mL was added to each well of a 24-well Nunc non-treated multidish. NSCs were allowed 24 hours to form neurospheres prior to transfection. NeuroMag, a commercial MNP was used for all transfections. mcGFP and NeuroMag particles were suspended in a solution of 3:1 DMEM: F12 and incubated for 20 minutes to allow the formation of complexes. It was ensured that no further mixing took place as this can dissociate the complexes. 50µl of solution was added to each well for transfection containing 125ng of mcGFP and 0.435µl of NeuroMag iron oxide nanoparticles (a ratio used previously (212)), 50µl of the same DMEM: F12 solution without DNA or nanoparticles was added to each control well.

Each plate was then placed on top of a nanoTherics magnefect-nano 24-magnet array system (**figure 2.8**). The programme was set to F=4Hz to produce an oscillating field for 30 minutes. The plate was then removed and placed at 37°C in 5% CO_2/ 95% humidified air. After 16 hours transfection of neurospheres was confirmed using an Axio Observer.Z1 in combination with an AxioCam MRm with Zen two.

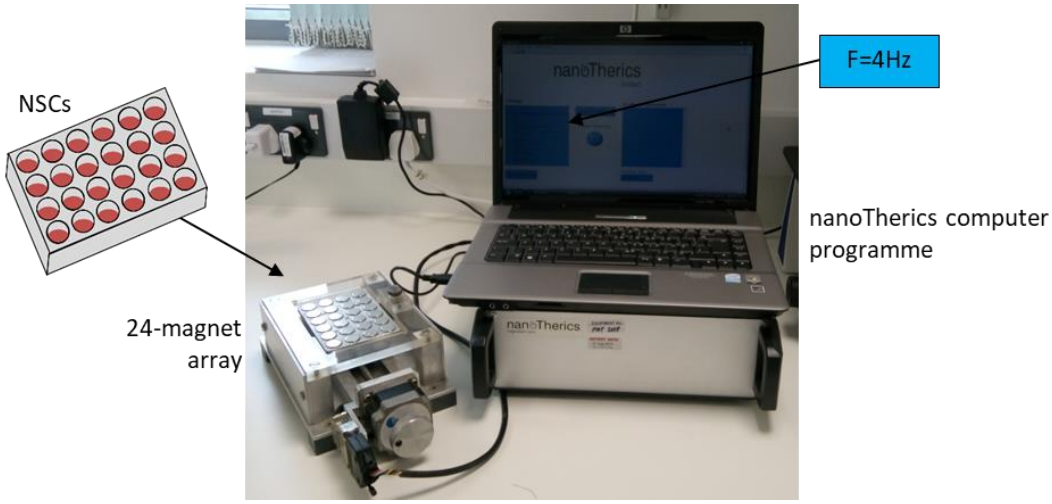

Figure 2.8: *nanoTherics magnefect-nano 24-magnet array system used in magnetofection of NSCs.*

2.7 Approaches to optimise method of achieving a 3D construct supporting growth of transfected NSCs

Multiple methods of constructing a biomaterial scaffold-genetically engineered cell construct have been used previously. It was therefore imperative to establish the most effective method of forming a DuraGen™-genetically engineered NSC construct. The flowchart demonstrates the multiple steps of optimisation that were required to reach the method used for the main research in chapter four (**figure 2.9**).

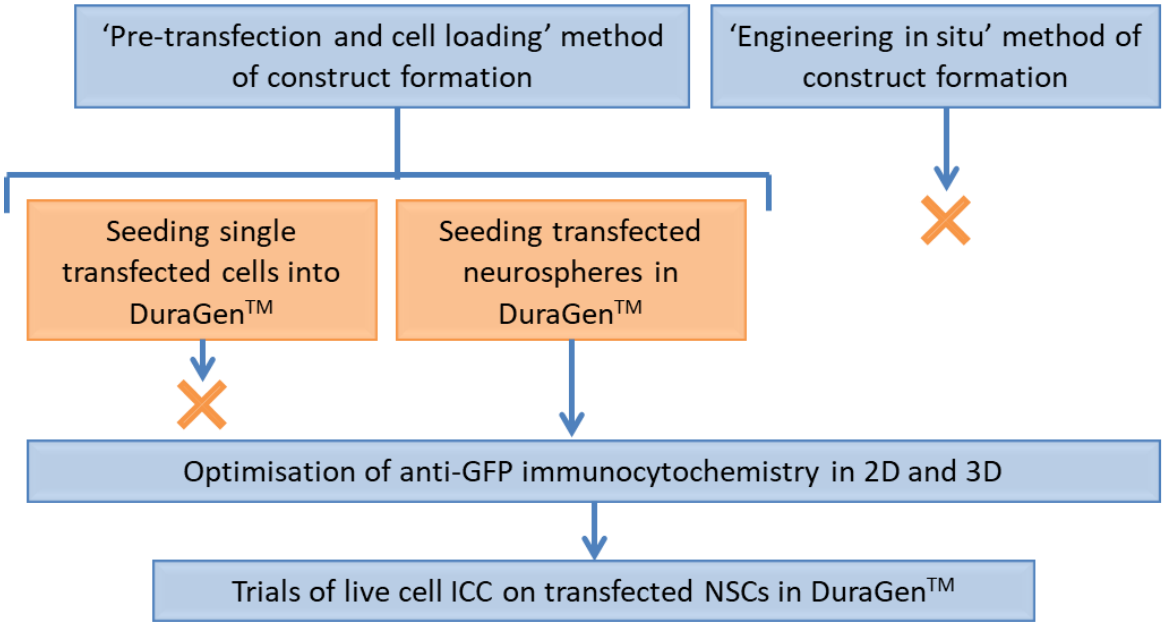

Figure 2.9: *Flowchart of optimisation experiments to produce a genetically engineered cellular 3D construct.*

2.7.1 Seeding single transfected cells into DuraGen™

Initially, in order to follow the DuraGen™ seeding protocols of section 2.5.1. NSCs were dissociated 24 hours after transfection (for details of dissociation see section 2.2.2). NSCs were resuspended at the lower density of $5x10^5$ cells/ mL due to low cell numbers post passage and seeded directly on to DuraGen™ slices of 250µm. They were then incubated for a further 24 hours before visualisation under light microscopy.

After 24 hours post seeding of transfected single cells into DuraGen™ the matrix appeared to have disintegrated. To investigate the conditions the DuraGen™ samples had been exposed to, the pH of each condition medium and some standard stock medium was measured using pH indicator strips.

2.7.2 Seeding transfected neurospheres into DuraGen™

Following the failure of single cell seeding of transfected NSCs, removing the second dissociation step and simply collecting and seeding the transfected NSCs as neurospheres onto the DuraGen™ was investigated. After transfection had been confirmed, at 24 hours the neurosphere suspension was added to the construct. The optimal method for this was assessed; either (1) neurospheres transferred directly on to DuraGen™ in the same slow, dropwise fashion as section 2.5.1, or (2) the DuraGen™ slice was added to the neurosphere suspension allowing cells to infiltrate the collagen matrix (**figure 2.10**). No difference in cell numbers was observed between the two methods therefore method one was used for the full characterisation of the construct. To avoid any further loss of the material all attempts to control or increase the density were precluded.

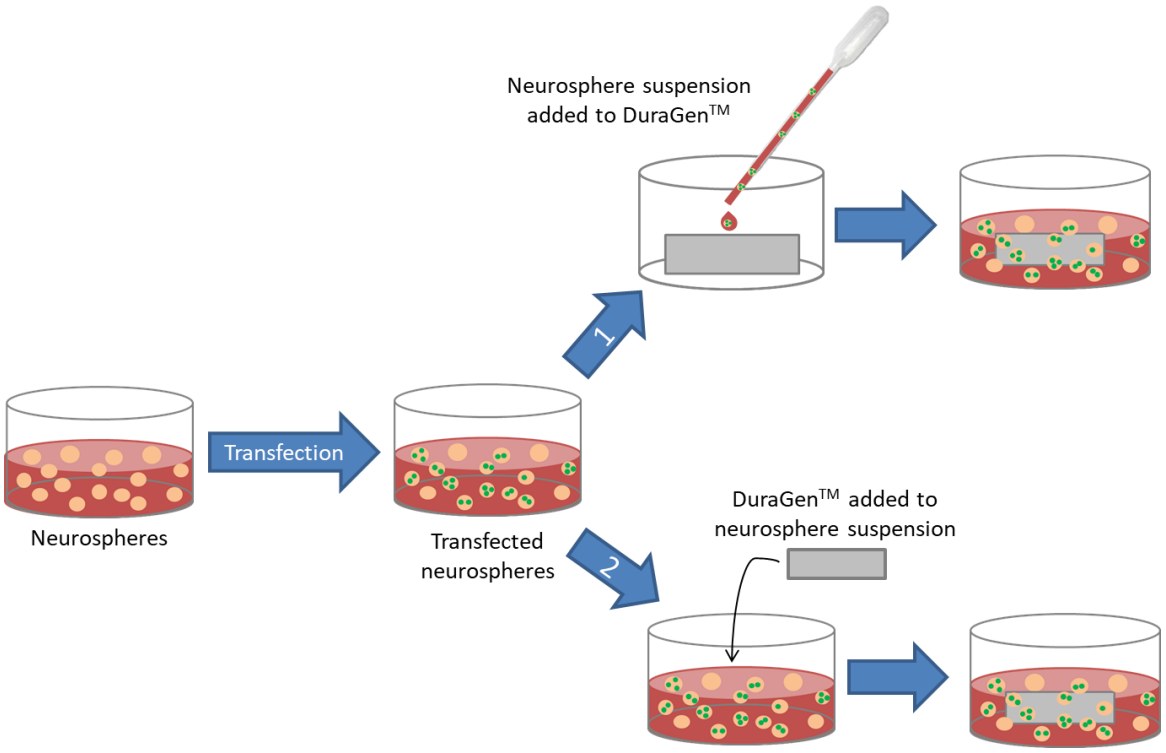

Figure 2.10: *Schematic representing two techniques to achieve DuraGen™ containing genetically engineered NSCs.*

2.7.3 In-situ engineering of NSCs

In order to simplify the 3D construct transfection protocol, a method to transfect the NSCs within the matrix was investigated. For the purpose of this thesis the method involving transfecting NSCs that are within the DuraGen™ construct was termed in-situ engineering. The benefit of this method is that it simplifies the process by removing a step. NSCs were seeded on to DuraGen™ at 250µm thickness and allowed to adhere to the material over the following 24 hours. Equivalent volumes of transfection reagents as described in section 2.6.2 were added to each well containing a cellular DuraGen™ sample. Control wells were treated identically except mcGFP and NeuroMag were omitted. Samples were subjected to one of three different conditions: (1) Oscillating magnetic field (F=4Hz), (2) static magnetic field (F=0Hz), or (3) no field. Plates were visualised at four, six, 16 and 24 hours to confirm transfection utilising an Axio Observer.Z1 in combination with an AxioCam MRm with Zen two. This method was unsuccessful initially; therefore, re-transfection without a magnetic field was carried out for all DuraGen™ samples.

3.7.4 Optimisation of anti-GFP ICC in two 2D and 3D

In previous studies utilising GFP the visually detectable levels of expression have been lower than the true value. These studies used an anti-GFP antibody to detect cells that did not demonstrate GFP expression under fluorescent microscopy but were in fact producing GFP. Figure 2.11 demonstrates the increased sensitivity for GFP expression provided by the use of anti-GFP antibody.

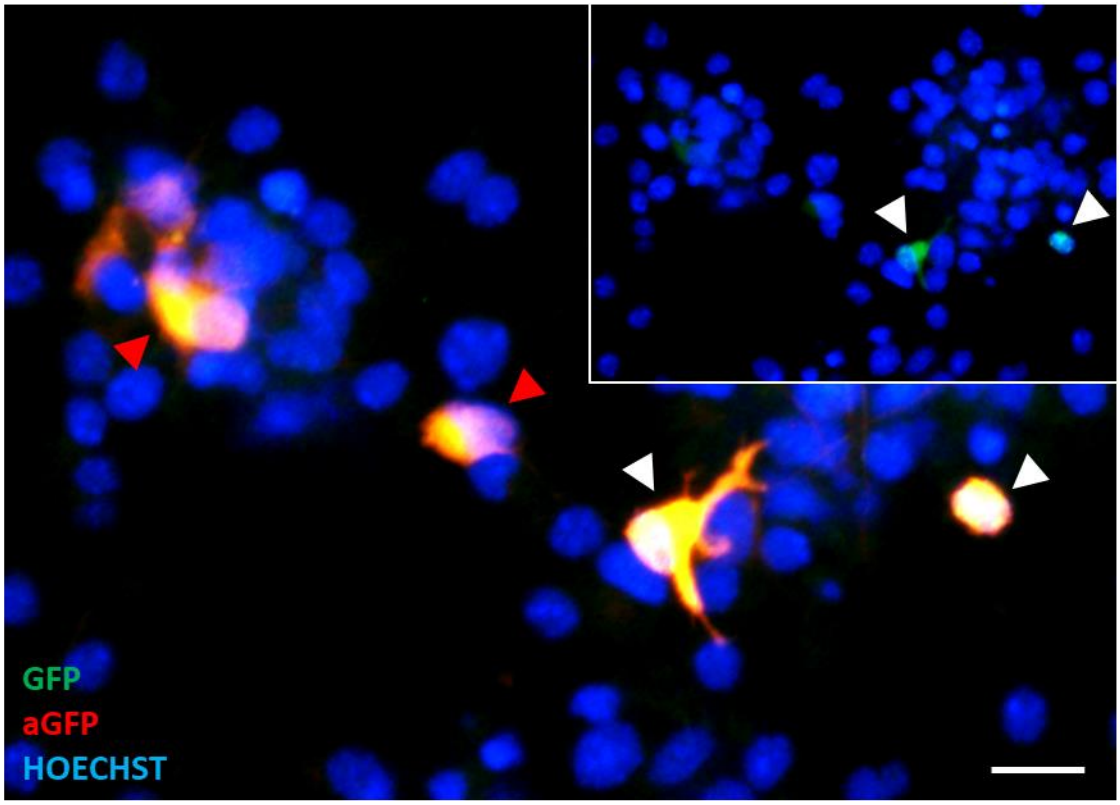

Figure 2.11: Anti-GFP antibody increases the detection of transfected NSCs. *Inset demonstrates GFP expression in transfected NSCs after 48 hours (white arrows).* Main image represents anti-GFP antibody robustly detecting NSCs expressing low levels of GFP *(red arrows). Scale bar = 25µm.*

To detect GFP in the DuraGen™ construct, the anti-GFP antibody was used. The method for ICC described in section 2.5.7 was utilised. After incubation with the primary antibody: anti-GFP at a dilution of 1:700, CY3 donkey anti-rabbit at 1:200 was used for secondary staining. Later the concentration of primary antibody was reduced to 1:1000.

Due to high background staining on the control samples and transfected samples, the exposure of the images was set so that control samples did not display background GFP staining. Exposure was kept constant throughout.

2.7.5 Trials of live cell ICC on transfected NSCs in DuraGen™

Live imaging of transfected NSCs in DuraGen™ demonstrated an increased intensity of GFP expression than when the same samples were fixed and imaged. Therefore, live cell ICC was attempted to examine whether omitting the fixation step could improve visualisation of the GFP expression. GFAP antibody was diluted (1:500) in pre-warmed differentiation medium. All medium was removed from each well and 400µl of the primary antibody dilution was added. This was incubated (37˚C) for 30 minutes before being washed off gently with medium. CY3 secondary antibody also diluted in medium (1:200 in 400µl) was added to each well. The constructs were observed regularly and at three hours no staining was evident. The protocol was revised, adding in one-hour incubation of primary antibody and no definitive staining was evident.

2.8 Characterisation of transfected NSCs within a surgical material

2.8.1 Magnetofection of NSCs with GFP

For characterisation purposes NSCs were transfected according to the methods stated in section 2.6.2.

2.8.2 Transfer of transfected NSCs to DuraGen™

24 hours after transfection GFP expression was confirmed using a Zeiss fluorescent microscope. Following confirmation of transfection, each well containing neurospheres suspended in 500µl of neurosphere medium were transferred via Gilson pipette onto pre-prepared DuraGen™ slices of 250µm thickness (see section 2.4.2 and 2.5.1 for details of DuraGen™ preparation). Transfected neurospheres and control neurospheres were transferred into corresponding wells containing DuraGen™ in a fresh 24-well plate to maintain continuity of conditions (**figure 2.12**). Constructs

were then incubated at 37°C in 5% CO_2/ 95% humidified air until their relevant assay time point (**table 2.3**).

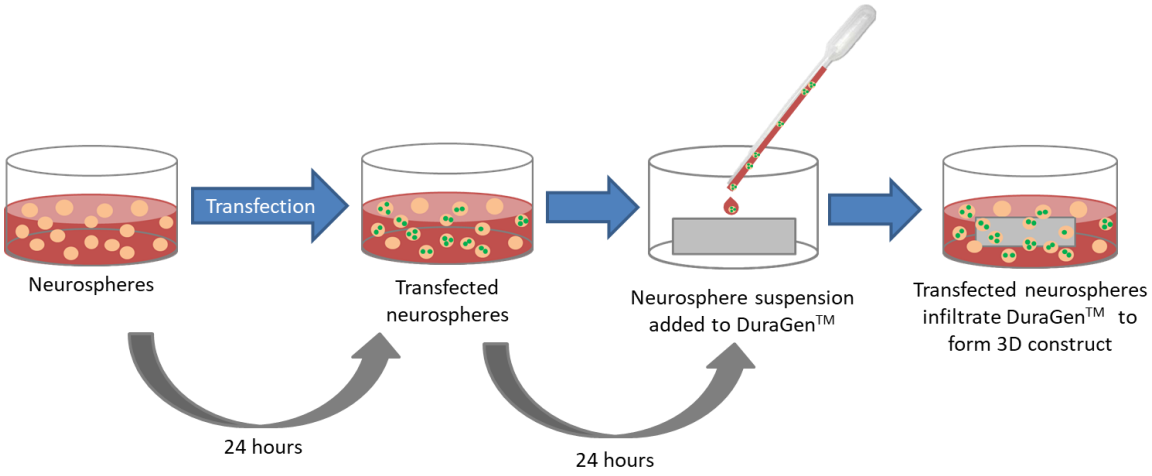

Figure 2.12*: Schematic depicting the optimised process of achieving transfected NSCs within the DuraGen™ matrix.*

2.8.3 Anti-GFP ICC

After fixation in 4% PFA (section 2.5.6), ICC protocols were as described in section 2.5.7. Briefly, constructs were incubated in blocking solution consisting of 5% NDS-0.3% triton X-100 in PBS. TurboGFP antibody was added at a concentration of 1:1000 and incubated at 4°C overnight. After three five-minute washes and subsequent blocking, CY3 (donkey anti-rabbit) was added diluted 1:200 in blocker for three hours at room temperature. Constructs were washed again, and the nuclei stained with Hoechst dye (as in section 2.5.7).

2.8.4 Investigating cell viability, proliferation and morphology

All assays were carried out in accordance with the methods given in sections 2.5.4-7 unless stated otherwise. Assay time points are given in table 2.3. Day 0 is the day of transfection and day one is when cells were added to the constructs. Both timings are given for clarity. For differentiation,

medium was changed at two days post transfection and one day post seeding into DuraGen™ (see section 2.5.2 for details of differentiation method).

Assay	Time point post transfection	Time point post seeding into construct
Live-dead	2 days	1 day
EDU Proliferation	2 days	1 day
Nestin (NSC marker)	2 days	1 day
Sox-2 (NSC marker)	2 days	1 day
Anti-GFP	2 days	1 day
GFAP/TUJ1/MBP	7 days	6 days
GFAP/ TUJ1/ MBP	9 days	8 days

Table 2.3: *Time points for assays utilised to assess the safety and efficacy of transfection of NSCs and transfer to collagen matrix.*

2.8.5 2D and 3D imaging of transfected cells in DuraGen™

Imaging was carried out following the method outlined in section 2.5.8.

2.8.6 Quantitative analysis of images

All fields both transfected and control were analysed by the method given in section 2.5.9. Transfected cells were identified by their green fluorescent stain associated with a cell nucleus. Although utilising NSCs within the neurosphere format has many benefits, one associated drawback is the reliability of cell counts due to the density of cells within the neurosphere. Previous studies

have dissociated the neurospheres to gain more accurate counts. Due to the neurospheres being within DuraGen™ in this study, it was not possible to dissociate the cells therefore transfection efficiency was based on the existence of at least one transfected NSC within the sphere. Proportions of neurospheres with at least one transfected NSC were counted.

2.8.7 Statistical analysis

All transfected and control groups were compared using MiniTab software. Where there were two groups for comparison, transfected versus control, a two sample T-test was performed. If there were multiple comparison groups, for example the differentiated cell type proportions in transfected versus control, two sample T-tests were performed for each comparison group.

Chapter 3: Investigating neurosurgical grade materials for the encapsulation of NSCs

3.1 Introduction

Neurosurgical grade materials offer a potential pre-approved biomaterial scaffold solution for stem cell delivery. There are multiple surgical materials available, each composed of different polymers and with distinct physical properties. Some are liquids or gels and others solid structures. Major pharmaceutical companies produce these materials on a large scale therefore translation of a stem cell therapy encapsulated within a surgical material to the clinical environment becomes more likely due to the existing infrastructure. The following two materials were selected for analysis in this chapter.

Firstly, DuraGen™ has demonstrated significant potential for the encapsulation of other cell types (details in section 1.3.6). To the best of our knowledge it appears DuraGen™ has never been tested for its capacity to allow the survival of NSCs or their differentiated progeny. Although evidence exists demonstrating DuraGen™ use in PNS implants and to support cortical neuron growth (details in section 1.3.6), it has never been considered as a CNS therapeutic option beyond its current indications for duraplasty. **Hence, this chapter study aims to establish whether DuraGen™ can support the growth of NSCs and allow them to differentiate to determine its utility as an implantable encapsulating cellular delivery device for the treatment of SCI.**

Secondly, DuraSeal™ was selected due to its properties and similarities with previously successful (unapproved) pre-clinical cell transplant materials (details in section 1.3.7). Additionally, it offers the benefit of being a liquid format. Although DuraSeal™ has shown promise in PNS graft, it has never been used to deliver any transplant cell type. Moreover, DuraSeal™ has never before been suggested for use in CNS therapies beyond its indication as a dural sealant. **Our study intends to investigate DuraSeal™ as a potential scaffold for the growth and differentiation of NSCs with the intention of utilising this as an injectable material for cell encapsulation for the treatment of SCI.**

3.2 Aims and objectives

Given the current lack of availability of a successful, FDA-approved substrate for NSC delivery to the site of SCI, this chapter will investigate the potential of two FDA-approved surgical materials to act as cell encapsulation devices for NSC transplantation. The specific objectives for this chapter are as follows:

I. To carry out pilot studies on DuraGen™ and DuraSeal™ to make an initial assessment of their capacity to support 3D NSC growth.

II. To characterise DuraGen™ and DuraSeal™'s structures using high resolution SEM to identify the pore size.

III. To optimise culture parameters for cell growth, ICC and microscopic analysis in DuraGen™.

IV. To establish whether DuraGen™ has any adverse effects on key cellular properties of NSCs: namely, viability, proliferation and differentiation.

V. To determine the 3-D spatial distribution of cells within DuraGen™.

3.3 Results

3.3.1 DuraSeal™ does not support 3D cell growth

Preliminary investigations into the potential use of DuraSeal™ proved that it is unlikely to be able to support cell growth. After standard application according to the manufacturer's guidelines, DuraSeal™ formed a gel-like material within the tube it was injected into. After the addition of food colouring dye to DuraSeal™ there was no immediate evidence of permeation of the dye through the gel. 24 hours later no change was visible and there was a distinct DuraSeal™-dye interface apparent (**Figure 3.1c**). As the dye appeared unable to diffuse through the DuraSeal™ matrix, the likelihood of the material supporting cellular infiltration or medium circulation becomes negligible.

This idea was corroborated by SEM which demonstrated a lack of porosity in the DuraSeal™ matrix (**Figure 3.1d**). This surgical material was therefore deemed unlikely to allow penetration of or provide protective encapsulation of transplantable cells. This material was rejected from further experiments in my thesis on this basis.

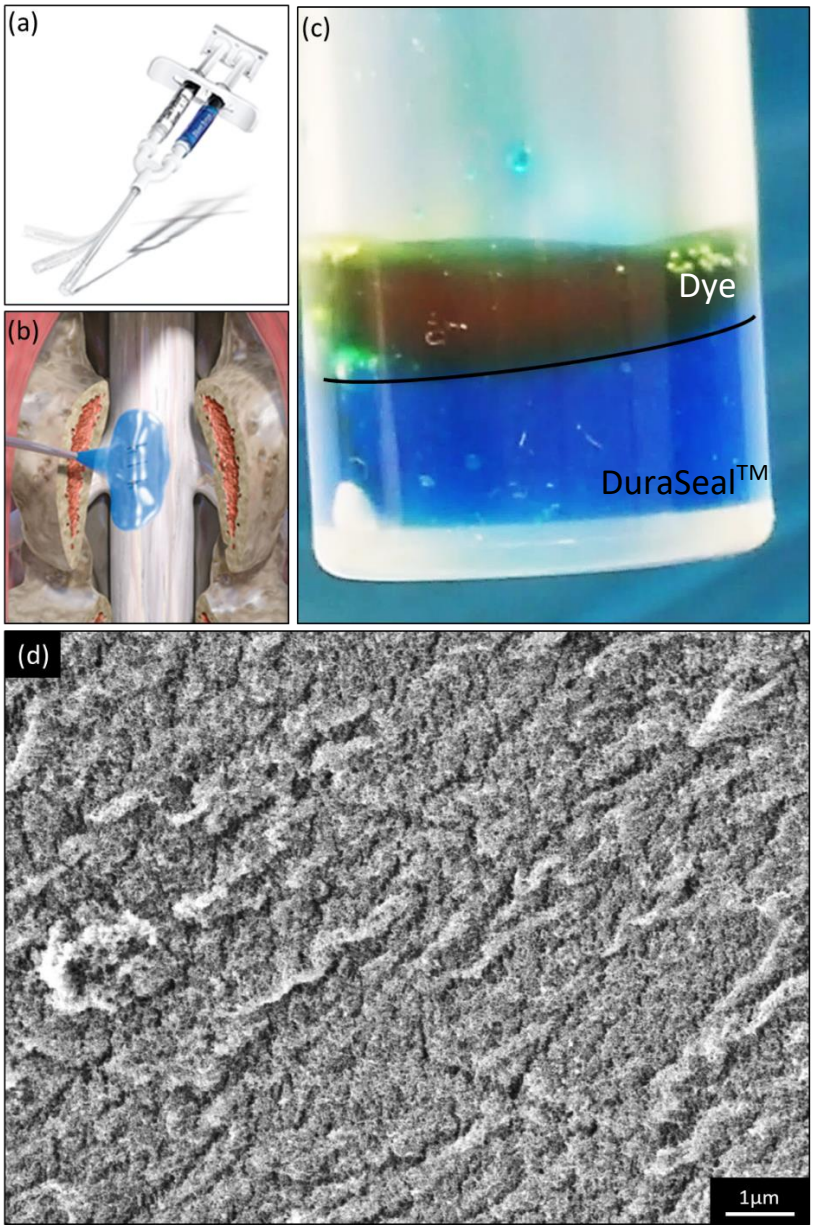

Figure 3.1: DuraSeal™ does not support permeation of liquid *(a) DuraSeal™ product comes as two separate components* (158)*. (b) DuraSeal™ is licensed for use as a dural sealant post spinal surgery* (219)*. (c) DuraSeal™ (blue) does not demonstrate permeation of a dye (red) after 24 hours. The black line indicates the DuraSeal™-dye interface. (d) SEM demonstrating the lack of porosity in DuraSeal™. Scale bar = 1µm.*

3.3.2 DuraGen™ supports NSC growth

DuraGen™ demonstrated the ability to rapidly (within 5-10 seconds) absorb medium (**figure 3.2a-b**) when applied to a dry sample. From a visual assessment, ca 25-40% expansion of the material was observed as the medium was absorbed. Under light microscopy DuraGen™ demonstrated an obvious, highly porous structure (**figure 3.2c**). Pore size appeared variable on visual inspection. SEM of DuraGen™ confirmed its highly porous structural network (**figure 3.2e-f**). The pore diameter was highly variable with an average size of 25.9 ± 14.3 μm. When seeded with dissociated NSCs, initial light microscopy showed cells infiltrating the material's pores. In order to prove that DuraGen™ can act as a cell delivery matrix, it was important to obtain early evidence that cells will adhere to the matrix. After ICC on pilot DuraGen™ samples, the adhesion of NSCs to the matrix was evident (**figure 3.2d**) and there was an irregular cell distribution throughout the material with no obvious pattern.

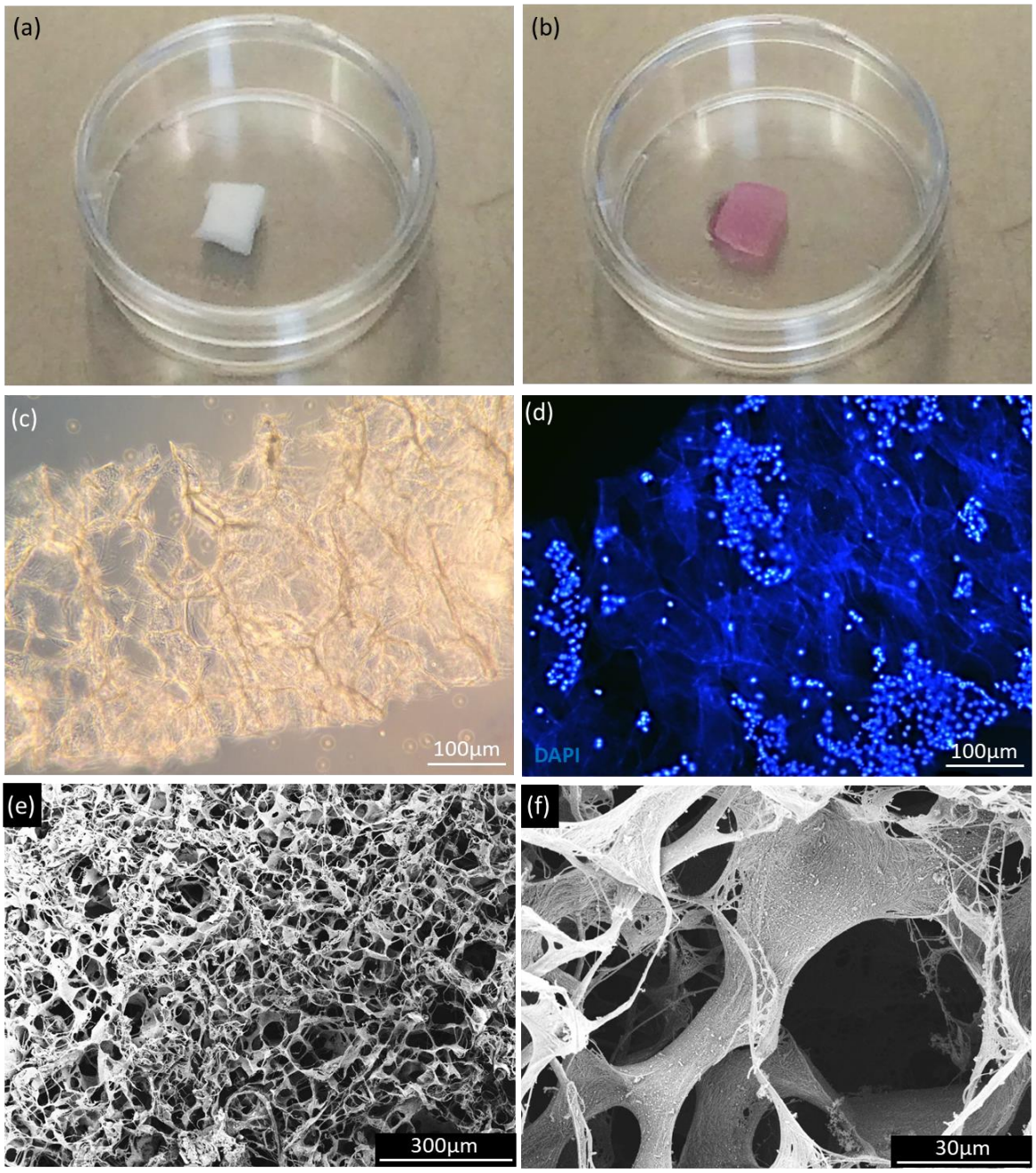

Figure 3.2: Porous DuraGen™ structure demonstrates cell adherence *(a) dry DuraGen™ sample before processing (b) DuraGen™ after application of media demonstrates absorption with evidence of swelling. (c) DuraGen™ under light microscopy demonstrates an obvious porous structure. (d) Balls of NSCs adhere to the DuraGen™ structure. (e) and (f) SEM at x100 magnification and x1000 magnification respectively show the porous structure of DuraGen™.*

3.3.3 Preliminary experiments established optimal parameters for cell growth, ICC and microscopic analysis in DuraGen™

3.3.3.1 DuraGen™ thickness optimisation

DuraGen™ seeded at full thickness c.a. five millimetres demonstrated presence of cells at the cut edges of the materials but none centrally (**Figure 3.3a**). When the thickness was reduced to 500µm, 250µm and 100µm it was observed that NSCs were distributed more evenly throughout the DuraGen™ sheet. It was evident that 250µm was the most suitable for cell growth and visualisation with ICC (**Figure 3.3c**). 250µm slices allowed the best visualisation of cell morphologies of all three slice thicknesses and also contained more cells than the thinnest slice (100µm). By contrast, 500µm sheets obscured clear visualisation of cellular morphologies (**Figure 3.3b**). Additionally, DuraGen™ sliced to a thickness of 100µm contained fewer cells (**Figure 3.3d**) and appeared more friable on handling. On this basis DuraGen™ was processed at 250µm for all further experiments.

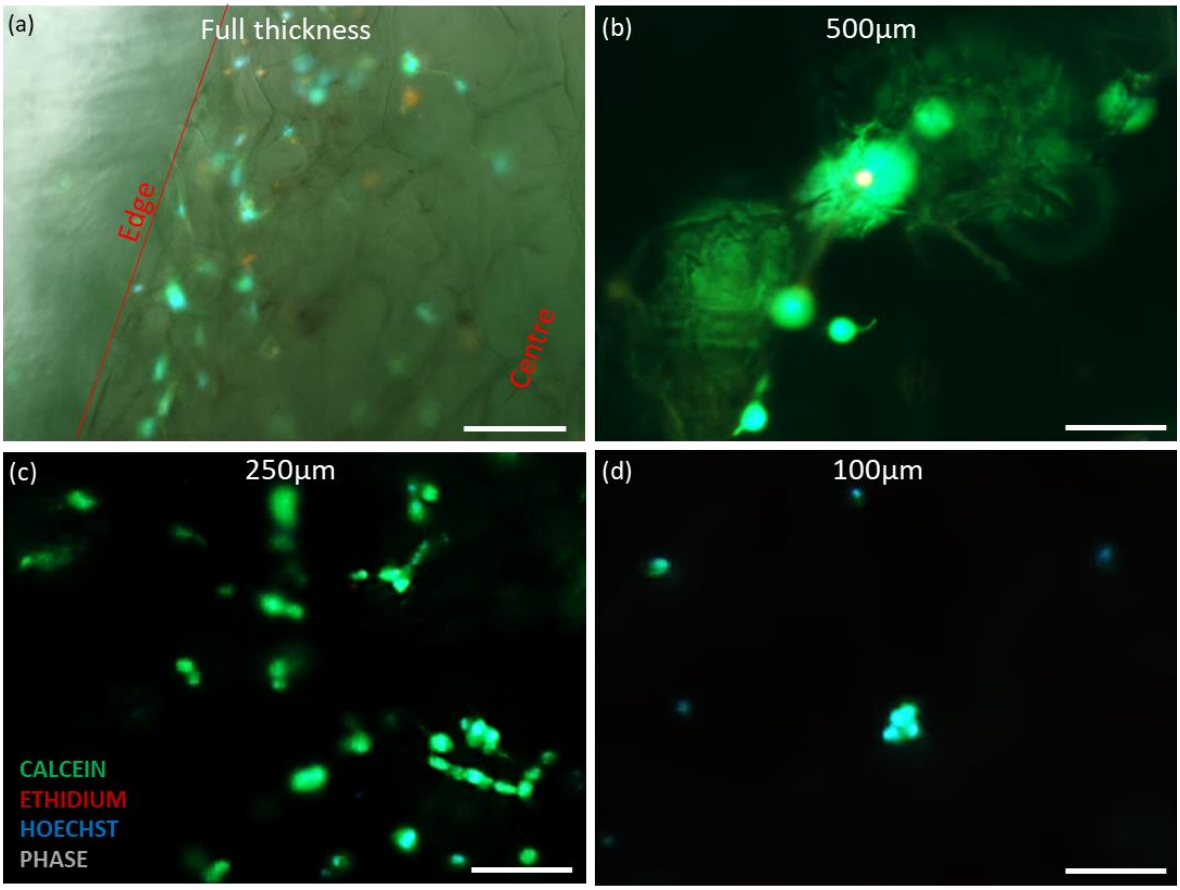

Figure 3.3: Early pilot studies show need for optimisation protocols. *(a) Image courtesy of Farhana Chowdhury: Human astrocytes growing at the edge of the full thickness DuraGen™ slice. Red line depicts the edge of the material. The edge and centre of the matrix are indicated. (b) 500µm slice of DuraGen™ obscures NSCs growing within matrix at 24 hours; (c) 250µm slice of DuraGen™ allows optimal visualisation of NSCs in 3D within the matrix at 24 hours; (d) the 100µm slice of DuraGen™ shows few NSCs within the matrix at 24 hours. Scale bar = 50µm in all images.*

3.3.3.2 Optimal cell seeding density for DuraGen™

Pilot investigations into optimal cell seeding density for DuraGen™ demonstrated higher numbers of cells adhered to the matrix, on visual inspection, with a higher seeding density ($1x10^6$ cells/mL) compared to the lower seeding density ($5x10^5$ cells/mL) (**figure 3.4a-b**). There was no significant

difference in cell viability at 24 hours after seeding between low and high seeding density groups (p-value=0.574, two sample T-test, n=3) (**figure 3.4c**). Therefore, it was established that $1x10^6$ cells/mL would be most suitable for all further analysis.

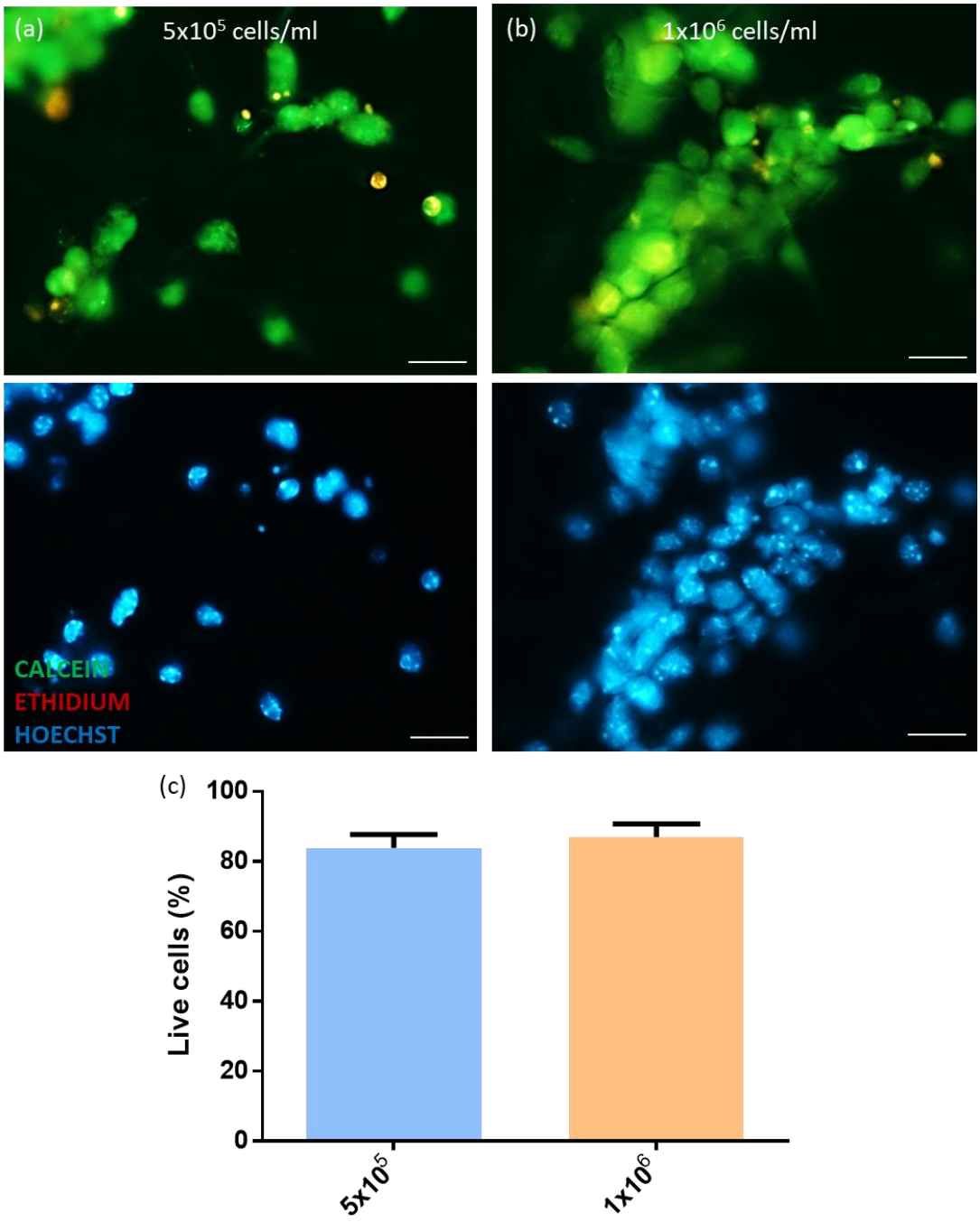

Figure 3.4: High cell viability in both high and low-density samples. *(a) Fewer cells adhered to DuraGen™ matrix at lower seeding density of 5x10^5 cells/mL. (b) High number of cells adhered to DuraGen™ with a higher seeding density of 1x10^6 cells/mL. The corresponding nuclei are displayed beneath images (a) and (b). Scale bars = 25µm. (c) Bar graph displays no difference in the cell viability at differing densities (p-value > 0.05, two-sample T-test, n=3).*

3.3.3.3 ICC protocols required optimisation for use with the DuraGen™ matrix

Preliminary experiments utilising standard monolayer ICC protocols did not sufficiently stain cells in the centre of the material. Moreover, the DuraGen™ fibres were also found to be stained confounding the interpretation of results (**figure 3.5a**). Briefly, standard ICC protocols involve overnight primary antibody incubation and a two-hour secondary antibody incubation. All washes are carried out three times for five minutes each. Therefore, the standard protocols utilised for collagen gels previously used in the laboratory were trialled with incubation times and washes increased (**for details see section 2.5.7**). After these adjustments were made, cell staining increased whilst background fibre staining decreased allowing better visualisation of cell morphologies. Vectashield with DAPI was applied to the matrix prior to microscopic analysis but this led to fibre staining also (**figure 3.5b**). By contrast, when incubated with Hoechst dye for one hour and washed three times this fibre staining decreased.

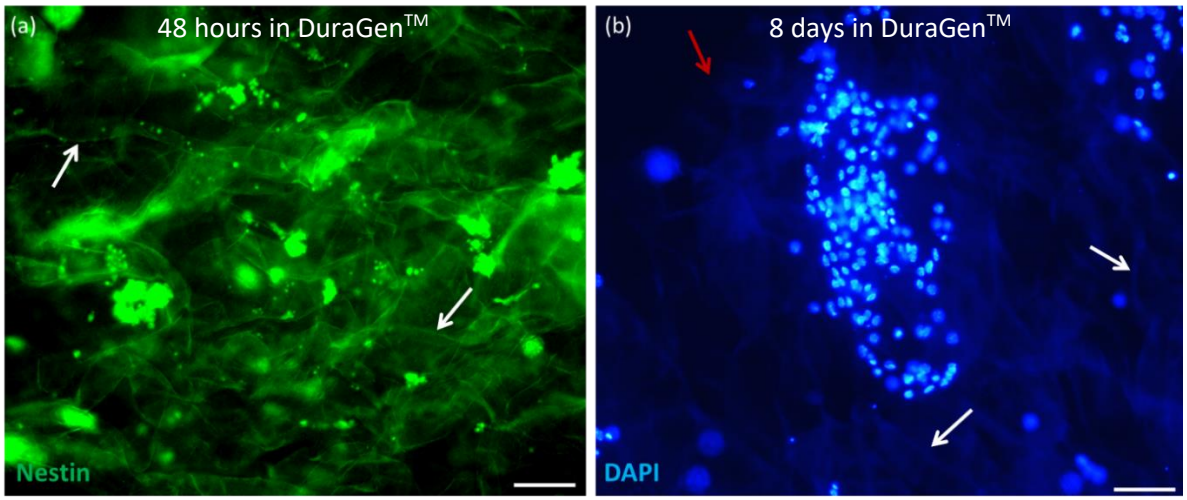

Figure 3.5: DuraGen™ fibres stained by ICC protocol requiring experimental optimisation *(a) NSCs in DuraGen™ at 48 hours with significant DuraGen™ fibre staining. Arrows indicates DuraGen™ fibres. (b) Nuclei of differentiated cells at day eight in DuraGen™ stained with Vectashield with DAPI demonstrating fibre staining. White arrows indicate the DuraGen™ fibres, red arrow indicates the edge of the DuraGen™ matrix. Scale bars = 100µm.*

3.3.4 DuraGen™ does not have adverse effects on the key cellular properties of NSCs

3.3.4.1 High NSC viability in DuraGen™ across all time points

To assess the safety of the biomaterial for NSCs, cell viability assays of live and dead cells along with counts of pyknotic nuclei were carried out at an early (24 hours), intermediate (eight days) and late time point (12 days). Pyknosis (defined as the condensation of chromatin within the nucleus caused by necrosis or apoptosis) was detected by evidence of a hyperdense, small and/or fragmenting nucleus (220) (**figure 3.6b**). NSCs and differentiated cells displayed high proportions of live cells across all time points (≥ 87.0 ± 3.74%) and a low proportion of pyknotic nuclei (≤ 7.48 ± 1.51%) (**figure 3.6a-d**). There was no significant difference between the proportions of live cells in DuraGen™ at any time point (p-value = 0.179, one-way ANOVA, n=3). There was no significant

difference in the proportions of pyknotic nuclei at all time points (p-value = 0.297, one-way ANOVA, n=3).

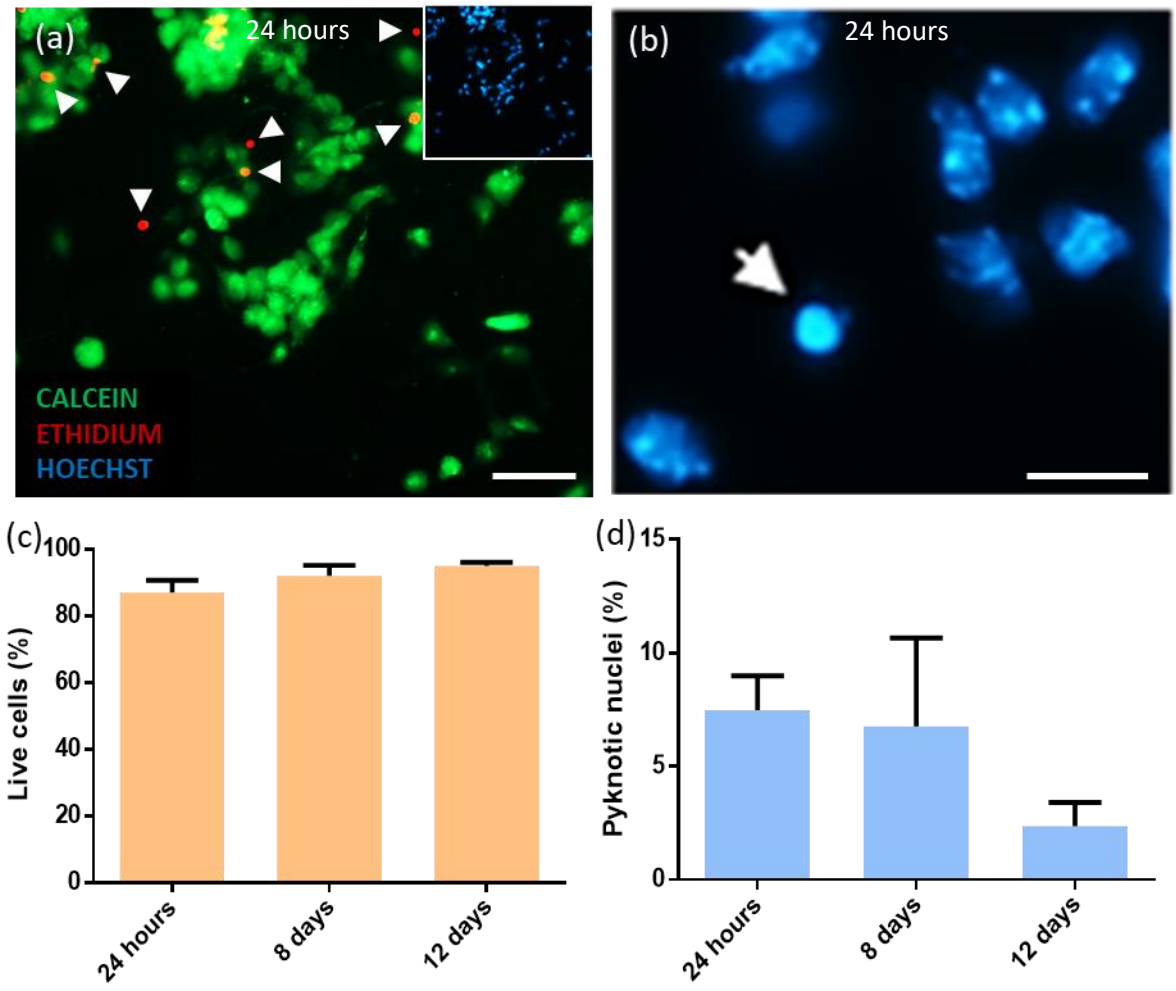

Figure 3.6: High cell viability in DuraGen™ across all time points. *(a) Representative fluorescence image at 24 hours demonstrating live cells stained with calcein and dead cells stained with ethidium homodimer-1 (arrows indicate dead cells), the insert demonstrates nuclei stained with Hoechst dye. Scale bar = 50µm. (b) Example pyknotic nucleus (arrow) surrounded by healthy nuclei. Scale bar = 20 µm. (c) Bar graph displays consistently high cell viability across all time points. The difference between time points was not significant (p-value > 0.05, one-way ANOVA, n=3). (d) Bar graph shows low proportion of pyknotic nuclei across all time points. The differences between time points were not significant (p-value > 0.05, one-way ANOVA, n=3).*

3.3.4.2 NSCs maintain stem cell phenotype in DuraGen™ matrix

The safety of a transplant substrate is often assessed by its ability to maintain the cells in a desired phenotype. In DuraGen™, a high proportion of nuclei were positive for nestin, a NSC cytoskeleton marker (93.1 ± 2.84%) and a similarly high proportion of nuclei were positive for Sox-2, a NSC-specific transcription factor (95.5 ± 0.42%), both at 48 hours. Cells demonstrated clear NSC morphologies with processes and were associated with rounded nuclei. NSCs were randomly orientated with no obvious pattern to the direction of processes. Processes extend into multiple planes within the matrix requiring a Z-stack imaging technique to fully detect them (**figure 3.7 and Video 3.1**).

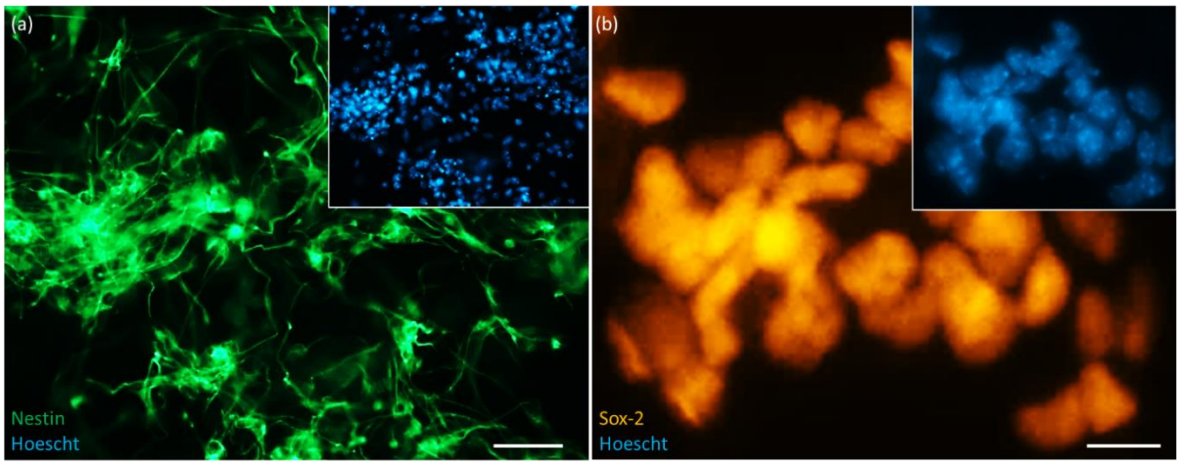

Figure 3.7: NSCs retain their stem cell phenotype in DuraGen™. *Representative fluorescence image (a) of a complex network of NSCs, inset: nuclei (**Video 3.1 in supplementary materials**). 93.9 ±2.84% of cells positive for nestin at 48 hours (n=3). Scale bar = 50µm. Representative fluorescence image (b) of a high level of Sox-2 staining of NSCs in DuraGen™. 95.5 ±0.42% of cells were positive for Sox-2 at 48 hours (n=3). Scale bar = 10µm.*

3.3.4.3 DuraGen™ allows proliferation of NSCs and astroglial lineage cells

NSCs are self-renewing, hence it was important to establish if DuraGen™ would support the proliferation of these cells. At all time points investigated, there was evidence of cell proliferation (**figure 3.8c**). At 24 hours, 25.6 ± 4.07% of cells expressed EdU (**figure 3.8a**). This decreased to 7.21 ± 1.41% at eight days once the cells had differentiated. The difference between the proliferation rate at 24 hours was statistically different to at eight days (p-value = 0.008, two sample T test, n=3). The majority of cells (ca. 71.8%) that showed EdU labelling in the differentiated population were astroglial lineage cells (GFAP positive) (**figure 3.8b**). Cells that proliferated and did not stain for astrocytic marker (EDU positive and GFAP negative) are likely to be undifferentiated NSCs.

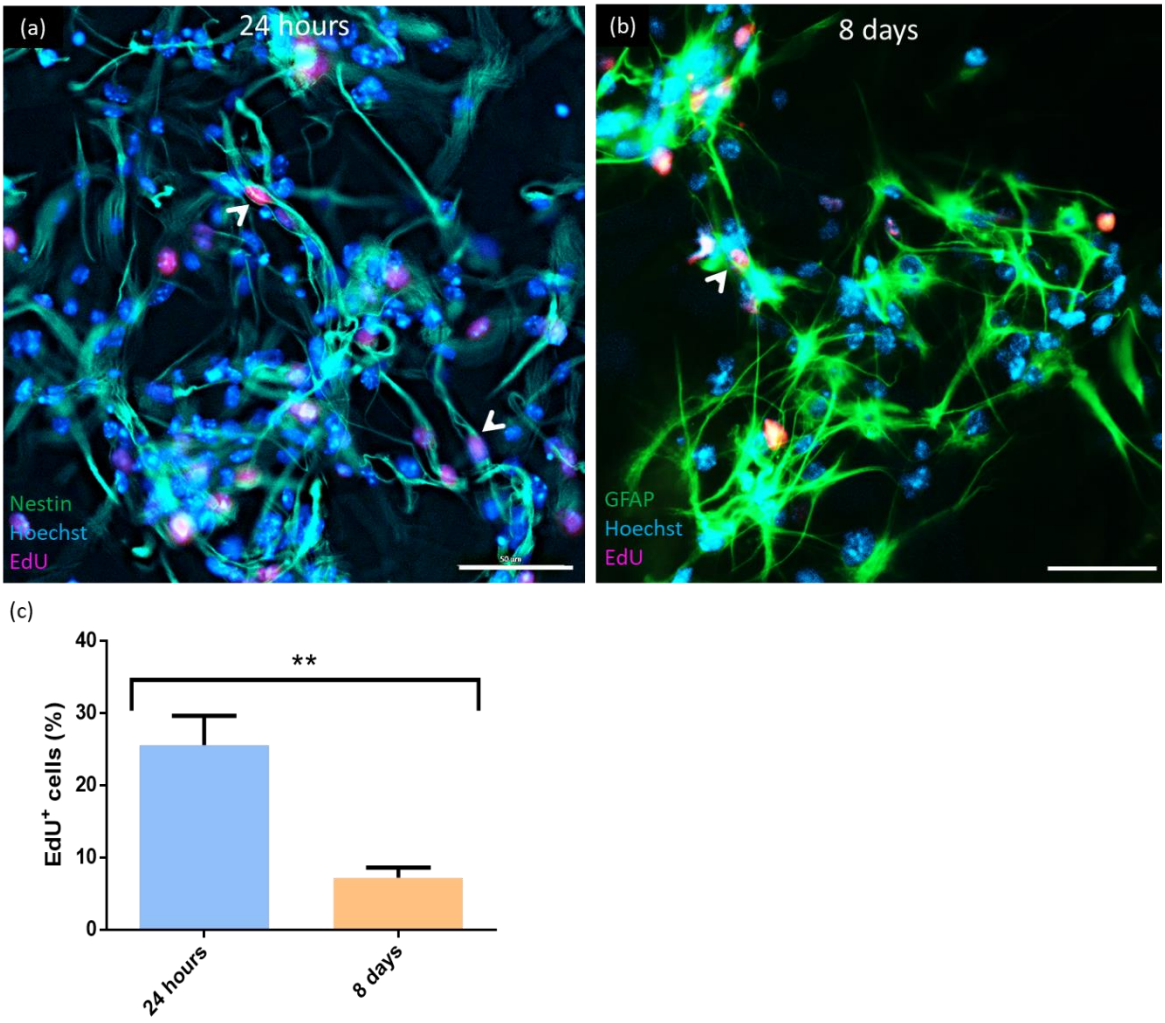

Figure 3.8: Cells proliferating at 24 hours and at eight days *in vitro*. *Representative fluorescence images demonstrating (a) proliferation of NSCs (nestin) observed at 24 hours in DuraGen™, arrows indicate proliferating NSCs, and (b) proliferation of differentiated cells. Arrow indicates proliferating astrocyte (GFAP). (c) 25.6 ±4.07% of cells proliferated after 24 hours and 7.21 ±1.41% of cells after eight days proliferated (EdU) within a 16-hour period. Statistical difference was analysed between the two time points and is: **p-value < 0.01 (two sample T-test, n=3). Scale bar = 50µm.*

3.3.4.4 DuraGen™ supports differentiation of NSC into astroglial lineage cells, neurons and oligodendrocytes

Six days following differentiation induction (eight days in DuraGen™) three classes of daughter cells – neurons, astroglial lineage cells and oligodendrocytes were observed (**figure 3.9**). The highest proportion (79.6 ± 6.28%) were that of astroglial lineage cells which demonstrated normal stellate morphologies. 18.6 ± 5.10% of cells were of the neuronal lineage, staining for TUJ1. Neurons demonstrated short processes at this early time point. Processes extended in multiple directions without an obvious pattern or directionality in growth. The smallest proportion of cells were oligodendrocytes, 2.12 ± 0.96% were positive for MBP (**figure 3.10**). The oligodendrocytes demonstrated highly branched morphologies often extending into multiple planes. Some nuclei did not stain for any marker, it is hypothesized that these are undifferentiated NSCs.

Across all time points there was no significant change in the proportion of each cell type, with time. Neurons demonstrated evidence of maturation across the time period displaying increasing complexity in their networks (**figure 3.9**). Axon length increased two-fold from day eight to day 16 ($p=0.02$, one-way ANOVA with Tukey and Fisher post hoc multiple comparison tests, $n=3$) (**figure 3.11a-c**). Triple staining of DuraGen™ revealed all three cell types in the same field (data not shown).

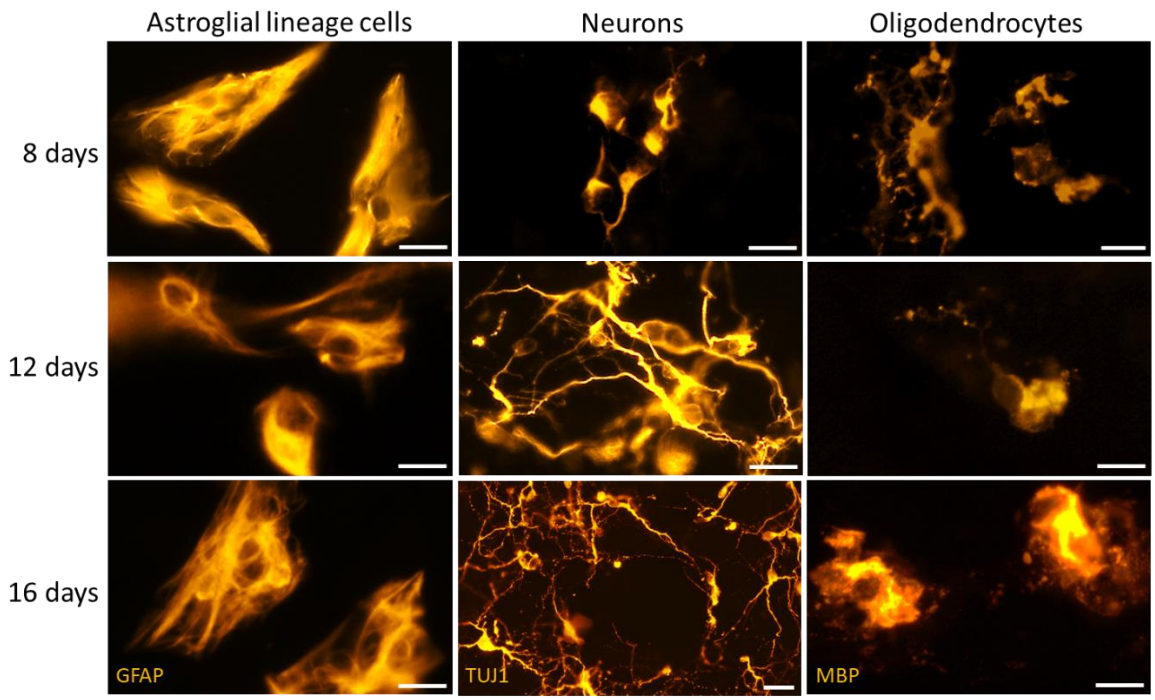

Figure 3.9*:* **DuraGen™ supports maturation of each cell type over time**. *(a) Astroglial lineage cells display normal morphology up to 16 days. (b) Axons increase in length and networks increase in complexity as time in vitro increases. (c) Oligodendrocytes display branched 3D morphology. Each scale bar = 25µm.*

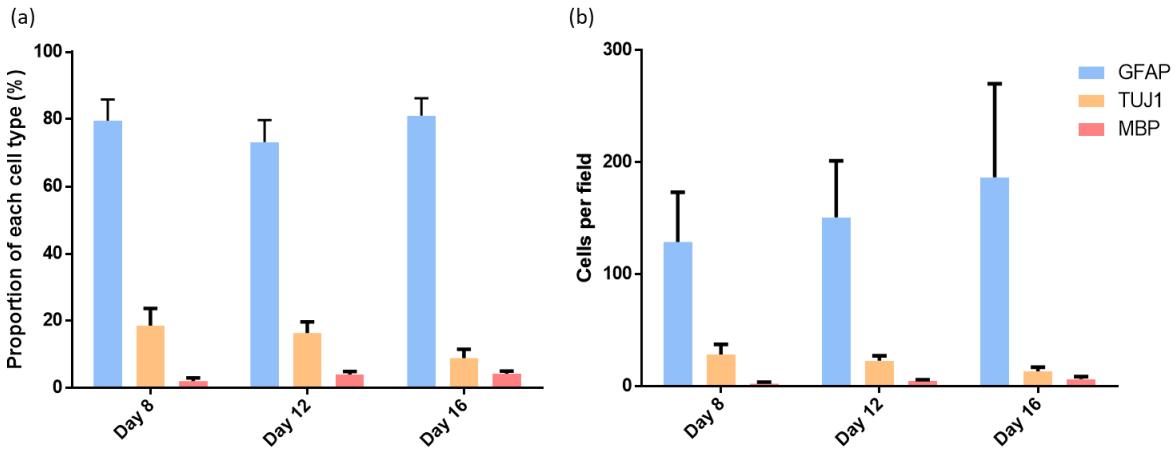

Figure 3.10: DuraGen™ demonstrated the capacity to support growth of all three types of daughter phenotypes. *(a) The proportions of each daughter cell type remain the same. (b) The absolute numbers of each cell type remain the same across the time points. There was no significant difference in proportion of each cell type across all time points (p-value > 0.05, one-way ANOVA, n=3).*

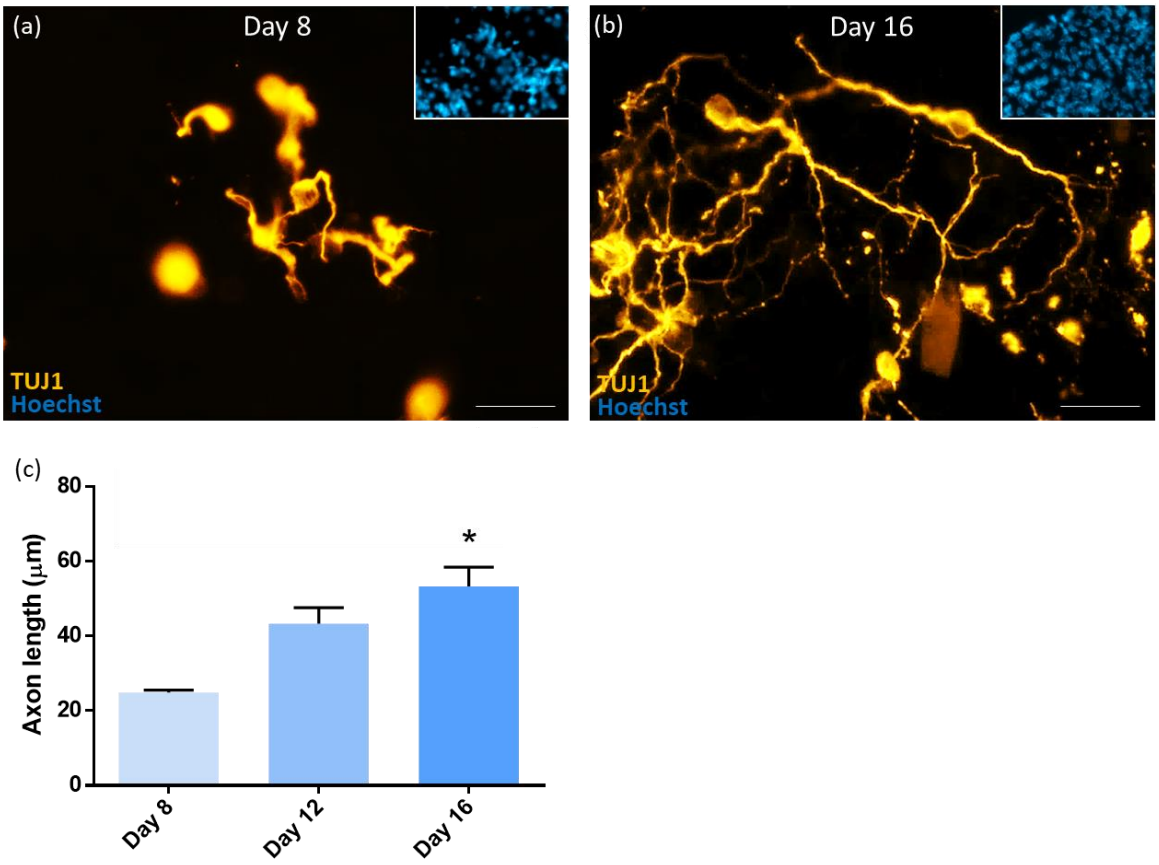

Figure 3.11: DuraGen™ allows extension of axons through matrix. *(a) Short processes of neurons growing in DuraGen™ at eight days. (c) Elongated processes of neurons growing in DuraGen™ at 16 days. (c) Axon length increased two-fold from day eight to day 16. Statistical difference is: *p-value < 0.05 vs day 8 (one-way ANOVA with Tukey and Fisher post hoc multiple comparison tests, n=3). Scale bar = 25μm.*

3.3.5 3-D spatial distribution of cells throughout the matrix

The distribution of the NSCs (48 hours) and later the differentiated cells (eight days) within the DuraGen™ matrix were investigated to study the distribution within the matrix. Within each field viewed microscopically, cells appeared to be grouped together. In some fields they followed the patterns of the fibres of the DuraGen™ matrix.

When viewing cellular distribution across the matrix in the horizontal plane (**figure 3.12**), cells were observed in all sections of the matrix and there was no significant increase in the number of cells in any specific region in NSCs (48 hours) or differentiated cells (eight days) ($p>0.05$, one-way ANOVA, n=3) (**figure 3.13a-b**). Previous studies investigating collagen materials have detected a high number of cells sinking to the bottom of the material (221). In DuraGen™ cells did not appear to sink to the base of the matrix but were distributed throughout the depth of the matrix at 48 hours and eight days (**figure 3.13c-d**).

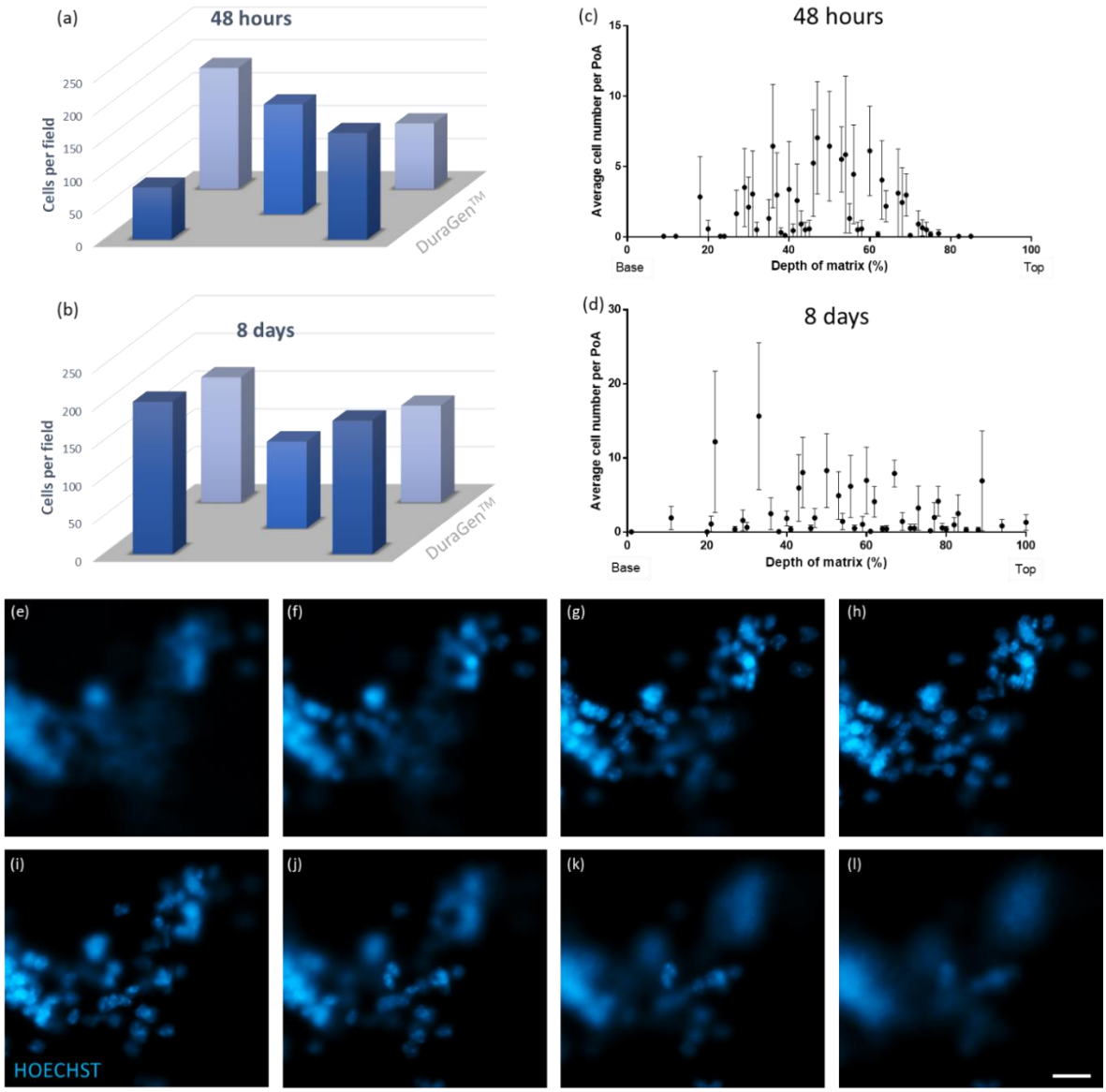

Figure 3.12: No difference in the spatial distribution in the horizontal or vertical plane. *(a) and (b) represent the average number of cells per field taken in each of the five spatial locations. No section of the material showed preferential distribution of NSCs (48 hours) or differentiated NSC (eight days) growth (p-value >0.05, one-way ANOVA for 48 hours and eight days, n=3). (c) and (d) represent the average number of cells per PoA considered to be each slice of a Z-stack. The cells were distributed throughout the depth of the matrix at both 48 hours and eight days (n=3). Fluorescent images (e-l)*

demonstrate a z-stack at eight days with nuclei distributed throughout the DuraGen™ matrix in 3D. Scale bar = 50µm.

3.4 Discussion

3.4.1 DuraGen™ supports NSC growth, proliferation and differentiation

We have demonstrated for the first time the capacity of a neurosurgical, collagen-based biomaterial to support the growth of NSCs, supporting the concept that it can be used as a cell delivery matrix. This chapter demonstrates that DuraGen™ can successfully support a population of NSCs without any significant impact on the cellular properties assessed. Importantly, high survival, maintenance of stem cell phenotype, continued proliferation and differentiation into all three daughter cell types within the material demonstrates its capacity to act as a protective matrix for the delivery of stem cells. To the best of our knowledge, this also represents the first time a surgical grade material has been shown to support a major neural cell transplant population.

The differentiation profile of NSCs in DuraGen™ did not widely differ from that previously seen on glass, thought to be the gold standard for *in vitro* culture, and from that of other types of collagen. Table 3.1 displays the differing differentiation profiles on a range of materials. When comparing DuraGen™ to monolayer NSC culture on glass and another type one collagen, rat tail collagen, there were similar proportions of astroglial lineage cells, neurons and oligodendrocytes. Rat tail collagen is a soft material. We do not know the stiffness of DuraGen™. Softer materials have been previously shown to promote neurogenesis (222). Neurogenesis is important when considering clinical translation. As described in section 1.1.4, the spinal cord is a 'non-permissive zone' for neuronal differentiation (24,28). Therefore, if neuronal differentiation can occur in DuraGen™ it might counteract the non-permissive environment at the SCI site.

	Astroglial lineage cells	Neurons	Oligodendrocytes
DuraGen™	79.6%	18.6%	2.12%
Glass	82%	12%	4%
Rat tail collagen	80%	16%	4%

Table 3.1: *Differentiation profiles of NSCs on a variety of material substrates. Figures for glass and rat tail collagen are from* (223)*.*

3.4.2 The pore size of DuraGen™ allows infiltration of NSCs

The pore size in DuraGen™ was highly varied and had an average size of 25.9 ± 14.3 µm. The average size of an NSC is approximately 15µm, hence they can easily pass through the material's pores. There is a broad range of pore size within biomaterial scaffolds. A 2mg/ml collagen gel has a pore size of 2.84 ± 0.94µm and a fibrin gel has a pore size of 1.69 ± 0.33 µm (224). Other materials utilised for cell transplantation have a nanoporous structure, such as alginate which has pores 5.2 – 7nm in size (225). Chitosan scaffolds and PEG hydrogels have larger pore sizes of 30-90 µm and 41-134 µm respectively (226,227). Brauker et al suggest that for cell encapsulation, a scaffold must have a pore size of 0.8-8µm (228). Lim et al describes a necessity for larger pore sizes, finding that greater than 90µm increased cell infiltration and vascularisation (226). Nonetheless, Integra LifeSciences report that DuraGen™ allows vascularisation to occur (142). The large variety in pore sizes of differing biomaterials suggests that none is the gold standard. It is likely that different cell types and different applications require different pore sizes. What is evident, is that pore size affects cellular behaviour and DuraGen™, with its mid-range pore size, has demonstrated the ability to support a viable population of NSCs.

3.4.3 The structure of DuraGen™ produces a random alignment of axons

DuraGen™'s fibrous structure has no directionality. The pores are randomly sized and spaced. This led to processes of the NSCs growing in all directions with no obvious pattern. When the NSCs had differentiated, the axons of the neurons also extended in a random alignment. Random alignment of axons could be problematic for the success of a transplant in SCI. For example, a rat contusion SCI study found that transplantation of NSCs caused uncontrolled axonal sprouting which led to allodynia in the rats (91).

There are some possible solutions to the alignment of cells within DuraGen™. Mechanical tension placed across the material could encourage linear growth. The matrix is amenable to stretch. Alternatively, magnetic alignment of collagen fibres has previously been demonstrated. Here, liquid collagen was subjected to a bipolar magnetic field during the setting process. This produced linear alignment of the collagen fibres (229). DuraGen™ is a pre-made material, to change the fibre alignment it would be necessary to change the manufacturing process. Growth factors encourage directional axonal growth. Bonner et al injected neuronal restricted- and glial restricted- precursors into dorsal column lesions in rats. After seven days, they injected lentiviral vectors, expressing BDNF, 2.5 or 5mm rostral to the lesion. This created a neurotrophin gradient. In the groups, exposed to the neurotrophin injection, there was an increase in directional axon growth (230). The use of a neurotrophin gradient with DuraGen™ may promote directional axonal growth through the matrix.

3.4.4 Pre-differentiated implantable neural circuit

We have for the first time produced a viable culture of the three major cell types of the CNS in a neurosurgical grade material. After differentiation induction, astroglial lineage cells, neurons and oligodendrocytes were successfully growing within the matrix. All three cell types were visualised in the same field. It was unclear whether the cell types were interacting with one another. All three cell types were often in close proximity but ICC with fluorescent microscopy could not provide

information on cell interactions. For instance, it would be important to discover whether the oligodendrocytes were myelinating the axons within the matrix.

The construct containing these three cell types, a neural circuit, could be transplanted into the site of a SCI. There are many benefits of a pre-differentiated implantable neural circuit. Firstly, it provides the opportunity to implant post-mitotic cells (neurons and oligodendrocytes) previously considered to be challenging to transplant (231). Secondly, pre-differentiated lineage cells have shown improved survival and integration into the CNS in rat SCI (96).

3.4.6 A clinical grade material has the potential to be accelerated to clinical trial

These initial trials utilising this FDA-approved biomaterial scaffold demonstrate the foundation to begin further research into the potential use of DuraGen™ for neuroregenerative therapies. Here we investigated two seeding densities and both demonstrated high viability. It is entirely feasible that the DuraGen™ matrix could be seeded with a higher density of cells than $1x10^6$ cells/ml to increase the numbers of cells delivered for clinical therapy.

We also utilised samples of DuraGen™ at an optimised thickness of 250µm to achieve the aims of this study. In clinical practice, it may be possible to use multiple, thin strips of DuraGen™ at the lesion site. SCI lesions are likely to be an irregular shape. It may offer the advantage of conformability if the DuraGen™ is sliced to 250µm. To utilise the full thickness of DuraGen™, an improved cell loading technique may be required. Where other researchers have utilised DuraGen™ at its full thickness, they have used alternative methods. For instance, Adesida et al seeded the matrix with a small of volume of very high-density meniscus fibrochondrocytes and allowed these to adhere to the material for 15 minutes. Then, following this incubation time the matrix was flooded with medium (147). This method was unnecessary for the aims of this trial but offers a different way to improve the cell density and distribution within larger sections of the

scaffold. This method may be useful for clinical manufacture. It offers the advantages of improving cell attachment so hence conserving precious cell transplant populations.

Chapter 4: Genetically engineering NSCs within a neurosurgical grade material

4.1 Introduction

A cell transplant population encapsulated within a supportive biomaterial scaffold addresses many pro-regenerative goals, such as encouraging axonal regeneration and bridging the cystic cavity. To maximise therapeutic benefit, cellular populations can be genetically engineered to produce trophic factors increasing the likelihood of enhanced regenerative outcomes. A construct formed of a genetically engineered cell population encapsulated within a biomaterial scaffold could constitute a single application, combinatorial therapy. To increase the therapeutic benefit of such a construct, the utilisation of a pre-approved neurosurgical grade biomaterial to encapsulate the cells could generate an implantable 'superconstruct' for regenerative applications. A combined nanoengineering and surgical biomaterial delivery approach has never been tested. **Our study intends to investigate the potential of a pre-approved neurosurgical grade biomaterial scaffold, DuraGen™, to encapsulate a transplantable population of NSCs engineered utilising clinically applicable magnetofection and minicircle technology.**

4.2 Aims and objectives

The specific objectives for this chapter are as follows:

I. To successfully genetically engineer NSCs using magnetofection technology and applied magnetic fields to express GFP.

II. To prove that DuraGen™ can support the growth of a genetically engineered population of NSCs.

III. To test two methods of producing the 'superconstruct': 'engineering in situ' versus 'pre-transfection and cell loading'.

IV. To assess the efficacy of transfection of NSCs in DuraGen™.

V. To establish if key safety parameters including cell viability, proliferation and differentiation are impacted by combining genetic engineering methodologies with DuraGen™ construct formation.

4.3 Results

4.3.4 Pilot experiment: In-situ engineering method demonstrated limited GFP expression

The ability to transfect NSCs that have been pre-loaded into the DuraGen™ matrix offers logistical benefits for larger scale manufacture. A protocol whereby cells could be grown within the matrix and then subsequently engineered could be manufactured more easily than engineering the population of cells and then loading into the material. Therefore, the 'engineering in-situ' method was trialled. After 24 hours post transfection, there was no visually detectable GFP expression in any applied field condition. In previous reports of magnetofection on monolayer cultures, NSCs expressed GFP after four hours with numbers peaking at 48 hours where ca. 32.2% were transfected (223). Re-transfection was carried out with no field for all previous conditions. After a further 24 hours, a negligible number of cells (<1%) expressed GFP in the repeat transfection experiment (**figure 4.1**). Due to the lack of success demonstrated with this method of transfection, a two-step method was investigated next.

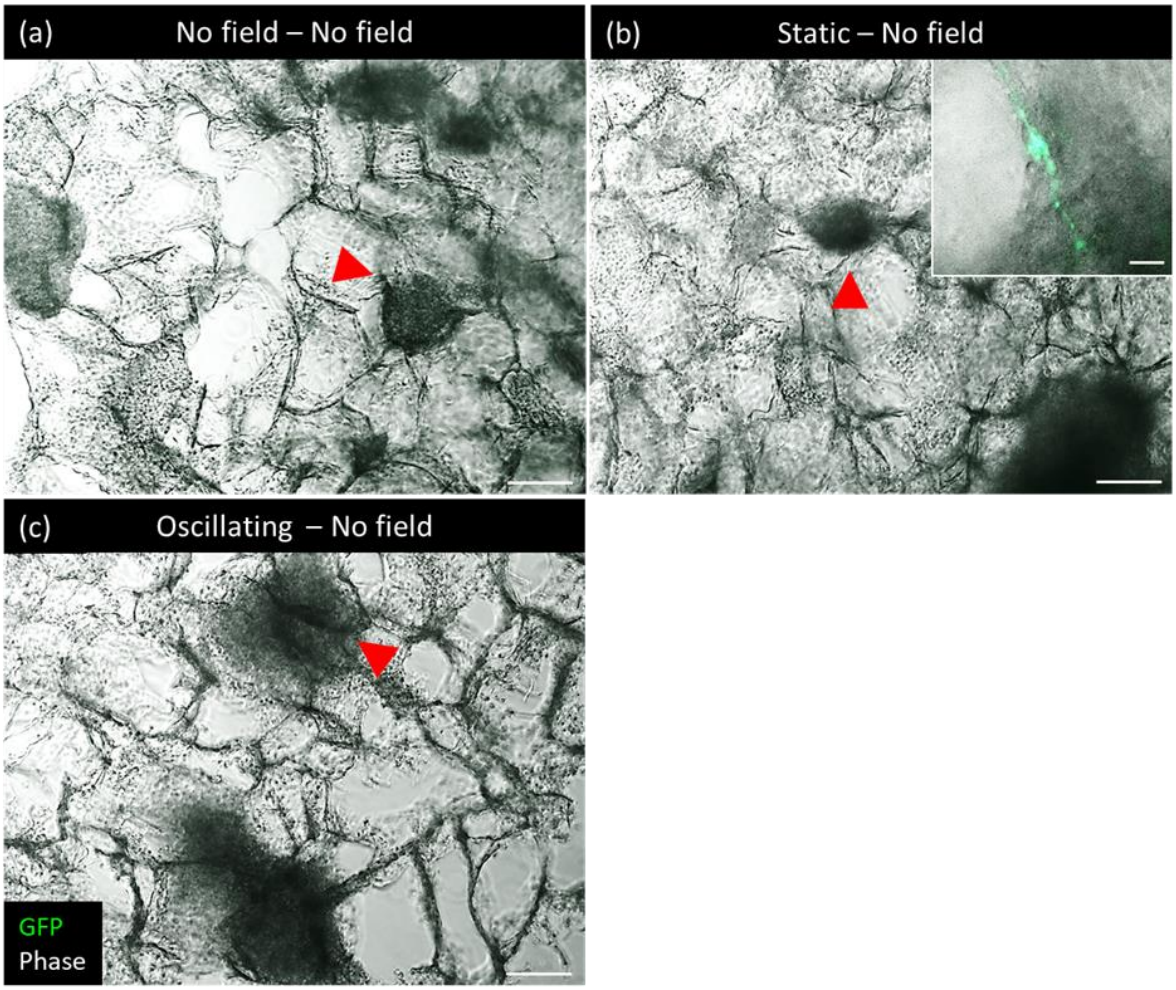

Figure 4.1: Limited success of in-situ engineering. *(a) Two sequential transfections with no magnetic field produced no GFP-expression. (b) Low number of NSCs expressing GFP in DuraGen™ after two successive transfections with mcGFP, the first with a static magnetic field and the second with no field. (c) Initial transfection in an oscillating field, followed by transfection without a magnetic field did not produce any GFP-expression. Red arrows indicate neurospheres within DuraGen™. Scale bar in main images = 100µm, insert = 25µm.*

4.3.5 Pilot experiment: A two-step method could be used to yield genetically engineered NSCs in DuraGen™

The next step was to trial the 'pre-transfection and cell loading' protocol. NSCs were transfected as neurospheres in suspension and then subsequently dissociated into single cells for seeding into DuraGen™ (for details see section 2.7.1).

Prior to transfection, neurospheres appeared evenly sized and round under phase microscopy. Transfection of neurospheres yielded a high proportion of neurospheres containing at least one transfected NSC at 24 hours (94.5 ± 3.62%) (n=3). No transfected cells were seen in any of the control conditions (**figure 4.2**). Post transfection, most neurospheres remained intact with some adhering to the base of the well. This also occurred in the controls.

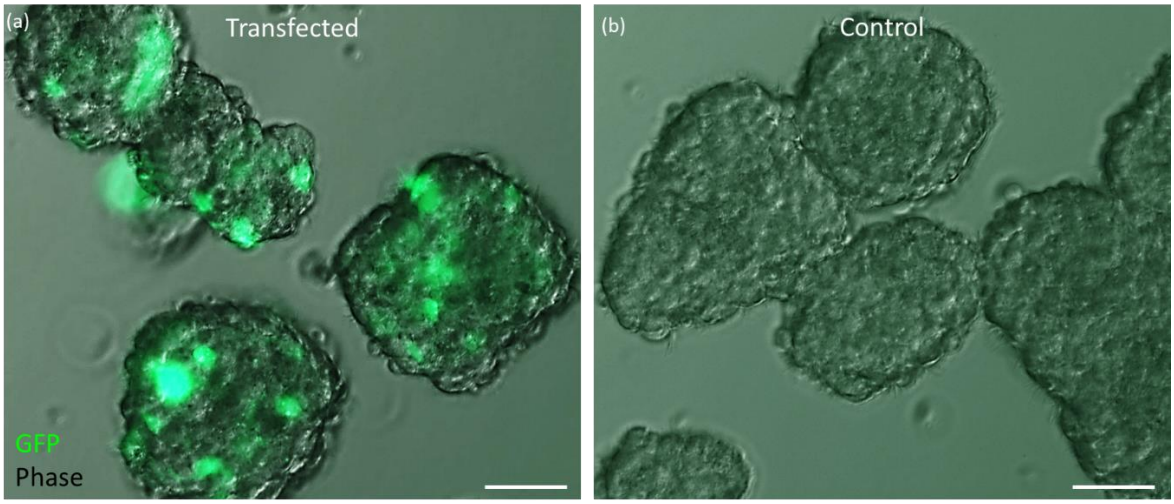

Figure 4.2: NSCs within neurospheres express GFP. *(a) Representative fluorescence image demonstrating transfected neurospheres at 24 hours, 94.5 ± 3.62% of neurospheres had at least one transfected NSC (n=3). (b) Control neurospheres at 24 hours. Scale bar = 50µm.*

For this pilot experiment, transfected neurospheres were dissociated and seeded into 250µm sheets of DuraGen™ (see methods section 2.5.1). Immediate visualisation revealed GFP-expressing NSCs within the matrix. After 24 hours, visualisation under light microscopy revealed that the DuraGen™ matrix had disintegrated in both transfected and control conditions (**figure 4.3**). pH tests of the medium revealed pH 8.5 for both transfected and control. The NSCs had been subjected to multiple passages within a relatively short space of time. This led to a decreasing number of cells in each subsequent passage. The most likely explanation for the disintegration is residual accutase and DNAse solution within the cell suspension, which could not be completely removed during passages due to small volumes of cell suspension. Accutase contains collagenolytic enzymes likely to break down DuraGen™ made predominantly of collagen.

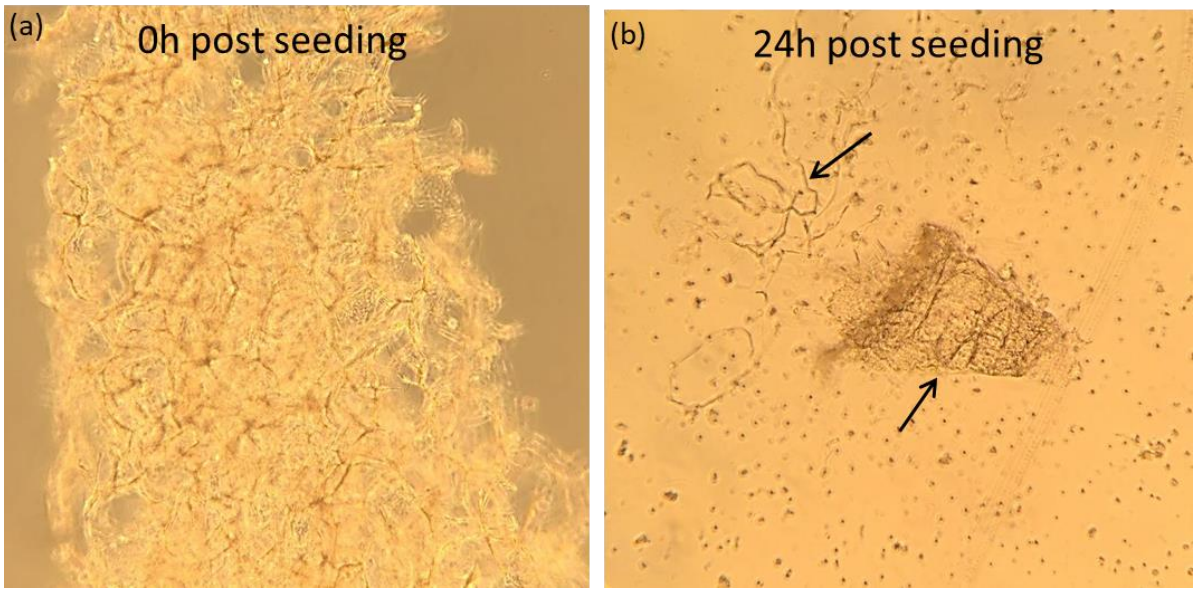

Figure 4.3: DuraGen™ disintegrates 24 hours after seeding with single transfected cells. *Intact DuraGen™ sample immediately after single cells were added (a). Fragments of DuraGen™ (arrows) seen 24 hours after single cell seeding.*

To remove the extra dissociation step identified as the cause of the disintegration, the alternative propagation format for NSCs was used, namely neurospheres. DuraGen™ seeding with neurospheres was trialled. Transfected neurospheres were seeded into DuraGen™ sheets and immediate visualisation under light microscopy was inconclusive in determining whether there was infiltration of the matrix. Seeding DuraGen™ with NSCs in the neurosphere format had not been tested until this stage so it was unknown whether the large balls of NSCs (average size: 100-200µm (232)) would be able to penetrate the pores (size: 25.9 ± 14.3µm) and adhere to the matrix. After 24 hours, nuclear staining revealed neurospheres adherent to the matrix (**figure 4.4**)

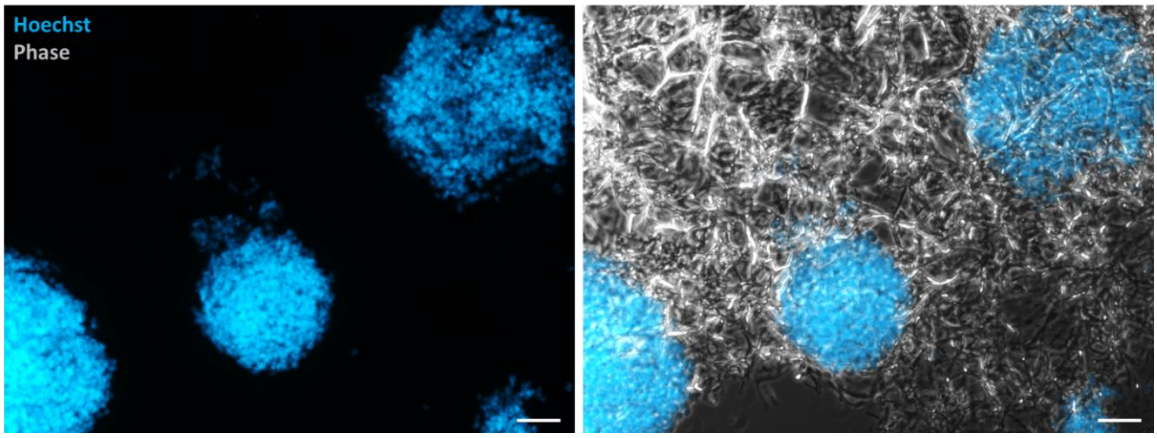

Figure 4.4: DuraGen™ permits neurosphere attachment. *NSCs 24 hours after seeding as neurospheres in to DuraGen™ matrix. Scale bar = 200µm.*

At 24 hours after seeding into DuraGen™ and 48 hours after transfection, GFP expression was observed in NSCs within the DuraGen™ matrix (**figure 4.5**). A high proportion of neurospheres demonstrated at least one NSC with GFP expression, detected by anti-GFP antibody, within DuraGen™ (82.0 ± 3.55%) (n=4). Approximately 7-10% of the NSCs were transfected, this is an estimate due to the reasons described in section 2.8.6. On visualisation, transfected cells were evenly distributed and displayed normal morphologies with normal, rounded nuclei. No transfected cells were detected in any of the control samples.

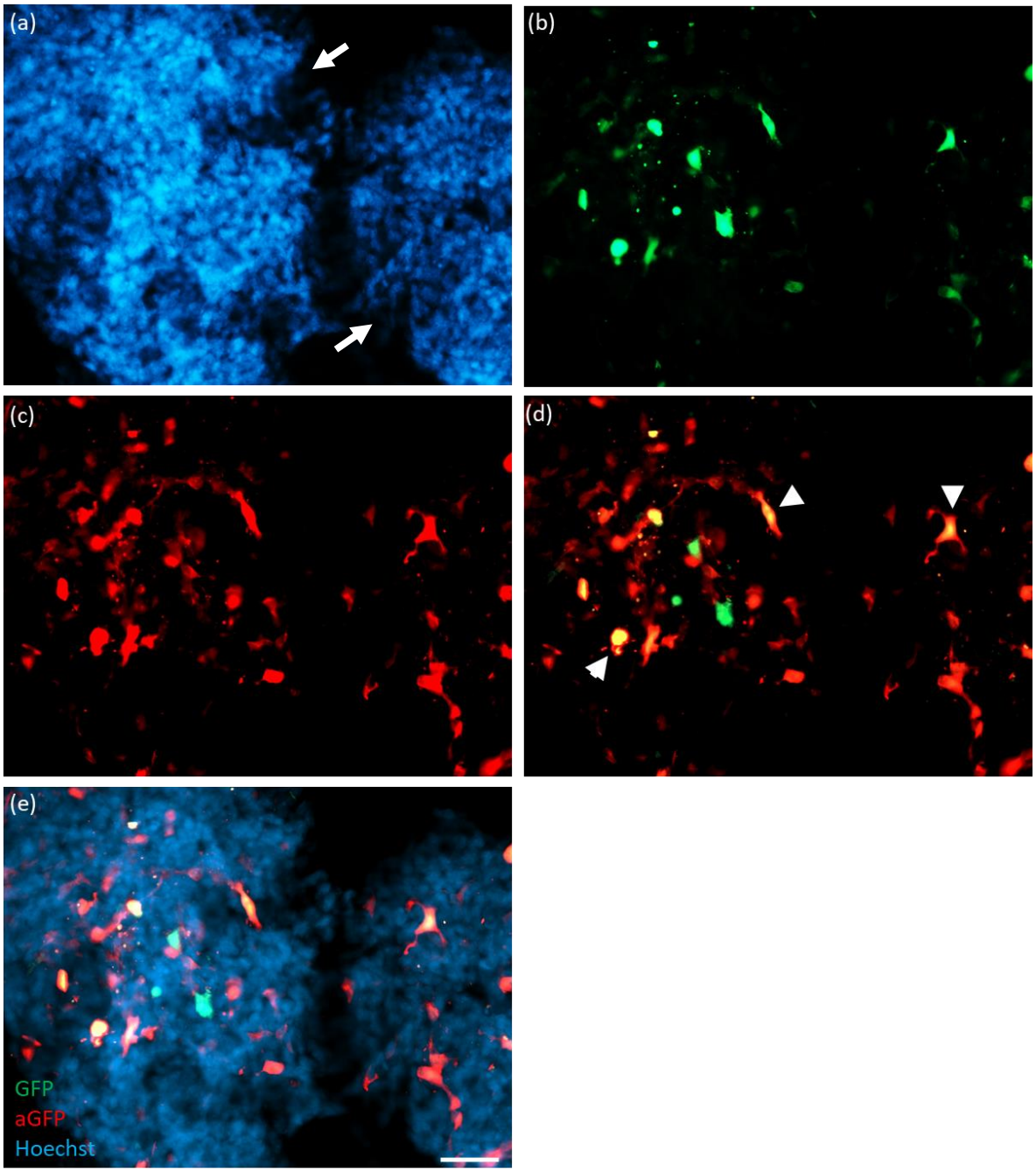

Figure 4.5: Transfected NSCs growing within DuraGen™ matrix. *82.0 ± 3.55% of neurospheres had at least one NSC expressing GFP within DuraGen™ matrix 48 hours post transfection/ 24 hours post seeding into DuraGen™ (n=4) (**video 4.1 in supplementary materials**). Representative fluorescent images (a-e) taken from the same field (a) nuclei of NSCs forming two neurospheres (arrows) (b) GFP expression (c) anti-GFP antibody (aGFP) detects GFP expression. (d) Double merged image*

displaying GFP expression detectability increased by anti-GFP. Arrows indicate NSCs expressing GFP (green) and anti-GFP (red). (e) Triple merged image demonstrates the proportion of GFP expression in NSCs within the DuraGen™ matrix. Scale bar = 50µm.

4.3.6 Genetic engineering and DuraGen™ construct formation did not negatively impact upon key safety parameters

The following safety assays were performed to establish if transfection and DuraGen™ loading impacted upon the properties of NSCs.

4.3.6.1 NSC viability unaffected by transfection and DuraGen™ loading

After 24 hours in DuraGen™, the transfected NSC population demonstrated high viability equivalent to that of the control. A high proportion of transfected NSCs were viable at 24 hours (92.8 ± 2.09%). There was no statistically detectable difference when compared to the control (p-value = 0.392, two sample T-test, n=4) (**figure 4.6c**). Furthermore, there was a low proportion of pyknotic nuclei in the transfected NSCs (5.76 $\pm$ 1.55%) which demonstrated no difference versus the control (p-value = 0.296, two sample T-test, n=4) (**figure 4.6d**). Visually, there was no detectable difference in the distribution of live and dead cells or pyknotic nuclei. The dead cells were evenly spaced throughout the matrix and no area preferentially exhibited dead cells. This indicates sufficient diffusion of nutrients throughout the 3D matrix.

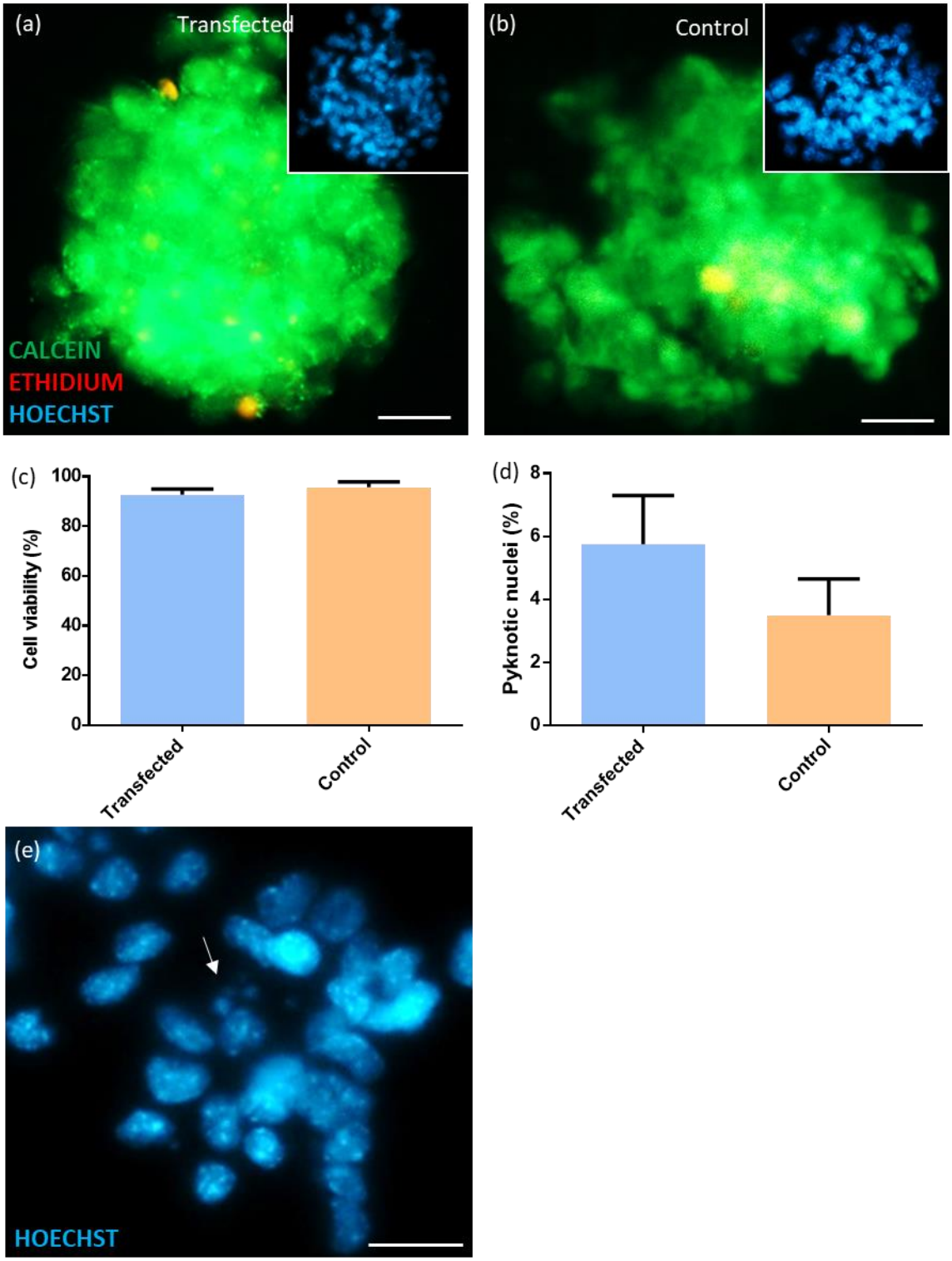

Figure 4.6: Cell viability unaffected by pre-transfection and cell loading. *Representative fluorescence images (a-b) of transfected NSCs (a) and control NSCs (b) in DuraGen™ at 48 hours post transfection/ 24 hours post-seeding in to DuraGen™. Scale bar = 25µm. Bar graph (c) displaying*

the high cell viability in both transfected NSC and control NSC populations growing in DuraGen™ (92.8 ± 2.09% and 95.7 ± 2.18% of the transfected NSC population and the control NSC population were live respectively) (p>0.05, two sample T-test, n=4). Bar graph (d) displaying low proportion of pyknotic nuclei in both transfected NSC and control NSC populations in DuraGen™ (5.76 ± 1.55% and 3.51 ± 1.15% of the transfected NSC and control NSC nuclei were pyknotic respectively) (p>0.05, two sample T-test, n=4). (e) Representative fluorescence image of a pyknotic nucleus (arrow) surrounded by normal nuclei. Scale bar = 25µm.

4.3.6.2 Transfected cell populations expressed as NSC markers

Transfection and cell loading did not impact the phenotype of the cells growing in DuraGen™. At 24 hours post seeding into DuraGen™ and 48 hours post transfection, the majority of cells were positive for NSC marker expression (93.9 ± 0.35%) (**figure 4.7a**). Proportions of cells expressing nestin in the transfected population did not differ from that in the control population (p-value = 0.304, two sample T-test, n=4) (**figure 4.7c**). The majority of nuclei also stained positive for NSC transcription factor expression (Sox-2). 96.7 ± 0.492% of the transfected NSC population and 97.3 ± 0.414% of the control NSC population were positive for Sox-2. This was not statistically different (p>0.05, two sample T-test, n=3). In the transfected and control groups, no difference was visualised in the NSC morphology or patterns of NSC marker staining (**figure 4.7a-b**). >95% of GFP-expressing cells at 48 hours post transfection were NSCs evidenced by the association of GFP-expression and NSC marker staining.

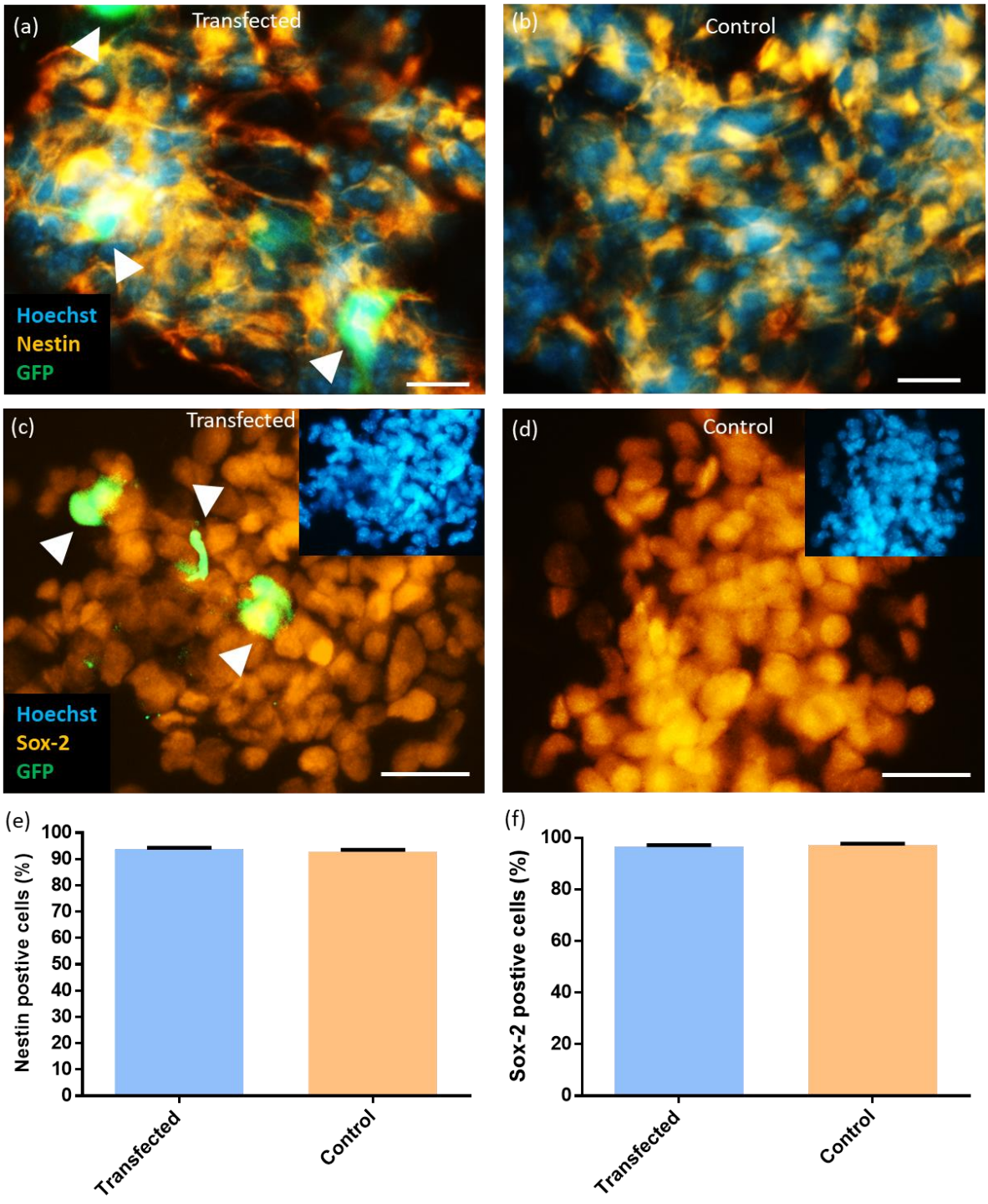

Figure 4.7: Cells maintain NSC phenotype after transfection. *Representative fluorescence images (a-b) of transfected NSCs (white arrows) (a) and control NSCs (b) expressing nestin in DuraGen™ at 48 hours post transfection/ 24 hours post-seeding in to DuraGen™. Scale bar = 25µm. Representative fluorescence images (c-d) of transfected NSCs (c) and control NSCs (d) expressing*

sox-2 in DuraGen™ at 48 hours post transfection/ 24 hours post-seeding in to DuraGen™. Scale bar = 25µm. Bar graph (e) displaying the proportions of nuclei associated with nestin in both transfected NSC and control NSC populations growing in DuraGen™ (93.9 ± 0.35% and 92.9 ± 0.69% of the transfected NSC population and the control NSC population were positive for nestin respectively) (p>0.05, two sample T-test, n=4). Bar graph (f) demonstrates the proportions of nuclei positive for Sox-2 (96.7 ± 0.492% and 97.3 ± 0.414% of the transfected NSC population and the control NSC population were positive for Sox-2 respectively) (p>0.05, two sample T-test, n=3).

4.3.6.3 Proliferation of NSCs unaffected by transfection and loading into DuraGen™

Transfection and subsequent loading into DuraGen™ did not impact on the NSC's ability to proliferate. At 24 hours in DuraGen™ and 48 hours post transfection, 58.7 ± 3.43% of NSCs in the transfected population were EdU labelled versus 66.4 ± 3.06% of the control NSC population (**figure 4.8**). This was not statistically significant (p-value > 0.05, two sample T-test, n=4).

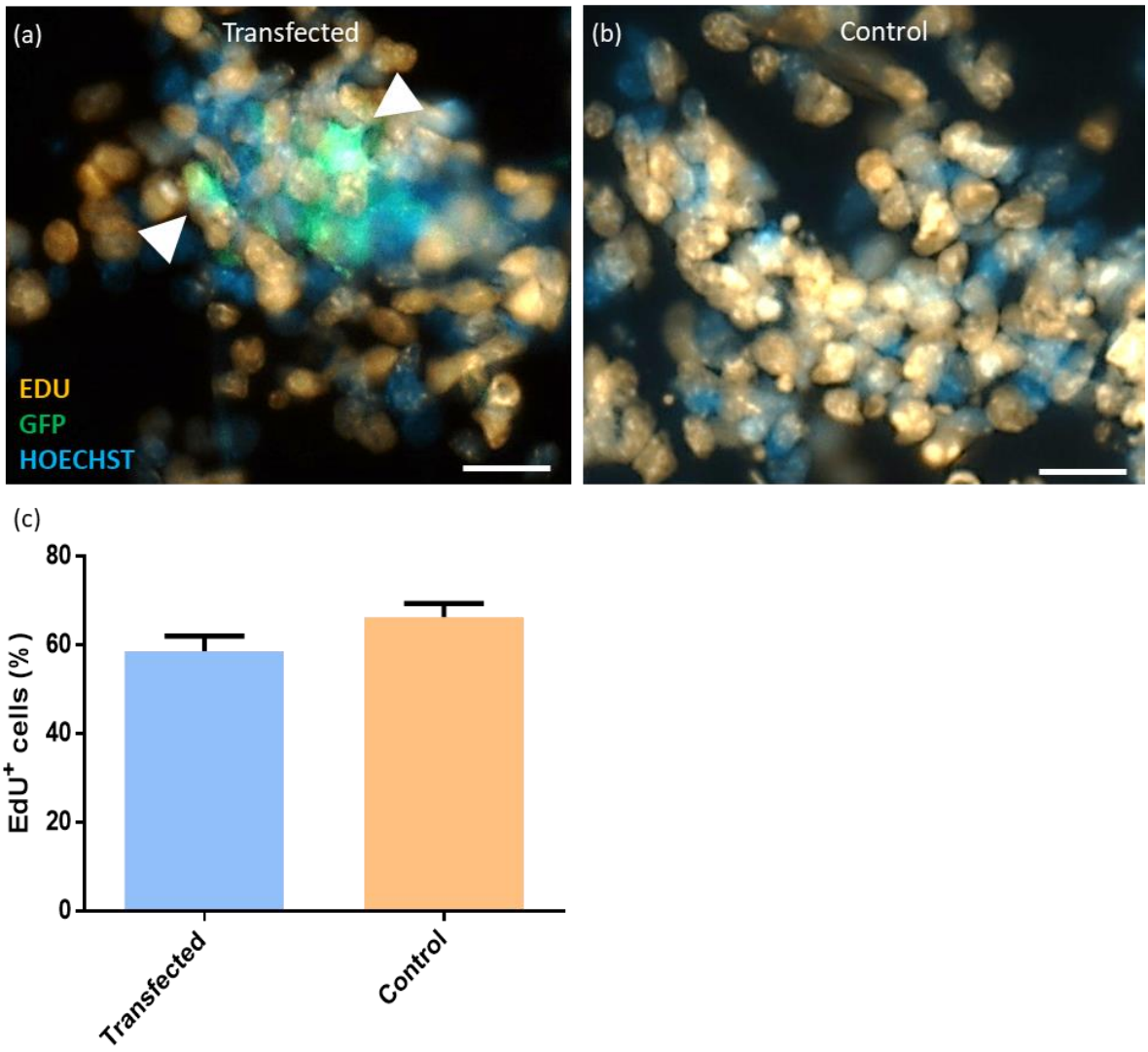

Figure 4.8: Cell proliferation unaffected by pre-transfection and cell loading. *Representative fluorescence images (a-b) of transfected NSCs (white arrows) (a) and control NSCs (b) in DuraGen™ at 48 hours post transfection/ 24 hours post-seeding in to DuraGen™. (c) Bar graph displaying the proliferation rates in both transfected NSC and control NSC populations growing in DuraGen™ (58.7 ± 3.43% and 66.4 ± 3.06% of the transfected NSC population and the control NSC population proliferated respectively) (p-value > 0.05, two sample T-test, n=4). Scale bar = 25µm.*

4.3.6.4 Transfected NSC populations show expected differentiation profiles in DuraGen™

NSC differentiation was not influenced by transfection. At nine days post transfection (eight days post seeding into DuraGen™/seven days after differentiation induction), all three differentiated cell types were present in the matrix (**figure 4.9a-c**). There were no differences in the proportions of each cell type when the transfected population were compared to the control population (p-values = 0.874, 0.883, 0.826 for astroglial lineage cells, neurons and oligodendrocytes respectively, two sample T-tests, n=4) (**figure 4.9d**).

NSCs differentiated predominantly into astroglial lineage cells (66.7 ± 8.76%) which displayed normal morphological features (**figure 4.9a**). All GFP positive cells co-expressed GFAP. There was no evidence of GFP expression in either neurons or oligodendrocytes. Neurons, which contributed the second largest proportion (11.0 ± 4.85%), displayed normal cell bodies with extension of axons into the matrix (**figure 4.9b**). The smallest proportion of cells were oligodendrocytes (0.830 ± 0.446%) which demonstrated their normal, highly processed morphology (**figure 4.9c**). The remaining proportion of cells are likely to be undifferentiated NSCs. Both neurons and oligodendrocytes were found in close spatial association with GFP-expressing cells assumed to be astroglial lineage cells (white arrows in **figure 4.9b-c**). GFP-expression in DuraGen™ was noted up to day nine post transfection when the experiments were terminated.

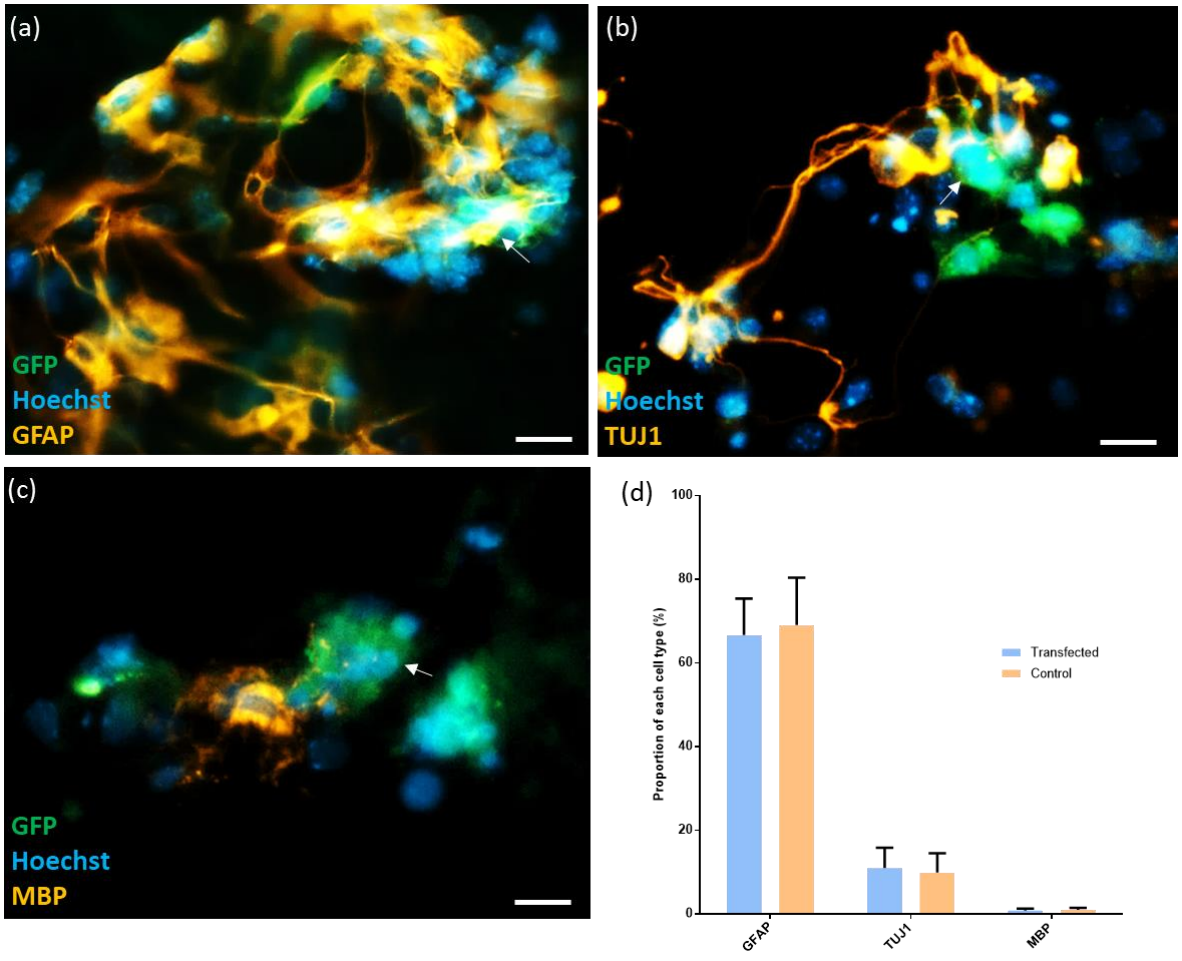

Figure 4.9: NSC differentiate into three types of daughter cells and astroglial lineage cells continue to express GFP. *Representative fluorescence images (a-c) of differentiated transfected NSCs: astroglial lineage cells (a), neurons (b) and oligodendrocytes (c) display normal morphologies in the presence of transfected astroglial lineage cells (arrows) in DuraGen™ at nine days post transfection/ eight days post-seeding in to DuraGen™. Scale bar = 25µm. Bar graph (d) demonstrates relative proportions of each cell type in transfected and control populations. Proportions of each cell type do not differ when transfected (p-values > 0.05, two sample T-tests, n=4).*

4.4 Discussion

4.4.1 Successful production of genetically engineered NSC-DuraGen™ construct

To the best of our knowledge, this is the first time a population of genetically engineered NSCs have been incorporated within a neurosurgical grade material. This chapter has demonstrated a successful method of producing genetically engineered NSCs within DuraGen™. The production of this construct did not reveal a negative impact of the biomaterial on the properties of the NSCs, indicating its safety.

4.4.2 Overall vision for the clinical application of the 'superconstruct'

The construct we have developed offers several potential benefits for the treatment for SCI. This pre-approved surgical material combined with the clinical benefits of magnetofection and minicircle technology offers a novel combinatorial therapy. Here, we used a GFP reporter protein to represent the potential to engineer NSCs with a therapeutic biomolecule. There are many proteins that could be expressed by this population of NSCs. BDNF would be a likely choice for a clinical therapy. It has the potential to improve neuronal survival and axonal growth, essential for regeneration in SCI (190). To engineer the NSCs using magnetofection and minicircle technology to express BDNF before DuraGen™ loading is likely to be possible as Fernandes and Chari have successfully magnetofected NSCs to express BDNF utilising DNA minicircles without negative implications to the NSC population (195).

4.4.3 Transfection efficiency within DuraGen™

The transfection efficiency of the neurospheres loaded into DuraGen™ proved difficult to establish due to the nature of the neurosphere format (section 2.8.6). The estimate given appears comparable to that of neurospheres transfected in previous studies utilising magnetofection

technology (233). The efficiency of transfection of NSCs within a neurosphere format is lower than that of a monolayer NSC culture and of other cell types (**table 4.1**). This has been demonstrated before (233).

Cell type	Magnetic field	Transfection efficiency	Ref
Neurospheres (NSCs)	F=4Hz	9.91%	(233)
Monolayer (NSCs)	F=4Hz	32.2%	(223)
Astrocytes	F=1Hz	54%	(211)
OECs	F=0Hz	57.7%	(192)

Table 4.1*: Transfection efficiencies for neural transplant cells utilising magnetofection technology.*

Viral vector transfection of neurospheres would likely yield a higher transfection efficiency for transplantable cells in DuraGen™. However, the use of viral vectors does not offer the clinical translation benefits of non-viral techniques such as magnetofection. With this in mind, a low level of therapeutic biomolecule release into the site of SCI might prove to be a safer therapy. If a small proportion of NSCs produce the therapeutic biomolecule, the overall concentration of the protein is likely to be lower. This would prevent a high level of sustained growth factor release and the risks associated with high growth factor release including malignant transformation (234).

Differentiated NSCs within DuraGen™ that maintained GFP-expression were positive for an astrocytic marker. In all experiments, transfected neurons or oligodendrocytes were never seen. This is in line with other studies utilising transfected NSCs, who found a high proportion of the differentiated cells to be astrocytes. Hughes et al used viral vectors to transfect neurospheres and after differentiation induction 96.6% of GFP-expressing cells were also GFAP positive (235).

Moreover, previous studies investigating magnetofection also demonstrated no GFP-expressing neurons or oligodendrocytes when transfected as neurospheres (223). Monolayer NSC transfection yielded mostly GFP-expressing astrocytes with less than ca 1% of the GFP-expressing cells co-expressing TUJ1 (212).

4.4.4 Failure of in-situ engineering method

The 'in situ engineering' protocol did not produce a useful level of transfection. This method would have been beneficial for clinical translation as it provided a simple method of production. In addition, it would have allowed control over the peak expression of therapeutic biomolecules. Studies have demonstrated a peak transfection efficiency of 48 hours with magnetofection protocols (212). To maximise the concentration of therapeutic biomolecules released into the site of the injury, rapid production and implantation into SCI site would be required.

The reason for the failure of this method remains unknown. Low transfection efficiency in collagen has been demonstrated before (141). Some potential reasons for the failure are outlined here. One hypothesis is that when the cells adhere to the matrix their behaviour changes and the cells may be less endocytotically active. Endocytosis is required for the MNP-DNA complexes to enter into the cells for transfection. Adams et al found that the cell membranes of NSCs growing on collagen substrates were 'less active' than those of cells growing on glass. They used field emission SEM to detect measures of membrane activity such as membrane ruffling, pitting, filopodia and nanopodia (141).

The stiffness of a biomaterial substrate has been suggested as a reason for a decrease in endocytosis. The softer the substrate the less endocytotic activity occurs (236). The stiffness of DuraGen^{TM} is currently unknown but it would be reasonable to assume that it is softer than standard *in vitro* culture substrates such as glass.

In addition, physical reasons were considered as to why the rate of transfection was negligible in DuraGen™. There is a possibility that the MNPs may have adhered to the fibrous structure of DuraGen™ or been unable to circulate within it. This would have prevented the MNP-DNA complexes coming into contact with the cells for successful transfection.

4.4.5 Why neurosphere loading is beneficial over single cell seeding in DuraGen™

After multiple optimisation steps, the resultant method for construct production was transfection as neurospheres and loading as neurospheres. This method removes the dissociation step involved with seeding single cells into DuraGen™. Simplifying the process will assist at the point of clinical scale up and reduce the risk of enzymatic breakdown of the matrix, as seen in the pilot study of this chapter. In addition to these practical benefits, neurospheres represent a desirable format for cell transplantation. They have been shown to improve NSC survival at transplantation (20% less cell death compared to dissociated NSC transplants) and they improve long-term survival. At two weeks there was a three and a half fold improvement in NSC survival in the neurosphere transplant population (62). The option to seed DuraGen™ with neurospheres as opposed to single cells adds an extra element of protection for the NSCs.

4.4.6 Possible use for magnetic resonance imaging (MRI) tracking

It is beneficial to have the ability to track cell transplants. Clinicians could ensure cells have reached and remained at their target site with the assistance of cell tracking. Moreover, if cells migrated from the site they could be tracked and off target effects, such as tumours, could be diagnosed quickly and treated. The ability to label transplanted cells for *in vivo* tracking is vital for clinical translation. Weinberg et al demonstrated that the use of a clinical grade nanoparticle could be utilised to non-invasively track transplanted cells using MRI (237). Additionally, Tickle et al has demonstrated MRI detection of nanoparticle-labelled astrocytes within polymer matrices designed

for cell transplant (238). Although the MNPs utilised in this study are not compatible with MRI, the potential to utilise compatible nanoparticles would offer increasing benefits of this 'superconstruct'.

Chapter 5: Conclusions and future directions

5.1 Summary of key thesis findings

This series of experiments has proven the utility of DuraGen™, a neurosurgical grade biomaterial scaffold, as a NSC encapsulation device for the first time. We have demonstrated that DuraGen™ does not negatively impact on a population of NSCs, which demonstrated high viability, maintenance of their phenotype, proliferative capacity and the ability to differentiate. Combinatorial neuroregenerative therapies involving the delivery of stem cells have a significant need for protective biomaterial scaffolds. These findings demonstrate the potential utility of a neurosurgical grade material. To progress cellular therapy to the treatment of SCI, barriers to clinical translation must be overcome. This neurosurgical material offers the benefit of FDA-approval to accelerate this process.

We have also demonstrated the ability to formulate a 'superconstruct' where the regenerative benefits of a genetically engineered NSC population were combined with the clinical translatable benefits of DuraGen™. The development of complex, combinatorial therapies demonstrates a key strategy for the treatment of neurological disease. Here we have developed a highly advanced construct with potential benefits for clinical translation that does not negatively impact upon the innate properties of the transplant cell population used.

Overall, the proven use of this surgical grade material introduces the concept that many existing, pre-approved medical products may be amenable to multiple functions for a variety of tissue engineering challenges.

5.2 The future direction for this research

The proof of concept experiments described here unlock multiple new research directions. Firstly, the next steps to these experiments should be further investigation into the impact of DuraGen™ on NSCs using more advanced methods. For instance, functional assessment of the neurons within

the construct utilising electrophysiological measures would allow a more detailed assessment of DuraGen™'s impact on cellular function. To further the concept of a pre-differentiated neural circuit within DuraGen™, an investigation into the cell-cell interactions within the culture would be important. SEM of the construct could reveal whether astroglial lineage cells are guiding neuronal growth or whether oligodendrocytes are myelinating axons.

It is important to recognise the significant impact physical properties of scaffolds, such as stiffness, has on the fate of cell transplant populations within the material. It would be beneficial to utilise elastography techniques to measure the stiffness of DuraGen™. This could then be compared to the native stiffness of the brain and spinal cord and other commonly used biomaterial scaffolds. Other physical properties important for cell encapsulation include the material's degradation rate. Integra Lifesciences report a degradation rate, when used for duraplasty, of two months (142). This rate could be affected by the presence of NSCs, therefore it would be useful to test the material's degradation rate whilst encapsulating cells. Here, we tested DuraGen™ up to 16 days only.

The inevitable next stage in testing the 'superconstruct' is to test its therapeutic benefit within experimental models of SCI. Organotypic slice culture offers the unique benefit of allowing visualisation of pathological and regenerative processes using a simple and tractable *in vitro* model system. Such testing could be carried out in rodent organotypic slice culture with rodent NSCs (15). Alternatively, our laboratory group have developed a method of culturing human organotypic slice models of neurological injury which could serve as a more representative model for DuraGen™ construct testing. Beyond *in vitro* investigations, the construct must be tested *in vivo* to elucidate whether it truly can promote spinal cord regeneration, including with behavioural testing to evaluate functional neurological recovery. During *in vivo* testing, it would be interesting to elucidate the cell release process from DuraGen™. It appears, from the suggested ideal properties of a biomaterial scaffold, that the scaffold should maintain the cells until they begin to form a structure

representative of neural tissue and at this point the scaffold would degrade (105). Another point of note is whether this minimally immunogenic material will protect the transplant cells from immune attack. This could be investigated by adding NSCs within DuraGen™ to a culture of microglia and observing the response. Furthermore, testing the immune response *in vivo* would provide a more representative outcome.

Controlling the direction of axonal growth presents a significant challenge for this cellular scaffold, as the growth of neurons was random within the material. There are multiple ways in which this could be overcome. In line with the work carried out by Bonner et al, a neurotrophin gradient could be manipulated in combination with the implantation of a DuraGen™ construct to encourage rostral and caudal axonal growth (230). This concept could be employed in one of two ways. Firstly, it could be used *in vivo* as intended. After a specified time, post implantation of the DuraGen™-NSC construct, neurotrophic factors could be injected rostrally and caudally via intraspinal injection. In theory, this would encourage directional growth of neurons from within the construct to connect with the lesion edges. The alternative option is to utilise the neurotrophin gradient to pre-align neurons within the construct prior to implantation. To do this the DuraGen™ could be secured in a position within a petri dish. Two inner chambers within the dish, separated by a semi-permeable membrane, at each pole would contain neurotrophic factors. This gradient would encourage neurons, differentiated from NSCs, to grow in the direction of the neurotrophin pools (**figure 5.1**). Once sufficient time for alignment had passed the construct could then be implanted in that alignment into the site of SCI. This removes the need to inject into healthy cord as was required in the previous method.

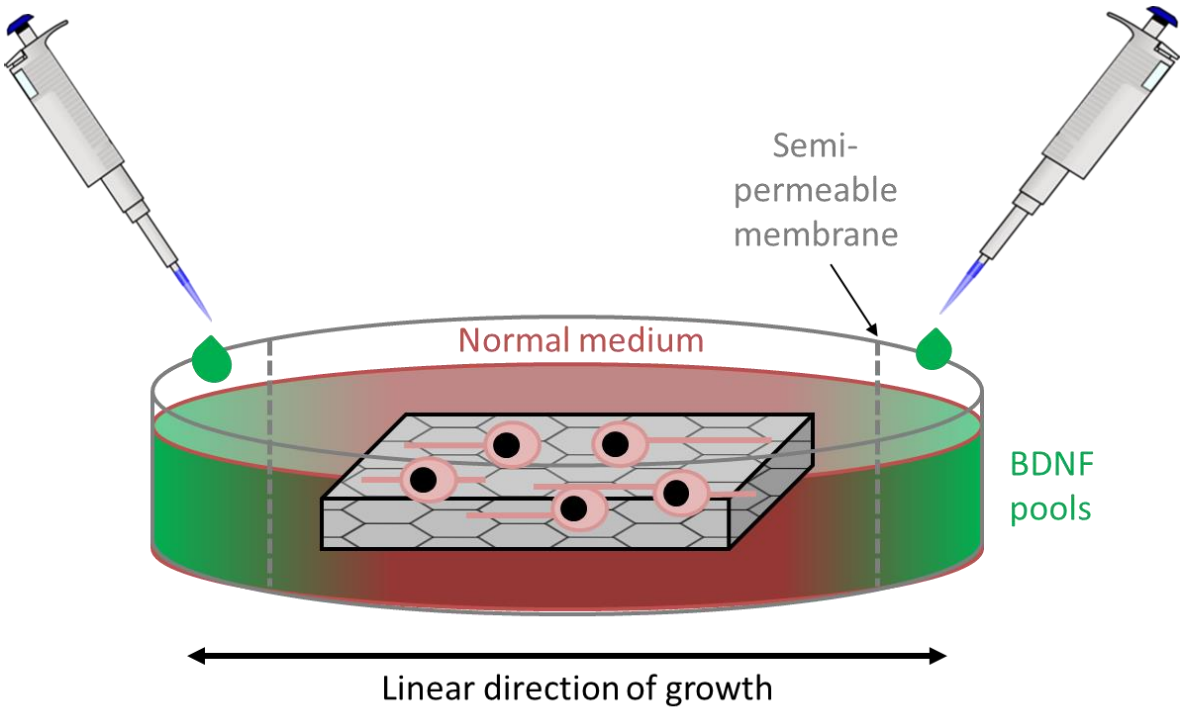

Figure 5.1: *Schematic representation of utilising a neurotrophin gradient to encourage linear axonal growth within DuraGen™.*

Other methods to achieve axonal alignment may exist. Axial tension has been demonstrated to encourage axonal elongation and growth (239). The nature of DuraGen™ makes it amenable to stretch. If NSCs could be grown and differentiated on samples of DuraGen™ that were under tension it could, in theory, align the axonal fibres. This construct could then be subsequently implanted, in the correct orientation, in to a lesion site.

Success has been demonstrated utilising electrical stimulation across the SCI lesion which improved function (40). I propose that the addition of this technology to the current approach of cellular transplantation within a biomaterial scaffold could increase regeneration. Harkema et al hypothesised that the epidural stimulation encouraged axonal regrowth. Combining electrical stimulation with a cell rich biomaterial scaffold, may target a sufficient number of the goals of regenerative therapy in a highly complex combinatorial therapy.

We investigated DuraGen™ as a matrix to encapsulate NSCs. However, as described in table 1.1 many neural transplant cell types have been tested for neurological applications. Each cell type offers individual benefits. I envisage that if DuraGen™ can support NSCs and their daughter cells, it can support a population of astrocytes, OECs, OPCs or Schwann cells. DuraGen™ could then be personalised to each individual condition. For example, in multiple sclerosis there is a loss of oligodendrocytes and OPCs leading to failed attempts at remyelination (240), so a DuraGen™ construct seeded with a population of OPCs or mature oligodendrocytes could potentially be investigated to target the largest lesions for remyelination. Moreover, a dopaminergic neuron culture within DuraGen™ has the potential for use as a cell replacement therapy in cases of severe Parkinson's disease. Complex mixed cultures of astrocytes, neurons and oligodendrocytes could replace lost tissue after tumour removal or traumatic brain injury.

Finally, and most importantly, the use of DuraGen™ here has uncovered the potential for pre-approved surgical materials to offer more than their current functions. In the introduction, several surgical materials were discussed for use as cell encapsulation devices. The next direction this research should be taken in is to investigate more of the available surgical materials for use as cell encapsulation devices, specifically fibrin glues, Floseal™ and Surgicel™. Many more materials exist beyond those described. One I wish to draw particular attention to is Vivostat™. This is an autologous fibrin sealant used for haemostasis and dural sealing in neurosurgery. The use of a patient's own blood to produce the sealant offers the benefit of immune rejection avoidance. If this biomaterial could be used to encapsulate cells for delivery it may also assist the transplanted cells in immune evasion. The potential for these pre-approved surgical materials can therefore be predicted to be far reaching. With the growing expense and delay in translating therapies to the clinic, it is vital that researchers capitalise on the resources and materials already available and routinely used in clinical practice.

Supplementary materials

Find attached CD-ROM with the following files:

Video 3.1: NSCs growing in 3D within DuraGen™ at 48 hours. Scale bar = 50 µm.

Video 4.1: Transfected neurospheres within DuraGen™ matrix, 48 hours post transfection (24 hours after DuraGen™ loading). Scale bar = 50 µm.

Bibliography

1. Gall A. A series of evidence-based guidelines for clinical management - chronic spinal cord injury: management of patients in acute hospital settings Clinical Standards Department Concise Guidance to Good Practice series [Internet]. 2008 [cited 2017 Dec 21]. Available from: www.bsrm.co.uk
2. NHS England. NHS Standard Contract for Spinal Cord Injuries (all ages) [Internet]. 2013 [cited 2017 Dec 21]. Available from: https://www.england.nhs.uk/commissioning/wp-content/uploads/sites/12/2014/04/d13-spinal-cord-0414.pdf
3. DeVivo MJ, Chen Y. Trends in New Injuries, Prevalent Cases, and Aging With Spinal Cord Injury. Arch Phys Med Rehabil [Internet]. 2011 [cited 2018 Apr 24];92(3):332–8. Available from: http://www.ncbi.nlm.nih.gov/pubmed/21353817
4. Wyndaele M, Wyndaele J-J. Incidence, prevalence and epidemiology of spinal cord injury: what learns a worldwide literature survey? Spinal Cord [Internet]. 2006 [cited 2018 Apr 24];44(9):523–9. Available from: http://www.nature.com/articles/3101893
5. Bárbara-Bataller E, Méndez-Suárez JL, Alemán-Sánchez C, Sánchez-Enríquez J, Sosa-Henríquez M. Change in the profile of traumatic spinal cord injury over 15 years in Spain. Scand J Trauma Resusc Emerg Med [Internet]. 2018 [cited 2018 Apr 24];26(1):27. Available from: https://sjtrem.biomedcentral.com/articles/10.1186/s13049-018-0491-4
6. World Health Organisation. Spinal cord injury [Internet]. WHO fact sheets. World Health Organization; 2016 [cited 2017 Dec 21]. Available from: http://www.who.int/mediacentre/factsheets/fs384/en/
7. Berkowitz M. Spinal cord injury : an analysis of medical and social costs. Demos; 1998.
8. Watson C, Paxinos G, Kayalioglu G. The Spinal Cord: A Christopher and Dana Reeve

Foundation Text and Atlas. Elsevier; 2009. 209-222 p.

9. Maynard FM, Bracken MB, Creasey G, Ditunno JF, Donovan WH, Ducker TB, et al. International Standards for Neurological and Functional Classification of Spinal Cord Injury. Spinal Cord [Internet]. 1997 [cited 2018 Feb 6];35(5):266–74. Available from: http://www.ncbi.nlm.nih.gov/pubmed/9160449

10. Faulkner JR, Herrmann JE, Woo MJ, Tansey KE, Doan NB, Sofroniew M V. Reactive Astrocytes Protect Tissue and Preserve Function after Spinal Cord Injury. J Neurosci [Internet]. 2004 [cited 2017 Dec 21];24(9):2143–55. Available from: http://www.ncbi.nlm.nih.gov/pubmed/14999065

11. David S, Kroner A. Repertoire of microglial and macrophage responses after spinal cord injury. Nat Rev Neurosci [Internet]. 2011 [cited 2018 Apr 24];12(7):388–99. Available from: http://www.nature.com/doifinder/10.1038/nrn3053

12. Prüss H, Kopp MA, Brommer B, Gatzemeier N, Laginha I, Dirnagl U, et al. Non-Resolving Aspects of Acute Inflammation after Spinal Cord Injury (SCI): Indices and Resolution Plateau. Brain Pathol [Internet]. 2011 [cited 2018 Apr 24];21(6):652–60. Available from: http://www.ncbi.nlm.nih.gov/pubmed/21418368

13. Ahuja CS, Nori S, Tetreault L, Wilson J, Kwon B, Harrop J, et al. Traumatic Spinal Cord Injury—Repair and Regeneration. Neurosurgery [Internet]. 2017 [cited 2017 Dec 21];80(3S):S9–22. Available from: http://www.ncbi.nlm.nih.gov/pubmed/28350947

14. Kjell J, Olson L. Rat models of spinal cord injury: from pathology to potential therapies. Dis Model Mech [Internet]. 2016 [cited 2017 Dec 21];9(10):1125–37. Available from: http://www.ncbi.nlm.nih.gov/pubmed/27736748

15. Weightman AP, Pickard MR, Yang Y, Chari DM. An in vitro spinal cord injury model to screen neuroregenerative materials. Biomaterials [Internet]. 2014 [cited 2017 Dec 21];35(12):3756–65. Available from: http://www.ncbi.nlm.nih.gov/pubmed/24484676

16. Pekny M, Johansson CB, Eliasson C, Stakeberg J, Wallén A, Perlmann T, et al. Abnormal reaction to central nervous system injury in mice lacking glial fibrillary acidic protein and vimentin. J Cell Biol [Internet]. 1999 [cited 2017 Dec 19];145(3):503–14. Available from: http://www.ncbi.nlm.nih.gov/pubmed/10225952

17. Ramón y Cajal S, DeFelipe J, Jones EG. Cajal's degeneration and regeneration of the nervous system. Oxford University Press; 1991. 769 p.

18. Richardson PM, McGuinness UM, Aguayo AJ. Axons from CNS neurones regenerate into PNS grafts. Nature [Internet]. 1980 [cited 2017 Dec 21];284(5753):264–5. Available from: http://www.nature.com/doifinder/10.1038/284264a0

19. Eric Huebner SA, Strittmatter SM. Axon Regeneration in the Peripheral and Central Nervous. [cited 2018 Jun 11]; Available from: https://www.ncbi.nlm.nih.gov/pmc/articles/PMC2846285/pdf/nihms162879.pdf

20. Fawcettt JW, Keynes RJ. Peripheral nerve regeneration. Annu Rev Neurosci [Internet]. 1990 [cited 2018 Jun 11];13:43–60. Available from: https://www.annualreviews.org/doi/pdf/10.1146/annurev.ne.13.030190.000355

21. Bradbury EJ, Moon LDF, Popat RJ, King VR, Bennett GS, Patel PN, et al. Chondroitinase ABC promotes functional recovery after spinal cord injury. Nature [Internet]. 2002 [cited 2018 Feb 6];416(6881):636–40. Available from: http://www.ncbi.nlm.nih.gov/pubmed/11948352

22. Barkho BZ, Song H, Aimone JB, Smrt RD, Kuwabara T, Nakashima K, et al. Identification of Astrocyte-expressed Factors That Modulate Neural Stem/Progenitor Cell Differentiation. Stem Cells Dev [Internet]. 2006 [cited 2018 Apr 24];15(3):407–21. Available from: http://www.ncbi.nlm.nih.gov/pubmed/16846377

23. Goldshmit Y, Spanevello MD, Tajouri S, Li L, Rogers F, Pearse M, et al. EphA4 Blockers Promote Axonal Regeneration and Functional Recovery Following Spinal Cord Injury in Mice. Priller J, editor. PLoS One [Internet]. 2011 [cited 2018 Apr 24];6(9):e24636. Available from:

http://dx.plos.org/10.1371/journal.pone.0024636

24. Lee-Liu D, Edwards-Faret G, Tapia VS, Larraín J. Spinal cord regeneration: Lessons for mammals from non-mammalian vertebrates. Genesis [Internet]. 2013 [cited 2017 Dec 21];51(8):529–44. Available from: http://www.ncbi.nlm.nih.gov/pubmed/23760835

25. Zukor KA, Kent DT, Odelberg SJ. Meningeal cells and glia establish a permissive environment for axon regeneration after spinal cord injury in newts. Neural Dev [Internet]. 2011 [cited 2018 Apr 24];6:1. Available from: http://www.ncbi.nlm.nih.gov/pubmed/21205291

26. Anderson MA, Burda JE, Ren Y, Ao Y, O'Shea TM, Kawaguchi R, et al. Astrocyte scar formation aids central nervous system axon regeneration. Nature [Internet]. 2016 [cited 2018 Jan 15];532(7598):195–200. Available from: http://www.nature.com/doifinder/10.1038/nature17623

27. Bush TG, Puvanachandra N, Horner CH, Polito A, Ostenfeld T, Svendsen CN, et al. Leukocyte Infiltration, Neuronal Degeneration, and Neurite Outgrowth after Ablation of Scar-Forming, Reactive Astrocytes in Adult Transgenic Mice. Neuron [Internet]. 1999 [cited 2018 Jan 22];23(2):297–308. Available from: http://www.sciencedirect.com/science/article/pii/S0896627300807813?via%3Dihub

28. Shihabuddin LS, Horner PJ, Ray J, Gage FH. Adult spinal cord stem cells generate neurons after transplantation in the adult dentate gyrus. J Neurosci [Internet]. 2000 [cited 2018 Apr 24];20(23):8727–35. Available from: http://www.ncbi.nlm.nih.gov/pubmed/11102479

29. Fehlings MG, Vaccaro A, Wilson JR, Singh A, W. Cadotte D, Harrop JS, et al. Early versus Delayed Decompression for Traumatic Cervical Spinal Cord Injury: Results of the Surgical Timing in Acute Spinal Cord Injury Study (STASCIS). Di Giovanni S, editor. PLoS One [Internet]. 2012 [cited 2017 Dec 19];7(2):e32037. Available from: http://dx.plos.org/10.1371/journal.pone.0032037

30. Chin L, Mesfin F, Dawodu ST, Kopell B. Spinal Cord Injuries Treatment & Management:

Approach Considerations, Prehospital Management, Emergency Department Management [Internet]. emedicine. 2017 [cited 2017 Dec 19]. Available from: https://emedicine.medscape.com/article/793582-treatment#d14

31. Esquenazi A, Talaty M, Packel A, Saulino M. The ReWalk Powered Exoskeleton to Restore Ambulatory Function to Individuals with Thoracic-Level Motor-Complete Spinal Cord Injury. Am J Phys Med Rehabil [Internet]. 2012 [cited 2018 Jun 11];91(11):911–21. Available from: https://insights.ovid.com/pubmed?pmid=23085703

32. Harrison SCW. Managing the urinary tract in spinal cord injury. Indian J Urol [Internet]. 2010 [cited 2018 Jun 11];26(2):245–52. Available from: http://www.ncbi.nlm.nih.gov/pubmed/20877604

33. Perkes SJ, Bowman J, Penkala S. Psychological therapies for the management of co-morbid depression following a spinal cord injury: A systematic review. J Health Psychol [Internet]. 2014 [cited 2018 Jun 11];19(12):1597–612. Available from: http://journals.sagepub.com/doi/10.1177/1359105313496445

34. Bracken MB, Shepard MJ, Collins WF, Holford TR, Young W, Baskin DS, et al. A Randomized, Controlled Trial of Methylprednisolone or Naloxone in the Treatment of Acute Spinal-Cord Injury. N Engl J Med [Internet]. 1990 [cited 2017 Dec 19];322(20):1405–11. Available from: http://www.ncbi.nlm.nih.gov/pubmed/2278545

35. Bracken MB, Shepard MJ, Holford TR, Leo-Summers L, Aldrich EF, Fazl M, et al. Administration of methylprednisolone for 24 or 48 hours or tirilazad mesylate for 48 hours in the treatment of acute spinal cord injury. Results of the Third National Acute Spinal Cord Injury Randomized Controlled Trial. National Acute Spinal Cord Injury. JAMA [Internet]. 1997 [cited 2017 Dec 19];277(20):1597–604. Available from: http://www.ncbi.nlm.nih.gov/pubmed/9168289

36. Nesathurai S. Steroids and spinal cord injury: revisiting the NASCIS 2 and NASCIS 3 trials. J

Trauma [Internet]. 1998 [cited 2017 Dec 19];45(6):1088–93. Available from: http://www.ncbi.nlm.nih.gov/pubmed/9867054

37. National Institute for Health and Care Excellence. Spinal injury: assessment and initial management [Internet]. NICE guideline [NG41]; 2016 [cited 2017 Dec 19]. Available from: https://www.nice.org.uk/guidance/ng41/chapter/recommendations#early-management-in-the-emergency-department-after-traumatic-spinal-cord-injury

38. Chengke L, Weiwei L, Xiyang W, Ping W, Xiaoyang P, Zhengquan X, et al. Effect of Infliximab Combined With Methylprednisolone on Expressions of NF-κB, TRADD, and FADD in Rat Acute Spinal Cord Injury. Spine (Phila Pa 1976) [Internet]. 2013 [cited 2018 Apr 25];38(14):861–9. Available from: http://www.ncbi.nlm.nih.gov/pubmed/23574812

39. Shultz RB, Wang Z, Nong J, Zhang Z, Zhong Y. Local delivery of thyroid hormone enhances oligodendrogenesis and myelination after spinal cord injury. J Neural Eng [Internet]. 2017 [cited 2018 Apr 25];14(3):036014. Available from: http://stacks.iop.org/1741-2552/14/i=3/a=036014?key=crossref.44de95fea4da30ede5869e9481f18824

40. Harkema S, Gerasimenko Y, Hodes J, Burdick J, Angeli C, Chen Y, et al. Effect of epidural stimulation of the lumbosacral spinal cord on voluntary movement, standing, and assisted stepping after motor complete paraplegia: a case study. Lancet [Internet]. 2011 [cited 2018 Apr 25];377(9781):1938–47. Available from: https://www.sciencedirect.com/science/article/pii/S0140673611605473

41. SlideHunter. SlideHunter PowerPoint templates [Internet]. [cited 2018 Jun 1]. Available from: https://slidehunter.com/powerpoint-templates/free-multi-level-circular-diagram-powerpoint-template/

42. Filous AR, Schwab JM. Determinants of Axon Growth, Plasticity, and Regeneration in the Context of Spinal Cord Injury. Am J Pathol [Internet]. 2018 [cited 2018 Feb 7];188(1):53–62. Available from:

https://www.sciencedirect.com/science/article/pii/S0002944017306326?via%3Dihub

43. Nakatomi H, Kuriu T, Okabe S, Yamamoto S, Hatano O, Kawahara N, et al. Regeneration of Hippocampal Pyramidal Neurons after Ischemic Brain Injury by Recruitment of Endogenous Neural Progenitors. Cell [Internet]. 2002 [cited 2018 Feb 5];110(4):429–41. Available from: https://www.sciencedirect.com/science/article/pii/S0092867402008620

44. Chu K, Kim M, Jeong S-W, Kim SU, Yoon B-W. Human neural stem cells can migrate, differentiate, and integrate after intravenous transplantation in adult rats with transient forebrain ischemia. Neurosci Lett [Internet]. 2003 [cited 2017 Dec 21];343(2):129–33. Available from: http://www.sciencedirect.com/science/article/pii/S0304394003001745?via%3Dihub

45. Lee HJ, Kim KS, Kim EJ, Choi HB, Lee KH, Park IH, et al. Brain Transplantation of Immortalized Human Neural Stem Cells Promotes Functional Recovery in Mouse Intracerebral Hemorrhage Stroke Model. Stem Cells [Internet]. 2007 [cited 2017 Dec 21];25(5):1204–12. Available from: http://doi.wiley.com/10.1634/stemcells.2006-0409

46. Dunnett SB, Bjorklund A. Mechanisms of function of neural grafts in the adult mammalian brain. J Exp Biol [Internet]. 1987 [cited 2018 Apr 28];132:265–89. Available from: https://pdfs.semanticscholar.org/cfea/0399edba9aa034563d8f1942aab05be09871.pdf

47. Dunnett SB, Bjorklund A. Mechanisms and use of neural transplants for brain repair. Prog Brain Res [Internet]. 2017 [cited 2018 Apr 28];230:1–51. Available from: https://www.sciencedirect.com/science/article/pii/S0079612316301601?via%3Dihub

48. Barker R. Stem cell therapies and neurological disorders of the brain: what is the truth? | Eurostemcell [Internet]. EuroStemCell. 2013 [cited 2018 Apr 28]. Available from: https://www.eurostemcell.org/stem-cell-therapies-and-neurological-disorders-brain-what-truth

49. Chu T, Zhou H, Li F, Wang T, Lu L, Feng S. Astrocyte transplantation for spinal cord injury:

Current status and perspective. Brain Res Bull [Internet]. 2014 [cited 2018 Apr 29];107:18–30. Available from: https://www.sciencedirect.com/science/article/pii/S0361923014000938?via%3Dihub

50. Bardehle S, Krüger M, Buggenthin F, Schwausch J, Ninkovic J, Clevers H, et al. Live imaging of astrocyte responses to acute injury reveals selective juxtavascular proliferation. Nat Neurosci [Internet]. 2013 [cited 2018 Apr 29];16(5):580–6. Available from: http://www.nature.com/articles/nn.3371

51. Ikeda O, Murakami M, Ino H, Yamazaki M, Nemoto T, Koda M, et al. Acute up-regulation of brain-derived neurotrophic factor expression resulting from experimentally induced injury in the rat spinal cord. Acta Neuropathol [Internet]. 2001 [cited 2018 Apr 29];102(3):239–45. Available from: http://www.ncbi.nlm.nih.gov/pubmed/11585248

52. Tom VJ, Doller CM, Malouf AT, Silver J. Astrocyte-Associated Fibronectin Is Critical for Axonal Regeneration in Adult White Matter. J Neurosci [Internet]. 2004 [cited 2018 Apr 29];24(42):9282–90. Available from: http://www.ncbi.nlm.nih.gov/pubmed/15496664

53. Lee M-Y, Kim C-J, Shin S-L, Moon S-H, Chun M-H. Increased ciliary neurotrophic factor expression in reactive astrocytes following spinal cord injury in the rat. Neurosci Lett [Internet]. 1998 [cited 2018 Apr 29];255(2):79–82. Available from: https://www.sciencedirect.com/science/article/pii/S0304394098007101?via%3Dihub

54. Bernstein JJ, Goldberg WJ. Grafted fetal astrocyte migration can prevent host neuronal atrophy: comparison of astrocytes from cultures and whole piece donors. Restor Neurol Neurosci [Internet]. 1991 [cited 2018 Apr 29];2(4):261–70. Available from: http://www.ncbi.nlm.nih.gov/pubmed/21551612

55. Wang JJ, Chuah MI, Yew DTW, Leung PC, Tsang DSC. Effects of astrocyte implantation into the hemisected adult rat spinal cord. Neuroscience [Internet]. 1995 [cited 2018 Apr 29];65(4):973–81. Available from:

https://www.sciencedirect.com/science/article/pii/030645229400519B?via%3Dihub

56. Zador Z, Stiver S, Wang V, Manley GT. Role of Aquaporin-4 in Cerebral Edema and Stroke. In: Aquaporins [Internet]. Berlin, Heidelberg: Springer Berlin Heidelberg; 2009 [cited 2018 Apr 29]. p. 159–70. Available from: http://link.springer.com/10.1007/978-3-540-79885-9_7

57. Sofroniew M V. Molecular dissection of reactive astrogliosis and glial scar formation. Trends Neurosci [Internet]. 2009 [cited 2018 Apr 29];32(12):638–47. Available from: https://www.sciencedirect.com/science/article/pii/S0166223609001532?via%3Dihub

58. Hayashi K, Hashimoto M, Koda M, Naito AT, Murata A, Okawa A, et al. Increase of sensitivity to mechanical stimulus after transplantation of murine induced pluripotent stem cell–derived astrocytes in a rat spinal cord injury model. J Neurosurg Spine [Internet]. 2011 [cited 2018 Apr 29];15(6):582–93. Available from: http://thejns.org/doi/10.3171/2011.7.SPINE10775

59. Joosten EAJ, Veldhuis WB, Hamers FPT. Collagen containing neonatal astrocytes stimulates regrowth of injured fibers and promotes modest locomotor recovery after spinal cord injury. J Neurosci Res [Internet]. 2004 [cited 2018 Feb 7];77(1):127–42. Available from: http://www.ncbi.nlm.nih.gov/pubmed/15197746

60. Zhu Y, Uezono N, Yasui T, Nakashima K. Neural stem cell therapy aiming at better functional recovery after spinal cord injury. Dev Dyn [Internet]. 2018 [cited 2018 Apr 29];247(1):75–84. Available from: http://www.ncbi.nlm.nih.gov/pubmed/28766845

61. Martino G, Pluchino S. The therapeutic potential of neural stem cells. Nat Rev Neurosci [Internet]. 2006 [cited 2018 Feb 16];7(5):395–406. Available from: http://www.nature.com/articles/nrn1908

62. Mothe AJ, Kulbatski I, Parr A, Mohareb M, Tator CH. Adult spinal cord stem/progenitor cells transplanted as neurospheres preferentially differentiate into oligodendrocytes in the adult rat spinal cord. Cell Transplant [Internet]. 2008 [cited 2018 May 23];17(7):735–51. Available

from: http://www.ncbi.nlm.nih.gov/pubmed/19044201

63. Takahashi K, Tanabe K, Ohnuki M, Narita M, Ichisaka T, Tomoda K, et al. Induction of Pluripotent Stem Cells from Adult Human Fibroblasts by Defined Factors. Cell [Internet]. 2007 [cited 2018 Apr 29];131(5):861–72. Available from: https://www.sciencedirect.com/science/article/pii/S0092867407014717?via%3Dihub

64. Bjorklund LM, Sanchez-Pernaute R, Chung S, Andersson T, Chen IYC, McNaught KSP, et al. Embryonic stem cells develop into functional dopaminergic neurons after transplantation in a Parkinson rat model. Proc Natl Acad Sci [Internet]. 2002 [cited 2018 Feb 5];99(4):2344–9. Available from: http://www.ncbi.nlm.nih.gov/pubmed/11782534

65. Amariglio N, Hirshberg A, Scheithauer BW, Cohen Y, Loewenthal R, Trakhtenbrot L, et al. Donor-Derived Brain Tumor Following Neural Stem Cell Transplantation in an Ataxia Telangiectasia Patient. Fischer A, editor. PLoS Med [Internet]. 2009 [cited 2018 Feb 5];6(2):e1000029. Available from: http://dx.plos.org/10.1371/journal.pmed.1000029

66. Setoguchi T, Nakashima K, Takizawa T, Yanagisawa M, Ochiai W, Okabe M, et al. Treatment of spinal cord injury by transplantation of fetal neural precursor cells engineered to express BMP inhibitor. Exp Neurol [Internet]. 2004 [cited 2018 Apr 29];189(1):33–44. Available from: http://www.ncbi.nlm.nih.gov/pubmed/15296834

67. Barnett SC, Riddell JS. Olfactory ensheathing cells (OECs) and the treatment of CNS injury: advantages and possible caveats. J Anat [Internet]. 2004 [cited 2018 Apr 29];204(1):57–67. Available from: http://www.ncbi.nlm.nih.gov/pubmed/14690478

68. Franklin RJM, Gilson JM, Franceschini IA, Barnett SC. Schwann cell-like myelination following transplantation of an olfactory bulb-ensheathing cell line into areas of demyelination in the adult CNS. Glia [Internet]. 1996 [cited 2018 Apr 29];17(3):217–24. Available from: http://doi.wiley.com/10.1002/%28SICI%291098-1136%28199607%2917%3A3%3C217%3A%3AAID-GLIA4%3E3.0.CO%3B2-Y

69. Chung RS, Woodhouse A, Fung S, Dickson TC, West AK, Vickers JC, et al. Olfactory ensheathing cells promote neurite sprouting of injured axons in vitro by direct cellular contact and secretion of soluble factors. Cell Mol Life Sci [Internet]. 2004 [cited 2018 Apr 29];61(10):1238–45. Available from: http://www.ncbi.nlm.nih.gov/pubmed/15141309

70. Féron F, Perry C, McGrath JJ, Mackay-Sim A. New techniques for biopsy and culture of human olfactory epithelial neurons. Arch Otolaryngol Head Neck Surg [Internet]. 1998 [cited 2018 Apr 29];124(8):861–6. Available from: http://www.ncbi.nlm.nih.gov/pubmed/9708710

71. Richter MW, Roskams AJ. Olfactory ensheathing cell transplantation following spinal cord injury: Hype or hope? Exp Neurol [Internet]. 2008 [cited 2018 Apr 29];209(2):353–67. Available from: https://www.sciencedirect.com/science/article/pii/S0014488607002439?via%3Dihub

72. Tetzlaff W, Okon EB, Karimi-Abdolrezaee S, Hill CE, Sparling JS, Plemel JR, et al. A Systematic Review of Cellular Transplantation Therapies for Spinal Cord Injury. J Neurotrauma [Internet]. 2011 Aug [cited 2018 Apr 30];28(8):1611–82. Available from: http://www.liebertonline.com/doi/abs/10.1089/neu.2009.1177

73. Sun Y, Xu C-C, Li J, Guan X-Y, Gao L, Ma L-X, et al. Transplantation of Oligodendrocyte Precursor Cells Improves Locomotion Deficits in Rats with Spinal Cord Irradiation Injury. Nait-Oumesmar B, editor. PLoS One [Internet]. 2013 [cited 2018 Apr 29];8(2):e57534. Available from: http://www.ncbi.nlm.nih.gov/pubmed/23460872

74. Kondo T, Raff M. Oligodendrocyte precursor cells reprogrammed to become multipotential CNS stem cells. Science [Internet]. 2000 [cited 2018 Apr 29];289(5485):1754–7. Available from: http://www.ncbi.nlm.nih.gov/pubmed/10976069

75. Belachew S, Chittajallu R, Aguirre AA, Yuan X, Kirby M, Anderson S, et al. Postnatal NG2 proteoglycan–expressing progenitor cells are intrinsically multipotent and generate

functional neurons. J Cell Biol [Internet]. 2003 [cited 2018 Apr 29];161(1):169–86. Available from: http://www.ncbi.nlm.nih.gov/pubmed/12682089

76. Rasouli A, Bhatia N, Dinh P, Cahill K, Suryadevara S, Gupta R. Resection of glial scar following spinal cord injury. J Orthop Res [Internet]. 2009 [cited 2018 Apr 29];27(7):931–6. Available from: http://www.ncbi.nlm.nih.gov/pubmed/19062171

77. Siebert JR, Conta Steencken A, Osterhout DJ. Chondroitin sulfate proteoglycans in the nervous system: inhibitors to repair. Biomed Res Int [Internet]. 2014 [cited 2018 Apr 29];2014:845323. Available from: http://www.ncbi.nlm.nih.gov/pubmed/25309928

78. Kohama I, Lankford KL, Preiningerova J, White FA, Vollmer TL, Kocsis JD. Transplantation of cryopreserved adult human Schwann cells enhances axonal conduction in demyelinated spinal cord. J Neurosci [Internet]. 2001 [cited 2018 Apr 29];21(3):944–50. Available from: http://www.ncbi.nlm.nih.gov/pubmed/11157080

79. Franklin RJ, Blakemore WF. Requirements for Schwann cell migration within CNS environments: a viewpoint. Int J Dev Neurosci [Internet]. 1993 [cited 2018 Apr 29];11(5):641–9. Available from: http://www.ncbi.nlm.nih.gov/pubmed/8116476

80. Tang Y, Yu P, Cheng L. Current progress in the derivation and therapeutic application of neural stem cells. Cell Death Dis [Internet]. 2017 [cited 2018 Feb 5];8(10):e3108. Available from: http://www.ncbi.nlm.nih.gov/pubmed/29022921

81. Pagano SF, Impagnatiello F, Girelli M, Cova L, Grioni E, Onofri M, et al. Isolation and Characterization of Neural Stem Cells from the Adult Human Olfactory Bulb. Stem Cells [Internet]. 2000 [cited 2018 Apr 29];18(4):295–300. Available from: http://www.ncbi.nlm.nih.gov/pubmed/10924096

82. Gage FH, Coates PW, Palmer TD, Kuhn HG, Fisher LJ, Suhonen JO, et al. Survival and differentiation of adult neuronal progenitor cells transplanted to the adult brain. Proc Natl Acad Sci U S A [Internet]. 1995 [cited 2018 Jun 11];92(25):11879–83. Available from:

http://www.ncbi.nlm.nih.gov/pubmed/8524867

83. Barazzetti G, Hurst SA, Mauron A. Adapting Preclinical Benchmarks for First-in-Human Trials of Human Embryonic Stem Cell-Based Therapies. Stem Cells Transl Med [Internet]. 2016 [cited 2018 Feb 6];5(8):1058–66. Available from: http://www.ncbi.nlm.nih.gov/pubmed/27334488

84. Acosta ND, Golub SH. The New Federalism: State Policies Regarding Embryonic Stem Cell Research. J Law, Med Ethics [Internet]. 2016 [cited 2018 Feb 6];44(3):419–36. Available from: http://www.ncbi.nlm.nih.gov/pubmed/27587447

85. Kim J, Efe JA, Zhu S, Talantova M, Yuan X, Wang S, et al. Direct reprogramming of mouse fibroblasts to neural progenitors. Proc Natl Acad Sci U S A [Internet]. 2011 [cited 2018 Apr 29];108(19):7838–43. Available from: http://www.ncbi.nlm.nih.gov/pubmed/21521790

86. Cheng L, Hu W, Qiu B, Zhao J, Yu Y, Guan W, et al. Generation of neural progenitor cells by chemical cocktails and hypoxia. Cell Res [Internet]. 2014 [cited 2018 Apr 29];24(6):665–79. Available from: http://www.nature.com/articles/cr201432

87. Su G, Zhao Y, Wei J, Xiao Z, Chen B, Han J, et al. Direct conversion of fibroblasts into neural progenitor-like cells by forced growth into 3D spheres on low attachment surfaces. Biomaterials [Internet]. 2013 [cited 2018 Apr 29];34(24):5897–906. Available from: https://www.sciencedirect.com/science/article/pii/S0142961213004997

88. Bunge MB. Efficacy of Schwann cell transplantation for spinal cord repair is improved with combinatorial strategies. J Physiol [Internet]. 2016 [cited 2018 Apr 30];594(13):3533–8. Available from: http://www.ncbi.nlm.nih.gov/pubmed/26876753

89. Reier PJ, Bregman BS, Wujek JR. Intraspinal transplantation of embyronic spinal cord tissue in neonatal and adult rats. J Comp Neurol [Internet]. 1986 [cited 2018 Apr 30];247(3):275–96. Available from: http://www.ncbi.nlm.nih.gov/pubmed/3522658

90. Björklund A, Lindvall O. Cell replacement therapies for central nervous system disorders. Nat

Neurosci [Internet]. 2000 [cited 2018 Apr 30];3(6):537–44. Available from: http://www.ncbi.nlm.nih.gov/pubmed/10816308

91. Hofstetter CP, Holmström NA V, Lilja JA, Schweinhardt P, Hao J, Spenger C, et al. Allodynia limits the usefulness of intraspinal neural stem cell grafts; directed differentiation improves outcome. Nat Neurosci [Internet]. 2005 [cited 2018 Feb 3];8(3):346–53. Available from: http://www.nature.com/articles/nn1405

92. Macias M, Syring M, Pizzi M, Crowe M, Alexanian A, Kurpad S. Pain with no gain: Allodynia following neural stem cell transplantation in spinal cord injury. Exp Neurol [Internet]. 2006 [cited 2018 Feb 3];201(2):335–48. Available from: http://www.ncbi.nlm.nih.gov/pubmed/16839548

93. Karimi-Abdolrezaee S, Eftekharpour E, Wang J, Morshead CM, Fehlings MG. Delayed Transplantation of Adult Neural Precursor Cells Promotes Remyelination and Functional Neurological Recovery after Spinal Cord Injury. J Neurosci [Internet]. 2006 [cited 2018 Jan 3];26(13):3377–89. Available from: http://www.ncbi.nlm.nih.gov/pubmed/16571744

94. Takahashi Y, Tsuji O, Kumagai G, Hara CM, Okano HJ, Miyawaki A, et al. Comparative Study of Methods for Administering Neural Stem/Progenitor Cells to Treat Spinal Cord Injury in Mice. Cell Transplant [Internet]. 2011 [cited 2018 Feb 4];20(5):727–39. Available from: http://www.ncbi.nlm.nih.gov/pubmed/21054930

95. Kumamaru H, Saiwai H, Kubota K, Kobayakawa K, Yokota K, Ohkawa Y, et al. Therapeutic Activities of Engrafted Neural Stem/Precursor Cells Are Not Dormant in the Chronically Injured Spinal Cord. Stem Cells [Internet]. 2013 [cited 2018 Jan 31];31(8):1535–47. Available from: http://www.ncbi.nlm.nih.gov/pubmed/23606608

96. Lepore AC, Han SSW, Tyler-Polsz CJ, Cai J, Rao MS, Fischer I. Differential fate of multipotent and lineage-restricted neural precursors following transplantation into the adult CNS. Neuron Glia Biol [Internet]. 2004 [cited 2018 Feb 5];1(2):113–26. Available from:

http://www.ncbi.nlm.nih.gov/pubmed/16520830

97. Salazar DL, Uchida N, Hamers FPT, Cummings BJ, Anderson AJ. Human Neural Stem Cells Differentiate and Promote Locomotor Recovery in an Early Chronic Spinal coRd Injury NOD-scid Mouse Model. Gelain F, editor. PLoS One [Internet]. 2010 [cited 2018 Apr 30];5(8):e12272. Available from: http://dx.plos.org/10.1371/journal.pone.0012272

98. Nemati SN, Jabbari R, Hajinasrollah M, Zare Mehrjerdi N, Azizi H, Hemmesi K, et al. Transplantation of adult monkey neural stem cells into a contusion spinal cord injury model in rhesus macaque monkeys. Cell J [Internet]. 2014 [cited 2018 Feb 5];16(2):117–30. Available from: http://www.ncbi.nlm.nih.gov/pubmed/24567941

99. Brock JH, Graham L, Staufenberg E, Im S, Tuszynski MH. Rodent Neural Progenitor Cells Support Functional Recovery after Cervical Spinal Cord Contusion. J Neurotrauma [Internet]. 2018 [cited 2018 Apr 30];35(9):1069–78. Available from: http://www.liebertpub.com/doi/10.1089/neu.2017.5244

100. Kumagai G, Okada Y, Yamane J, Nagoshi N, Kitamura K, Mukaino M, et al. Roles of ES Cell-Derived Gliogenic Neural Stem/Progenitor Cells in Functional Recovery after Spinal Cord Injury. Hashimoto K, editor. PLoS One [Internet]. 2009 [cited 2018 May 18];4(11):e7706. Available from: http://dx.plos.org/10.1371/journal.pone.0007706

101. Moviglia G, Fernandez Viña R, Brizuela J, Saslavsky J, Vrsalovic F, Varela G, et al. Combined protocol of cell therapy for chronic spinal cord injury. Report on the electrical and functional recovery of two patients. Cytotherapy [Internet]. 2006 [cited 2018 Jun 11];8(3):202–9. Available from: http://files.rodrigo-nogueira.webnode.com/200000097-2337724354/Arq_1.pdf

102. Tabakow P, Raisman G, Fortuna W, Czyz M, Huber J, Li D, et al. Functional Regeneration of Supraspinal Connections in a Patient with Transected Spinal Cord following Transplantation of Bulbar Olfactory Ensheathing Cells with Peripheral Nerve Bridging. Cell Transplant

[Internet]. 2014 [cited 2018 Jun 11];23(12):1631–55. Available from: http://journals.sagepub.com/doi/10.3727/096368914X685131

103. Curtis E, Martin JR, Gabel B, Sidhu N, Rzesiewicz TK, Mandeville R, et al. A First-in-Human, Phase I Study of Neural Stem Cell Transplantation for Chronic Spinal Cord Injury. Cell Stem Cell [Internet]. 2018 [cited 2018 Jun 11];22(6):941–950.e6. Available from: https://www.sciencedirect.com/science/article/pii/S1934590918302327?via%3Dihub

104. Willyard C. Stem cells: A time to heal. Nature [Internet]. 2013 [cited 2018 Feb 5];503(7475):S4–6. Available from: http://www.nature.com/articles/503S4a

105. Liu S, Schackel T, Weidner N, Puttagunta R. Biomaterial-Supported Cell Transplantation Treatments for Spinal Cord Injury: Challenges and Perspectives. Front Cell Neurosci [Internet]. 2018 [cited 2018 Feb 3];11:430. Available from: http://www.ncbi.nlm.nih.gov/pubmed/29375316

106. Swanger SA, Neuhuber B, Himes BT, Bakshi A, Fischer I. Analysis of allogeneic and syngeneic bone marrow stromal cell graft survival in the spinal cord. Cell Transplant [Internet]. 2005 [cited 2018 Feb 4];14(10):775–86. Available from: http://www.ncbi.nlm.nih.gov/pubmed/16454352

107. Mooney DJ, Vandenburgh H. Cell Delivery Mechanisms for Tissue Repair. Cell Stem Cell [Internet]. 2008 [cited 2018 Jan 31];2(3):205–13. Available from: https://www.sciencedirect.com/science/article/pii/S1934590908000696

108. Mothe AJ, Tam RY, Zahir T, Tator CH, Shoichet MS. Repair of the injured spinal cord by transplantation of neural stem cells in a hyaluronan-based hydrogel. Biomaterials [Internet]. 2013 [cited 2018 Feb 4];34(15):3775–83. Available from: http://www.ncbi.nlm.nih.gov/pubmed/23465486

109. Amer MH, White LJ, Shakesheff KM. The effect of injection using narrow-bore needles on mammalian cells: administration and formulation considerations for cell therapies. J Pharm

Pharmacol [Internet]. 2015 [cited 2018 May 1];67(5):640–50. Available from: http://www.ncbi.nlm.nih.gov/pubmed/25623928

110. Pearse DD, Sanchez AR, Pereira FC, Andrade CM, Puzis R, Pressman Y, et al. Transplantation of Schwann cells and/or olfactory ensheathing glia into the contused spinal cord: Survival, migration, axon association, and functional recovery. Glia [Internet]. 2007 [cited 2018 May 1];55(9):976–1000. Available from: http://www.ncbi.nlm.nih.gov/pubmed/17526000

111. Fan W, Liu P, Wang G, Pu J, Xue X, Zhao J. Transplantation of hypoxic preconditioned neural stem cells benefits functional recovery via enhancing neurotrophic secretion after spinal cord injury in rats. J Cell Biochem [Internet]. 2018 [cited 2018 Apr 30];119(6):4339–51. Available from: http://doi.wiley.com/10.1002/jcb.26397

112. Mortazavi MM, Verma K, Tubbs RS, Theodore N. Cellular and paracellular transplants for spinal cord injury: a review of the literature. Child's Nerv Syst [Internet]. 2011 [cited 2017 Dec 20];27(2):237–43. Available from: http://www.ncbi.nlm.nih.gov/pubmed/20972681

113. Straley KS, Foo CWP, Heilshorn SC. Biomaterial Design Strategies for the Treatment of Spinal Cord Injuries. J Neurotrauma [Internet]. 2010 [cited 2018 Feb 5];27(1):1–19. Available from: http://www.ncbi.nlm.nih.gov/pubmed/19698073

114. Bento AR, Quelhas P, Oliveira MJ, Pêgo AP, Amaral IF. Three-dimensional culture of single embryonic stem-derived neural/stem progenitor cells in fibrin hydrogels: neuronal network formation and matrix remodelling. J Tissue Eng Regen Med [Internet]. 2017 [cited 2018 Feb 7];11(12):3494–507. Available from: http://doi.wiley.com/10.1002/term.2262

115. Liu C, Huang Y, Pang M, Yang Y, Li S, Liu L, et al. Tissue-engineered regeneration of completely transected spinal cord using induced neural stem cells and gelatin-electrospun poly (lactide-co-glycolide)/polyethylene glycol scaffolds. Sensebé L, editor. PLoS One [Internet]. 2015 [cited 2018 Feb 5];10(3):e0117709. Available from: http://dx.plos.org/10.1371/journal.pone.0117709

116. Lin C, Liu C, Zhang L, Huang Z, Zhao P, Chen R, et al. Interaction of iPSC-derived neural stem cells on poly(L-lactic acid) nanofibrous scaffolds for possible use in neural tissue engineering. Int J Mol Med [Internet]. 2017 [cited 2018 Feb 7]; Available from: http://www.spandidos-publications.com/10.3892/ijmm.2017.3299

117. Lu P, Wang Y, Graham L, McHale K, Gao M, Wu D, et al. Long-Distance Growth and Connectivity of Neural Stem Cells after Severe Spinal Cord Injury. Cell [Internet]. 2012 [cited 2018 Feb 7];150(6):1264–73. Available from: http://www.ncbi.nlm.nih.gov/pubmed/22980985

118. Kadoya K, Lu P, Nguyen K, Lee-Kubli C, Kumamaru H, Yao L, et al. Spinal cord reconstitution with homologous neural grafts enables robust corticospinal regeneration. Nat Med [Internet]. 2016 [cited 2018 Feb 7];22(5):479–87. Available from: http://www.ncbi.nlm.nih.gov/pubmed/27019328

119. Teng YD, Lavik EB, Qu X, Park KI, Ourednik J, Zurakowski D, et al. Functional recovery following traumatic spinal cord injury mediated by a unique polymer scaffold seeded with neural stem cells. Proc Natl Acad Sci [Internet]. 2002 [cited 2018 Feb 7];99(5):3024–9. Available from: http://www.ncbi.nlm.nih.gov/pubmed/11867737

120. Du B-L, Xiong Y, Zeng C-G, He L-M, Zhang W, Quan D-P, et al. Transplantation of artificial neural construct partly improved spinal tissue repair and functional recovery in rats with spinal cord transection. Brain Res [Internet]. 2011 [cited 2018 Feb 7];1400:87–98. Available from: http://www.ncbi.nlm.nih.gov/pubmed/21658682

121. Wang J-M, Zeng Y-S, Wu J-L, Li Y, Teng YD. Cograft of neural stem cells and schwann cells overexpressing TrkC and neurotrophin-3 respectively after rat spinal cord transection. Biomaterials [Internet]. 2011 [cited 2018 Feb 7];32(30):7454–68. Available from: http://www.ncbi.nlm.nih.gov/pubmed/21783247

122. Li X, Xiao Z, Han J, Chen L, Xiao H, Ma F, et al. Promotion of neuronal differentiation of neural

progenitor cells by using EGFR antibody functionalized collagen scaffolds for spinal cord injury repair. Biomaterials [Internet]. 2013 [cited 2018 Feb 7];34(21):5107–16. Available from: http://www.ncbi.nlm.nih.gov/pubmed/23591390

123. Fouad K, Schnell L, Bunge MB, Schwab ME, Liebscher T, Pearse DD. Combining Schwann Cell Bridges and Olfactory-Ensheathing Glia Grafts with Chondroitinase Promotes Locomotor Recovery after Complete Transection of the Spinal Cord. J Neurosci [Internet]. 2005 [cited 2018 Feb 7];25(5):1169–78. Available from: http://www.ncbi.nlm.nih.gov/pubmed/15689553

124. Wang C, Sun C, Hu Z, Huo X, Yang Y, Liu X, et al. Improved Neural Regeneration with Olfactory Ensheathing Cell Inoculated PLGA Scaffolds in Spinal Cord Injury Adult Rats. Neurosignals [Internet]. 2017 [cited 2018 Feb 7];25(1):1–14. Available from: http://www.ncbi.nlm.nih.gov/pubmed/28359049

125. Hong LTA, Kim Y-M, Park HH, Hwang DH, Cui Y, Lee EM, et al. An injectable hydrogel enhances tissue repair after spinal cord injury by promoting extracellular matrix remodeling. Nat Commun [Internet]. 2017 [cited 2018 Feb 7];8(1):533. Available from: http://www.nature.com/articles/s41467-017-00583-8

126. King VR, Alovskaya A, Wei DYT, Brown RA, Priestley J V. The use of injectable forms of fibrin and fibronectin to support axonal ingrowth after spinal cord injury. Biomaterials [Internet]. 2010 [cited 2018 Jan 17];31(15):4447–56. Available from: http://www.ncbi.nlm.nih.gov/pubmed/20206381

127. Novikova LN, Mosahebi A, Wiberg M, Terenghi G, Kellerth J-O, Novikov LN. Alginate hydrogel and matrigel as potential cell carriers for neurotransplantation. J Biomed Mater Res Part A [Internet]. 2006 [cited 2018 Feb 5];77A(2):242–52. Available from: http://www.ncbi.nlm.nih.gov/pubmed/16392134

128. Zhuo F, Liu X, Gao Q, Wang Y, Hu K, Cai Q. Injectable hyaluronan-methylcellulose composite

hydrogel crosslinked by polyethylene glycol for central nervous system tissue engineering. Mater Sci Eng C [Internet]. 2017 [cited 2018 Jan 3];81:1–7. Available from: https://www.sciencedirect.com/science/article/pii/S0928493117317836#bb0145

129. Gupta D, Tator CH, Shoichet MS. Fast-gelling injectable blend of hyaluronan and methylcellulose for intrathecal, localized delivery to the injured spinal cord. Biomaterials [Internet]. 2006 [cited 2018 Feb 6];27(11):2370–9. Available from: https://www.sciencedirect.com/science/article/pii/S0142961205010410?via%3Dihub

130. Hidalgo San Jose L, Stephens P, Song B, Barrow D. Microfluidic Encapsulation Supports Stem Cell Viability, Proliferation, and Neuronal Differentiation. Tissue Eng Part C Methods [Internet]. 2018 [cited 2018 Feb 6]; Available from: http://www.ncbi.nlm.nih.gov/pubmed/29258387

131. Olson HE, Rooney GE, Gross L, Nesbitt JJ, Galvin KE, Knight A, et al. Neural Stem Cell– and Schwann Cell–Loaded Biodegradable Polymer Scaffolds Support Axonal Regeneration in the Transected Spinal Cord. Tissue Eng Part A [Internet]. 2009 [cited 2018 Feb 6];15(7):1797–805. Available from: http://www.ncbi.nlm.nih.gov/pubmed/19191513

132. Nomura H, Zahir T, Kim H, Katayama Y, Kulbatski I, Morshead CM, et al. Extramedullary Chitosan Channels Promote Survival of Transplanted Neural Stem and Progenitor Cells and Create a Tissue Bridge After Complete Spinal Cord Transection. Tissue Eng Part A [Internet]. 2008 [cited 2018 Feb 6];14(5):649–65. Available from: http://www.ncbi.nlm.nih.gov/pubmed/18419246

133. Bozkurt G, Mothe AJ, Zahir T, Kim H, Shoichet MS, Tator CH. Chitosan Channels Containing Spinal Cord-Derived Stem/Progenitor Cells for Repair of Subacute Spinal Cord Injury in the Rat. Neurosurgery [Internet]. 2010 [cited 2018 Feb 6];67(6):1733–44. Available from: http://www.ncbi.nlm.nih.gov/pubmed/21107205

134. Van Norman GA. Drugs, Devices, and the FDA: Part 1: An Overview of Approval Processes

for Drugs. JACC Basic to Transl Sci [Internet]. 2016 [cited 2018 May 1];1(3):170–9. Available from: https://www.sciencedirect.com/science/article/pii/S2452302X1600036X

135. Fargen KM, Frei D, Fiorella D, McDougall CG, Myers PM, Hirsch JA, et al. The FDA approval process for medical devices: an inherently flawed system or a valuable pathway for innovation? J Neurointerv Surg [Internet]. 2013 [cited 2018 May 1];5(4):269–75. Available from: http://www.ncbi.nlm.nih.gov/pubmed/22764203

136. Sade B, Oya S, Lee JH. Non-watertight dural reconstruction in meningioma surgery: results in 439 consecutive patients and a review of the literature. J Neurosurg [Internet]. 2011 [cited 2018 Jan 3];114(3):714–8. Available from: http://www.ncbi.nlm.nih.gov/pubmed/20707618

137. Integra LifeSciences Corporation. DuraGen® Plus matrix « Integra LifeSciences: Europe, Middle East and Africa [Internet]. 2010 [cited 2018 Jan 3]. Available from: http://www.integralife.eu/products/neuro/duraplasty/duragen-plus-matrix-2/

138. Integra LifeSciences Corporation. Dural Regeneration Matrix: Product information leaflet [Internet]. 2009 [cited 2018 Jan 3]. Available from: https://www.integralife.com/file/general/1453795521-1.pdf

139. Pena C (FDA). Department of health and human services [Internet]. 2015 [cited 2018 Jan 3]. Available from: https://www.accessdata.fda.gov/cdrh_docs/pdf15/K150825.pdf

140. Shin SS, Grandhi R, Henchir J, Yan HQ, Badylak SF, Dixon CE. Neuroprotective effects of collagen matrix in rats after traumatic brain injury. Restor Neurol Neurosci [Internet]. 2015 [cited 2018 Jan 3];33(2):95–104. Available from: https://content.iospress.com/articles/restorative-neurology-and-neuroscience/rnn140430

141. Adams CF, Dickson AW, Kuiper J-H, Chari DM. Nanoengineering neural stem cells on biomimetic substrates using magnetofection technology. Nanoscale. 2016;8(41).

142. Integra LifeSciences Corporation. Ultra Pure Collagen ™ Dural repair [Internet]. 2009 [cited

2018 Feb 6]. Available from: http://www.cardion.cz/file/90/duragen-ultrapure-collagen.pdf

143. Gafni Y, Pelled G, Zilberman Y, Turgeman G, Apparailly F, Yotvat H, et al. Gene Therapy Platform for Bone Regeneration Using an Exogenously Regulated, AAV-2-Based Gene Expression System. Mol Ther [Internet]. 2004 [cited 2018 Jan 3];9(4):587–95. Available from: https://www.sciencedirect.com/science/article/pii/S1525001603004131?via%3Dihub

144. Steinhardt Y, Aslan H, Regev E, Zilberman Y, Kallai I, Gazit D, et al. Maxillofacial–Derived Stem Cells Regenerate Critical Mandibular Bone Defect. Tissue Eng Part A [Internet]. 2008 [cited 2018 Jan 3];14(11):1763–73. Available from: http://www.ncbi.nlm.nih.gov/pubmed/18636943

145. Kallai I, van Lenthe GH, Ruffoni D, Zilberman Y, Müller R, Pelled G, et al. Quantitative, structural, and image-based mechanical analysis of nonunion fracture repaired by genetically engineered mesenchymal stem cells. J Biomech [Internet]. 2010 [cited 2018 Jan 3];43(12):2315–20. Available from: http://www.ncbi.nlm.nih.gov/pubmed/20471652

146. Kimelman-Bleich N, Pelled G, Zilberman Y, Kallai I, Mizrahi O, Tawackoli W, et al. Targeted Gene-and-host Progenitor Cell Therapy for Nonunion Bone Fracture Repair. Mol Ther [Internet]. 2011 [cited 2018 Jan 3];19(1):53–9. Available from: http://www.ncbi.nlm.nih.gov/pubmed/20859259

147. Adesida AB, Mulet-Sierra A, Laouar L, Jomha NM. Oxygen Tension Is a Determinant of the Matrix-Forming Phenotype of Cultured Human Meniscal Fibrochondrocytes. Awad HA, editor. PLoS One [Internet]. 2012 [cited 2018 Jan 3];7(6):e39339. Available from: http://www.ncbi.nlm.nih.gov/pubmed/22720095

148. Murphy MB, Suzuki RK, Sand TT, Chaput CD, Gregory CA. Short Term Culture of Human Mesenchymal Stem Cells with Commercial Osteoconductive Carriers Provides Unique Insights into Biocompatibility. J Clin Med [Internet]. 2013 [cited 2018 Feb 5];2(3):49–66. Available from: http://www.mdpi.com/2077-0383/2/3/49

149. Geng X, Hong Q, Wang W, Zheng W, Li O, Cai G, et al. Biological Membrane-Packed Mesenchymal Stem Cells Treat Acute Kidney Disease by Ameliorating Mitochondrial-Related Apoptosis. Sci Rep [Internet]. 2017 [cited 2018 Jan 3];7:41136. Available from: http://www.nature.com/articles/srep41136

150. Gersey ZC, Burks SS, Anderson KD, Dididze M, Khan A, Dietrich WD, et al. First human experience with autologous Schwann cells to supplement sciatic nerve repair: report of 2 cases with long-term follow-up. Neurosurg Focus [Internet]. 2017 [cited 2017 Dec 19];42(3):E2. Available from: http://thejns.org/doi/10.3171/2016.12.FOCUS16474

151. Hoffmann A, Pelled G, Turgeman G, Eberle P, Zilberman Y, Shinar H, et al. Neotendon formation induced by manipulation of the Smad8 signalling pathway in mesenchymal stem cells. J Clin Invest [Internet]. 2006 [cited 2018 Feb 5];116(4):940–52. Available from: http://www.jci.org/cgi/doi/10.1172/JCI22689

152. Rabinowitz L, Monnerie H, Shashidhara S, Le Roux PD. Growth of rat cortical neurons on DuraGen, a collagen-based dural graft matrix. Neurol Res [Internet]. 2005 [cited 2018 Jan 3];27(8):887–94. Available from: http://www.ncbi.nlm.nih.gov/pubmed/16354551

153. De Kok IJ, Jere D, Padilla RJ, Cooper LF. Evaluation of a collagen scaffold for cell-based bone repair. Int J Oral Maxillofac Implants [Internet]. 2014 [cited 2018 Feb 5];29(1):e122-9. Available from: http://www.ncbi.nlm.nih.gov/pubmed/24451880

154. Triplett RG, Nevins M, Marx RE, Spagnoli DB, Oates TW, Moy PK, et al. Pivotal, randomized, parallel evaluation of recombinant human bone morphogenetic protein-2/absorbable collagen sponge and autogenous bone graft for maxillary sinus floor augmentation. J Oral Maxillofac Surg [Internet]. 2009 [cited 2018 Feb 5];67(9):1947–60. Available from: https://www.sciencedirect.com/science/article/pii/S0278239109005898?via%3Dihub

155. Croutze R, Jomha N, Uludag H, Adesida A. Matrix forming characteristics of inner and outer human meniscus cells on 3D collagen scaffolds under normal and low oxygen tensions. BMC

Musculoskelet Disord [Internet]. 2013 [cited 2018 Feb 5];14(1):353. Available from: http://www.ncbi.nlm.nih.gov/pubmed/24330551

156. Tai K, Pelled G, Sheyn D, Bershteyn A, Han L, Kallai I, et al. Nanobiomechanics of Repair Bone Regenerated by Genetically Modified Mesenchymal Stem Cells. Tissue Eng Part A [Internet]. 2008 [cited 2018 Feb 5];14(10):1709–20. Available from: http://www.ncbi.nlm.nih.gov/pubmed/18620480

157. Kim KD, Wright NM. Polyethylene Glycol Hydrogel Spinal Sealant (DuraSeal Spinal Sealant) as an Adjunct to Sutured Dural Repair in the Spine. Spine (Phila Pa 1976) [Internet]. 2011 [cited 2018 May 12];36(23):1906–12. Available from: http://www.ncbi.nlm.nih.gov/pubmed/22008746

158. Integra LifeSciences. DuraSeal® Xact Spinal Sealant System [Internet]. 2016 [cited 2018 May 11]. Available from: http://www.integralife.eu/products/neuro/duraplasty/duraseal-xact-sealant-system-adhesion-barrier-2/

159. Naghdi P, Tiraihi T, Ganji F, Darabi S, Taheri T, Kazemi H. Survival, proliferation and differentiation enhancement of neural stem cells cultured in three-dimensional polyethylene glycol-RGD hydrogel with tenascin. J Tissue Eng Regen Med [Internet]. 2016 [cited 2018 May 12];10(3):199–208. Available from: http://www.ncbi.nlm.nih.gov/pubmed/25312025

160. Oda Y, Tani K, Isozaki A, Haraguchi T, Itamoto K, Nakazawa H, et al. Effects of polyethylene glycol administration and bone marrow stromal cell transplantation therapy in spinal cord injury mice. J Vet Med Sci [Internet]. 2014 [cited 2018 May 12];76(3):415–21. Available from: http://www.ncbi.nlm.nih.gov/pubmed/24270802

161. Borgens RB, Shi R, Bohnert D. Behavioral recovery from spinal cord injury following delayed application of polyethylene glycol. J Exp Biol [Internet]. 2002 [cited 2018 May 12];205(Pt 1):1–12. Available from: http://www.ncbi.nlm.nih.gov/pubmed/11818407

162. Duerstock BS, Borgens RB. Three-dimensional morphometry of spinal cord injury following polyethylene glycol treatment. J Exp Biol [Internet]. 2002 [cited 2018 May 12];205(Pt 1):13–24. Available from: http://www.ncbi.nlm.nih.gov/pubmed/11818408

163. Liu-Snyder P, Logan MP, Shi R, Smith DT, Borgens RB. Neuroprotection from secondary injury by polyethylene glycol requires its internalization. J Exp Biol [Internet]. 2007 [cited 2018 May 12];210(8):1455–62. Available from: http://www.ncbi.nlm.nih.gov/pubmed/17401128

164. Neuman BJ, Radcliff K, Rihn J. Cauda equina syndrome after a TLIF resulting from postoperative expansion of a hydrogel dural sealant. Clin Orthop Relat Res [Internet]. 2012 [cited 2018 Feb 17];470(6):1640–5. Available from: http://www.ncbi.nlm.nih.gov/pubmed/21952743

165. Lee S-H, Park C-W, Lee S-G, Kim W-K. Postoperative Cervical Cord Compression Induced by Hydrogel Dural Sealant (DuraSeal®). Korean J Spine [Internet]. 2013 [cited 2018 Feb 17];10(1):44–6. Available from: http://www.ncbi.nlm.nih.gov/pubmed/24757459

166. Lin K-L, Yang D-Y, Chu I-M, Cheng F-C, Chen C-J, Ho S-P, et al. DuraSeal as a Ligature in the Anastomosis of Rat Sciatic Nerve Gap Injury. J Surg Res [Internet]. 2010 [cited 2018 Feb 17];161(1):101–10. Available from: http://www.ncbi.nlm.nih.gov/pubmed/19482304

167. Isaacs J, Klumb I, McDaniel C. Preliminary investigation of a polyethylene glycol hydrogel “nerve glue”. J Brachial Plex Peripher Nerve Inj [Internet]. 2009 [cited 2018 Feb 17];4:16. Available from: http://www.ncbi.nlm.nih.gov/pubmed/19754963

168. Janmey PA, Winer JP, Weisel JW. Fibrin gels and their clinical and bioengineering applications. J R Soc Interface [Internet]. 2009 [cited 2018 Mar 7];6(30):1–10. Available from: http://www.ncbi.nlm.nih.gov/pubmed/18801715

169. Zhang X, Wang H, Ma X, Adila A, Wang B, Liu F, et al. Preservation of the cardiac function in infarcted rat hearts by the transplantation of adipose-derived stem cells with injectable fibrin scaffolds. Exp Biol Med [Internet]. 2010 [cited 2018 Feb 17];235(12):1505–15.

Available from: http://www.ncbi.nlm.nih.gov/pubmed/21127347

170. Kim YS, Sung CH, Chung SH, Kwak SJ, Koh YG. Does an Injection of Adipose-Derived Mesenchymal Stem Cells Loaded in Fibrin Glue Influence Rotator Cuff Repair Outcomes? A Clinical and Magnetic Resonance Imaging Study. Am J Sports Med [Internet]. 2017 [cited 2018 Feb 17];45(9):2010–8. Available from: http://www.ncbi.nlm.nih.gov/pubmed/28448728

171. Chen S-J, Chang C-M, Tsai S-K, Chang Y-L, Chou S-J, Huang S-S, et al. Functional Improvement of Focal Cerebral Ischemia Injury by Subdural Transplantation of Induced Pluripotent Stem Cells with Fibrin Glue. Stem Cells Dev [Internet]. 2010 [cited 2018 Feb 17];19(11):1757–67. Available from: http://www.ncbi.nlm.nih.gov/pubmed/20192839

172. Graziano F, Certo F, Basile L, Maugeri R, Grasso G, Meccio F, et al. Autologous fibrin sealant (Vivostat(®)) in the neurosurgical practice: Part I: Intracranial surgical procedure. Surg Neurol Int [Internet]. 2015 [cited 2018 Feb 17];6:77. Available from: http://www.ncbi.nlm.nih.gov/pubmed/25984391

173. Johnstone P, Kwei JS-S, Filobbos G, Lewis D, Jeffery S. Successful application of keratinocyte suspension using autologous fibrin spray. Burns [Internet]. 2017 [cited 2018 Feb 17];43(3):e27–30. Available from: http://www.ncbi.nlm.nih.gov/pubmed/27345775

174. Gärtner A, Pereira T, Armada-da-Silva P, Amado S, Veloso A, Amorim I, et al. Effects of umbilical cord tissue mesenchymal stem cells (UCX®) on rat sciatic nerve regeneration after neurotmesis injuries. J Stem Cells Regen Med [Internet]. 2014 [cited 2018 Feb 17];10(1):14–26. Available from: http://www.ncbi.nlm.nih.gov/pubmed/25075157

175. Sinis N, Manoli T, Schiefer JL, Werdin F, Jaminet P, Kraus A, et al. Application of 2 Different Hemostatic Procedures During Microsurgical Median Nerve Reconstruction in the Rat Does Not Hinder Axonal Regeneration. Neurosurgery [Internet]. 2011 [cited 2018 Feb 17];68(5):1399–404. Available from: http://www.ncbi.nlm.nih.gov/pubmed/21311369

176. Xu L, Wu F, Yuan W, Jin T. Controlled-release implant system formulated using biodegradable hemostatic gauze as scaffold. Int J Pharm [Internet]. 2008 [cited 2018 Jun 1];355(1–2):249–58. Available from: https://www.sciencedirect.com/science/article/pii/S0378517307010599

177. Finn MD, Schow SR, Schneiderman ED. Osseous regeneration in the presence of four common hemostatic agents. J Oral Maxillofac Surg [Internet]. 1992 [cited 2018 Jun 1];50(6):608–12. Available from: http://www.ncbi.nlm.nih.gov/pubmed/1593323

178. Pan H-C, Yang D-Y, Chiu Y-T, Lai S-Z, Wang Y-C, Chang M-H, et al. Enhanced regeneration in injured sciatic nerve by human amniotic mesenchymal stem cell. J Clin Neurosci [Internet]. 2006 [cited 2018 Jun 1];13(5):570–5. Available from: http://www.ncbi.nlm.nih.gov/pubmed/16769515

179. Stewart AN, Matyas JJ, Welchko RM, Goldsmith AD, Zeiler SE, Hochgeschwender U, et al. SDF-1 overexpression by mesenchymal stem cells enhances GAP-43-positive axonal growth following spinal cord injury. Restor Neurol Neurosci [Internet]. 2017 [cited 2018 Feb 11];35(4):395–411. Available from: http://www.medra.org/servlet/aliasResolver?alias=iospress&doi=10.3233/RNN-160678

180. Stewart AN, Kendziorski G, Deak ZM, Brown DJ, Fini MN, Copely KL, et al. Co-transplantation of mesenchymal and neural stem cells and overexpressing stromal-derived factor-1 for treating spinal cord injury. Brain Res [Internet]. 2017 [cited 2018 Feb 11];1672:91–105. Available from: http://www.ncbi.nlm.nih.gov/pubmed/28734802

181. Zhao Y, Tang F, Han G, Wang N, Yin N, Chen B, et al. Clinical study of NeuroRegen scaffold combined with human mesenchymal stem cells for the repair of chronic complete spinal cord injury. Cell Transplant [Internet]. 2017 [cited 2017 Dec 19];26(5):1–28. Available from: http://journals.sagepub.com/doi/10.3727/096368917X695038

182. Shakhbazau A, Shcharbin D, Bryszewska M, Kumar R, Wobma HM, Kallos MS, et al. Non-viral

engineering of skin precursor-derived Schwann cells for enhanced NT-3 production in adherent and microcarrier culture. Curr Med Chem [Internet]. 2012 [cited 2018 Feb 11];19(32):5572–9. Available from: http://www.ncbi.nlm.nih.gov/pubmed/22834817

183. Lavdas AA, Chen J, Papastefanaki F, Chen S, Schachner M, Matsas R, et al. Schwann cells engineered to express the cell adhesion molecule L1 accelerate myelination and motor recovery after spinal cord injury. Exp Neurol [Internet]. 2010 [cited 2018 Feb 12];221(1):206–16. Available from: https://www.sciencedirect.com/science/article/pii/S0014488609004567?via%3Dihub

184. Cai P, Sun G, Cai P, Oudega M, Xiao R, Wang X, et al. Survival of transplanted neurotrophin-3 expressing human neural stem cells and motor function in a rat model of spinal cord injury. Neural Regen Res. 2009;4(7):485–91.

185. Bohl D, Liu S, Blanchard S, Hocquemiller M, Haase G, Heard J-M. Directed Evolution of Motor Neurons from Genetically Engineered Neural Precursors. Stem Cells [Internet]. 2008 [cited 2018 Feb 12];26(10):2564–75. Available from: http://doi.wiley.com/10.1634/stemcells.2008-0371

186. Ruitenberg MJ, Levison DB, Lee S V., Verhaagen J, Harvey AR, Plant GW. NT-3 expression from engineered olfactory ensheathing glia promotes spinal sparing and regeneration. Brain [Internet]. 2005 [cited 2018 Feb 12];128(4):839–53. Available from: https://academic.oup.com/brain/article-lookup/doi/10.1093/brain/awh424

187. Ruitenberg MJ, Plant GW, Hamers FPT, Wortel J, Blits B, Dijkhuizen PA, et al. Ex vivo adenoviral vector-mediated neurotrophin gene transfer to olfactory ensheathing glia: Effects on rubrospinal tract regeneration, lesion size, and functional recovery after implantation in the injured rat spinal cord. J Neurosci [Internet]. 2003 [cited 2018 Feb 12];23(18):7045–58. Available from: https://www.ncbi.nlm.nih.gov/pubmed/12904465

188. Taha MF. Cell based-gene delivery approaches for the treatment of spinal cord injury and

neurodegenerative disorders. Curr Stem Cell Res Ther [Internet]. 2010 [cited 2018 May 18];5(1):23–36. Available from: http://www.ncbi.nlm.nih.gov/pubmed/19951254

189. Carwardine D, Wong L-F, Fawcett JW, Muir EM, Granger N. Canine olfactory ensheathing cells from the olfactory mucosa can be engineered to produce active chondroitinase ABC. J Neurol Sci [Internet]. 2016 [cited 2018 Feb 11];367:311–8. Available from: https://www.sciencedirect.com/science/article/pii/S0022510X16303422?via%3Dihub

190. Zhao M, Chen B, Wei X, Hou S. Implantation of neurotrophin gene modified bone derived mesenchymal stem cells to repair spinal cord complete transection injury in adult rats. Int J Clin Exp Pathol [Internet]. 2016 [cited 2018 Feb 11];9(2):695–704. Available from: http://www.ijcep.com/files/ijcep0018237.pdf

191. Deng L-X, Deng P, Ruan Y, Xu ZC, Liu N-K, Wen X, et al. A Novel Growth-Promoting Pathway Formed by GDNF-Overexpressing Schwann Cells Promotes Propriospinal Axonal Regeneration, Synapse Formation, and Partial Recovery of Function after Spinal Cord Injury. J Neurosci [Internet]. 2013 [cited 2018 May 17];33(13):5655–67. Available from: http://www.ncbi.nlm.nih.gov/pubmed/23536080

192. Delaney AM, Adams CF, Fernandes AR, Al-Shakli AF, Sen J, Carwardine DR, et al. A fusion of minicircle DNA and nanoparticle delivery technologies facilitates therapeutic genetic engineering of autologous canine olfactory mucosal cells. Nanoscale [Internet]. 2017 [cited 2018 Feb 11];9(25):8560–6. Available from: http://www.ncbi.nlm.nih.gov/pubmed/28613324

193. Sharma AD, Brodskiy PA, Petersen EM, Dagdeviren M, Ye E-A, Mallapragada SK, et al. High throughput characterization of adult stem cells engineered for delivery of therapeutic factors for neuroprotective strategies. J Vis Exp [Internet]. 2015 [cited 2018 Feb 11];(95):e52242. Available from: http://www.ncbi.nlm.nih.gov/pubmed/25590859

194. Hur E-M, Hong Yang I, Kim D-H, Byun J, Xu W-L, Nicovich PR, et al. Engineering neuronal

growth cones to promote axon regeneration over inhibitory molecules. Proc Natl Acad Sci U S A [Internet]. 2011 [cited 2018 Feb 11];108(12):5057–62. Available from: http://www.pnas.org/content/pnas/108/12/5057.full.pdf

195. Fernandes AR, Chari DM. Part II: Functional delivery of a neurotherapeutic gene to neural stem cells using minicircle DNA and nanoparticles: Translational advantages for regenerative neurology. J Control Release. 2016;238.

196. Haastert K, Mauritz C, Matthies C, Grothe C. Autologous adult human Schwann cells genetically modified to provide alternative cellular transplants in peripheral nerve regeneration. J Neurosurg [Internet]. 2006 [cited 2018 Feb 12];104(5):778–86. Available from: http://thejns.org/doi/10.3171/jns.2006.104.5.778

197. Baum C, Kustikova O, Modlich U, Li Z, Fehse B. Mutagenesis and Oncogenesis by Chromosomal Insertion of Gene Transfer Vectors. Hum Gene Ther [Internet]. 2006 [cited 2018 May 18];17(3):253–63. Available from: http://www.ncbi.nlm.nih.gov/pubmed/16544975

198. Patra S, Andrew AA. Human, Social, and Environmental Impacts of Human Genetic Engineering. J Biomed Sci [Internet]. 2015 [cited 2018 May 17];04(02). Available from: http://www.jbiomeds.com/biomedical-sciences/human-social-and-environmental-impacts-of-human-genetic-engineering.php?aid=7264

199. Abou-El-Enein M, Bauer G, Reinke P, Renner M, Schneider CK. A roadmap toward clinical translation of genetically-modified stem cells for treatment of HIV. Trends Mol Med [Internet]. 2014 [cited 2018 May 17];20(11):632–42. Available from: http://www.ncbi.nlm.nih.gov/pubmed/25262540

200. Hwang DH, Kim HM, Kang YM, Joo IS, Cho C-S, Yoon B-W, et al. Combination of Multifaceted Strategies to Maximize the Therapeutic Benefits of Neural Stem Cell Transplantation for Spinal Cord Repair. Cell Transplant [Internet]. 2011 [cited 2018 Feb 7];20(9):1361–80.

Available from: http://www.ncbi.nlm.nih.gov/pubmed/21396156

201. Du B-L, Zeng X, Ma Y-H, Lai B-Q, Wang J-M, Ling E-A, et al. Graft of the gelatin sponge scaffold containing genetically-modified neural stem cells promotes cell differentiation, axon regeneration, and functional recovery in rat with spinal cord transection. J Biomed Mater Res Part A [Internet]. 2015 [cited 2018 May 12];103(4):1533–45. Available from: http://www.ncbi.nlm.nih.gov/pubmed/25046856

202. Deng L-X, Hu J, Liu N, Wang X, Smith GM, Wen X, et al. GDNF modifies reactive astrogliosis allowing robust axonal regeneration through Schwann cell-seeded guidance channels after spinal cord injury. Exp Neurol [Internet]. 2011 [cited 2018 May 12];229(2):238–50. Available from: http://www.ncbi.nlm.nih.gov/pubmed/21316362

203. Gao M, Lu P, Bednark B, Lynam D, Conner JM, Sakamoto J, et al. Templated agarose scaffolds for the support of motor axon regeneration into sites of complete spinal cord transection. Biomaterials [Internet]. 2013 [cited 2018 May 12];34(5):1529–36. Available from: http://www.ncbi.nlm.nih.gov/pubmed/23182350

204. Kubinová Š. New trends in spinal cord tissue engineering. Futur Neurol [Internet]. 2015 [cited 2018 May 12];10(2):129–45. Available from: https://www.futuremedicine.com/doi/pdf/10.2217/fnl.14.71

205. Kim TK, Eberwine JH. Mammalian cell transfection: the present and the future. Anal Bioanal Chem [Internet]. 2010 [cited 2018 Feb 17];397(8):3173–8. Available from: http://www.ncbi.nlm.nih.gov/pubmed/20549496

206. Thomas CE, Ehrhardt A, Kay MA. Progress and problems with the use of viral vectors for gene therapy. Nat Rev Genet [Internet]. 2003 [cited 2018 Feb 15];4(5):346–58. Available from: http://www.nature.com/articles/nrg1066

207. Jordan M, Wurm F. Transfection of adherent and suspended cells by calcium phosphate. Methods [Internet]. 2004 [cited 2018 Feb 17];33(2):136–43. Available from:

https://www.sciencedirect.com/science/article/pii/S1046202303003050

208. Yarmush ML, Golberg A, Serša G, Kotnik T, Miklavčič D. Electroporation-Based Technologies for Medicine: Principles, Applications, and Challenges. Annu Rev Biomed Eng [Internet]. 2014 [cited 2018 Feb 17];16(1):295–320. Available from: http://www.annualreviews.org/doi/10.1146/annurev-bioeng-071813-104622

209. Inoue T, Krumlauf R. An impulse to the brain--using in vivo electroporation. Nat Neurosci [Internet]. 2001 [cited 2018 May 14];4(Supp):1156–8. Available from: http://www.ncbi.nlm.nih.gov/pubmed/11687822

210. Shirahata Y, Ohkohchi N, Itagak H, Satomi S. New Technique for Gene Transfection Using Laser Irradiation. J Investig Med [Internet]. 2001 [cited 2018 May 14];49(2):184–90. Available from: http://www.ncbi.nlm.nih.gov/pubmed/11288759

211. Pickard M, Chari D. Enhancement of magnetic nanoparticle-mediated gene transfer to astrocytes by 'magnetofection': effects of static and oscillating fields. Nanomedicine [Internet]. 2010 [cited 2018 May 23];5(2):217–32. Available from: http://www.ncbi.nlm.nih.gov/pubmed/20148634

212. Pickard MR, Barraud P, Chari DM. The transfection of multipotent neural precursor/stem cell transplant populations with magnetic nanoparticles. Biomaterials [Internet]. 2011 [cited 2018 Mar 1];32(9):2274–84. Available from: https://www.sciencedirect.com/science/article/pii/S0142961210015449?via%3Dihub

213. Scherer F, Anton M, Schillinger U, Henke J, Bergemann C, Krüger A, et al. Magnetofection: enhancing and targeting gene delivery by magnetic force in vitro and in vivo. Gene Ther [Internet]. 2002 [cited 2018 May 14];9(2):102–9. Available from: http://www.ncbi.nlm.nih.gov/pubmed/11857068

214. Dobson J. Gene therapy progress and prospects: magnetic nanoparticle-based gene delivery. Gene Ther [Internet]. 2006 [cited 2018 May 14];13(4):283–7. Available from:

http://www.ncbi.nlm.nih.gov/pubmed/16462855

215. Pickard M, Adams C, Barraud P, Chari D. Using Magnetic Nanoparticles for Gene Transfer to Neural Stem Cells: Stem Cell Propagation Method Influences Outcomes. J Funct Biomater [Internet]. 2015 [cited 2018 Feb 16];6(4):259–76. Available from: http://www.ncbi.nlm.nih.gov/pubmed/25918990

216. Gracey Maniar LE, Maniar JM, Chen Z-Y, Lu J, Fire AZ, Kay MA. Minicircle DNA Vectors Achieve Sustained Expression Reflected by Active Chromatin and Transcriptional Level. Mol Ther [Internet]. 2013 [cited 2018 Feb 16];21(1):131–8. Available from: http://www.ncbi.nlm.nih.gov/pubmed/23183534

217. Fernandes AR, Chari DM. Part I: Minicircle vector technology limits DNA size restrictions on ex vivo gene delivery using nanoparticle vectors: Overcoming a translational barrier in neural stem cell therapy. J Control Release. 2016;238.

218. Biosciences S. Minicircle DNA Vector Technology Cat. #MNXXX Series: user manual. 2012. p. 2.

219. Integra LifeSciences Corporation. Seal to heal with DuraSeal [Internet]. 2016. Available from: http://sealtoheal.com/index.php/use-duraseal/for-spinal-use/

220. Kroemer G, Galluzzi L, Vandenabeele P, Abrams J, Alnemri ES, Baehrecke EH, et al. Classification of cell death: recommendations of the Nomenclature Committee on Cell Death 2009. Cell Death Differ [Internet]. 2009 [cited 2018 Apr 22];16(1):3–11. Available from: http://www.ncbi.nlm.nih.gov/pubmed/18846107

221. Delaney AM. Optimising canine olfactory ensheathing cell therapy using tissue engineering tools. Keele University; 2016.

222. Engler AJ, Sen S, Sweeney HL, Discher DE. Matrix Elasticity Directs Stem Cell Lineage Specification. Cell [Internet]. 2006 [cited 2018 May 22];126(4):677–89. Available from: http://www.ncbi.nlm.nih.gov/pubmed/16923388

223. Adams C. Assessment of magnetic particles for neural stem cell- based therapies. Keele University; 2015.

224. Moreno-Arotzena O, Meier J, del Amo C, García-Aznar J. Characterization of Fibrin and Collagen Gels for Engineering Wound Healing Models. Materials (Basel) [Internet]. 2015 [cited 2018 May 22];8(4):1636–51. Available from: http://www.mdpi.com/1996-1944/8/4/1636

225. Simpliciano C, Clark L, Asi B, Chu N, Mercado M, Diaz S, et al. Cross-Linked Alginate Film Pore Size Determination Using Atomic Force Microscopy and Validation Using Diffusivity Determinations *. J Surf Eng Mater Adv Technol [Internet]. 2013 [cited 2018 May 22];3:1–12. Available from: http://dx.doi.org/10.4236/jsemat.2013.34A1001

226. Lim TC, Bang CP, Chian KS, Leong KF. Development of cryogenic prototyping for tissue engineering. Virtual Phys Prototyp [Internet]. 2008 [cited 2018 May 22];3(1):25–31. Available from: http://www.tandfonline.com/doi/abs/10.1080/17452750701799303

227. Chiu Y-C, Cheng M-H, Engel H, Kao S-W, Larson JC, Gupta S, et al. The role of pore size on vascularization and tissue remodeling in PEG hydrogels. Biomaterials [Internet]. 2011 [cited 2018 May 22];32(26):6045–51. Available from: https://www.sciencedirect.com/science/article/pii/S0142961211004881

228. Brauker JH, Carr-Brendel VE, Martinson LA, Crudele J, Johnston WD, Johnson RC. Neovascularization of synthetic membranes directed by membrane microarchitecture. J Biomed Mater Res [Internet]. 1995 [cited 2018 May 22];29(12):1517–24. Available from: http://doi.wiley.com/10.1002/jbm.820291208

229. Dubey N, Letourneau PC, Tranquillo RT. Neuronal contact guidance in magnetically aligned fibrin gels: effect of variation in gel mechano-structural properties. Biomaterials [Internet]. 2001 [cited 2018 Mar 7];22(10):1065–75. Available from: https://www.ncbi.nlm.nih.gov/pubmed/11352087

230. Bonner JF, Blesch A, Neuhuber B, Fischer I. Promoting directional axon growth from neural progenitors grafted into the injured spinal cord. J Neurosci Res [Internet]. 2009 [cited 2018 May 22];88(6). Available from: http://www.ncbi.nlm.nih.gov/pubmed/19908250

231. Carlson AL, Bennett NK, Francis NL, Halikere A, Clarke S, Moore JC, et al. Generation and transplantation of reprogrammed human neurons in the brain using 3D microtopographic scaffolds. Nat Commun [Internet]. 2016 [cited 2018 Jun 1];7:10862. Available from: http://www.nature.com/doifinder/10.1038/ncomms10862

232. Lee VM, Louis SA, Reynolds BA. Mini-review: Neural Stem Cells. Stem cell Technol [Internet]. 2015 [cited 2018 Jun 9]; Available from: https://cdn.stemcell.com/media/files/minireview/MR29019-Neural_Stem_Cells.pdf?_ga=2.179222820.1878140984.1528564899-524324965.1526993768

233. Adams CF, Pickard MR, Chari DM. Magnetic nanoparticle mediated transfection of neural stem cell suspension cultures is enhanced by applied oscillating magnetic fields. Nanomedicine Nanotechnology, Biol Med [Internet]. 2013 [cited 2018 Feb 15];9(6):737–41. Available from: http://linkinghub.elsevier.com/retrieve/pii/S1549963413002657

234. Herberts CA, Kwa MSG, Hermsen HPH. Risk factors in the development of stem cell therapy. J Transl Med [Internet]. 2011 [cited 2018 May 23];9:29. Available from: http://www.ncbi.nlm.nih.gov/pubmed/21418664

235. Hughes SM, Moussavi-Harami F, Sauter SL, Davidson BL. Viral-Mediated Gene Transfer to Mouse Primary Neural Progenitor Cells. Mol Ther [Internet]. 2002 [cited 2018 May 23];5(1):16–24. Available from: https://www.sciencedirect.com/science/article/pii/S152500160190512X

236. Huang C, Butler PJ, Tong S, Muddana HS, Bao G, Zhang S. Substrate Stiffness Regulates Cellular Uptake of Nanoparticles. Nano Lett [Internet]. 2013 [cited 2018 May

23];13(4):1611–5. Available from: http://www.ncbi.nlm.nih.gov/pubmed/23484640

237. Weinberg D, Adams CF, Chari DM. Deploying clinical grade magnetic nanoparticles with magnetic fields to magnetolabel neural stem cells in adherent versus suspension cultures. RSC Adv. 2015;5(54).

238. Tickle J, Chari D. Non-invasive imaging of a nanoparticle-labelled transplant population within polymer matrices for neural cell therapy [In press]. Nanomedicine. 2018;

239. Bray D. Axonal growth in response to experimentally applied mechanical tension. Dev Biol [Internet]. 1984 [cited 2018 May 25];102(2):379–89. Available from: https://www.sciencedirect.com/science/article/pii/0012160684902021

240. Chari D, Blakemore W. New insights into remyelination failure in multiple sclerosis: implications for glial cell transplantation. Mult Scler [Internet]. 2002 [cited 2018 May 25];8(4):271–7. Available from: http://msj.sagepub.com/cgi/doi/10.1191/1352458502ms842oa